Doctoral Dissertation

Myoglobin reconstituted with cobalt corrinoids as a model of cobalamin-dependent methyltransferase

(コバルトコリノイド錯体含有ミオグロビンを用いた
コバラミン依存型メチル基転移酵素のモデル研究)

Yoshitsugu Morita

January 2016

Graduate School of Engineering,

Osaka University

Contents

	Page
General Introduction	1
Chapter 1	
1-1. Introduction	11
1-2. Results and Discussion	12
1-3. Summary	18
1-4. Experimental Section	18
References and Notes	21
Chapter 2	
2-1. Introduction	23
2-2. Results and Discussion	24
2-3. Summary	36
2-4. Experimental Section	36
References and Notes	40
Chapter 3	
3-1. Introduction	44
3-2. Results and Discussion	45
3-3. Summary	56
3-4. Experimental Section	56
References and Notes	61
Conclusion	65
Acknowledgments	68

General Introduction

Cofactor-containing metalloenzyme

Metalloenzymes containing cofactors such as several heme derivatives, vitamin B_{12}, F_{430} are responsible for the catalysis of essential reactions in organisms. For example, horseradish peroxidase (HRP) and cytochrome $P450_{cam}$, which contain iron protoporphyrin IX (heme *b*) as a cofactor, promote one-electron

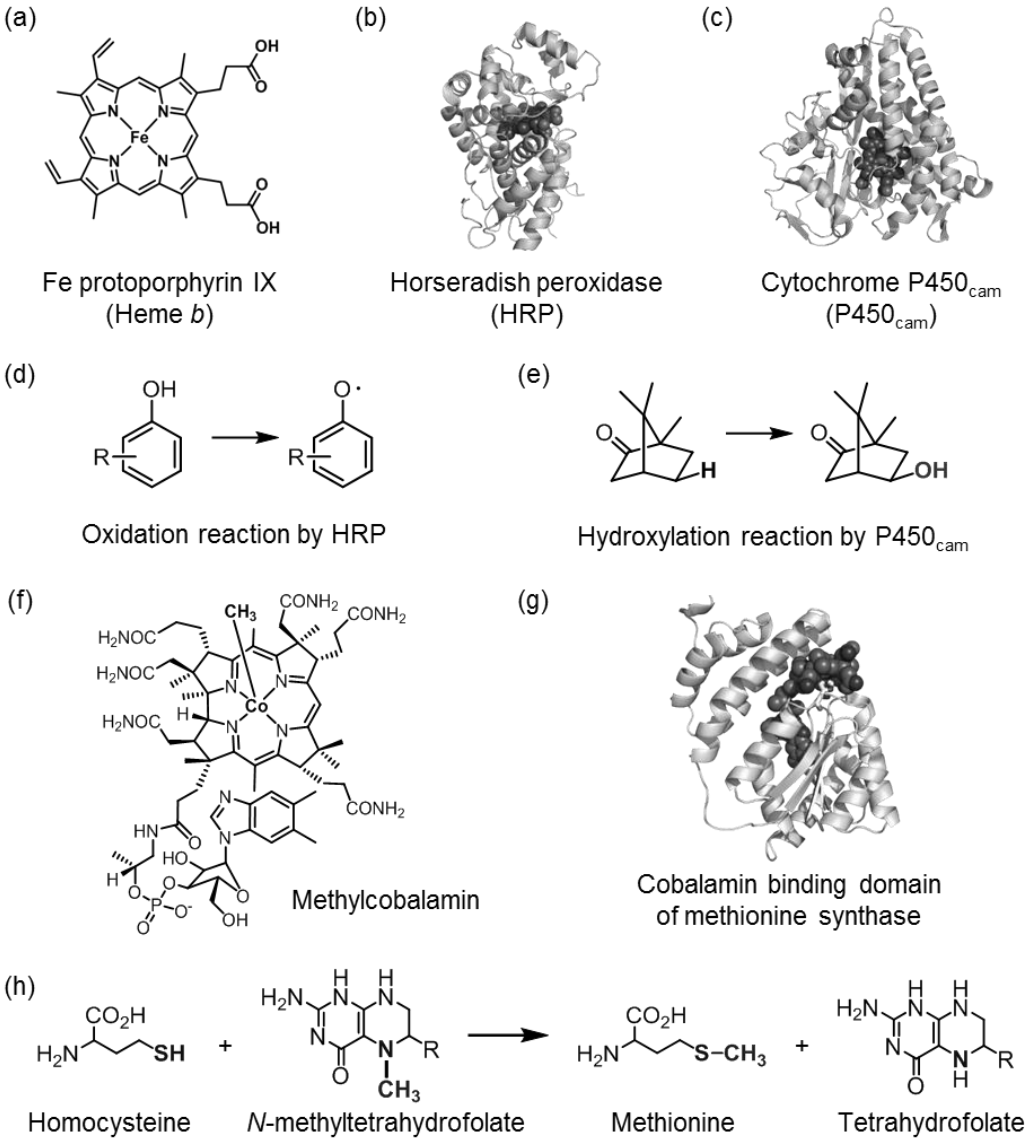

Figure 1. (a) Chemical structure of iron protoporphyrin IX as a cofactor. Structures of (b) horseradish peroxidase (PDB ID: 1H58) and (c) cytochrome $P450_{cam}$ (PDB ID: 2CPP). (d) and (e) Representative reaction schemes catalyzed by HRP and $P450_{cam}$. (f) Chemical structure of methylcobalamin. (g) Crystal structure of the cobalamin-binding domain of methionine synthase (PDB ID: 1BMT). (h) Transmethylation catalyzed by methionine synthase.

oxidation of phenol derivatives and hydroxylation of camphor, respectively (Figure 1a–e). These reactions are not readily carried out by conventional organic synthesis under mild conditions at ambient temperature and pressure in water. HRP oxidizes phenol derivatives using hydrogen peroxide in organisms (Figure 1d). The heme cofactor is coordinated with a histidine residue in the HRP matrix.[1] Cytochrome $P450_{cam}$ contains the same heme cofactor with a Fe–S(cys) coordination[2] and mediates the regioselective hydroxylation of camphor using dioxygen in the protein matrix (Figure 1e). Thus, the coordination environments control the reactivity of the heme cofactors and promote oxidation or hydroxylation reactions.

On the other hand, methionine synthase is also a cofactor-dependent enzyme. It contains methylcobalamin as an organometallic cofactor (Figure 1f,g) and catalyzes a methyl group transfer from *N*-methyltetrahydrofolate to homocysteine, generating methionine and tetrahydrofolate (Figure 1h).[3] The cobalamin derivatives have been received much attention as an important cofactor not only from the field of coordination chemistry but also from the field of bioinorganic and bioorganometallic chemistry.[3,4]

Cobalamin derivatives and the Co–C bond cleavages

Methylcobalamin and adenosylcobalamin are known as organometallic cofactors in most living organisms (Figure 2a).[4] Their precursor, cobalamin, is a cobalt complex with a corrin framework which is a tetrapyrrole ligand similar to a well-known porphyrin framework. In contrast to porphyrin, corrin has four highly saturated pyrrole rings and smaller framework size due to lacking one of the meso carbon atoms and connecting the C1–C19 bond in the corrin framework (Figure 2b). In addition, corrin acts as a monoanionic ligand compared to a dianionic ligand of porphyrin. Furthermore, the cobalamin derivatives form an intramolecular coordination bond with a peripherally-attached 6,7-dimethylbenzimidazole (DMB) moiety at the 17-position of the framework, and the axial coordination stabilizes the Co–C bond of methylcobalamin (Figure 2a).[5]

The cobalamin-dependent enzymes promote either homolytic or heterolytic cleavage of the Co–C bond of the cobalamin derivatives for their enzymatic reaction.[6] For example, methylmalonyl CoA mutase promotes the homolysis of the Co–C bond of adenosylcobalamin to catalyze a radical rearrangement reaction (Figure 2c). In contrast, methionine synthase promotes the heterolysis of the Co–C bond of methylcobalamin toward the transmethylation (Figure 1h and Figure 2d). Thus, the protein matrices control the reactivity of the cobalamin derivatives, and the mechanism has been investigated. In the case of homolysis, the cobalamin-dependent enzymes promote the dissociation of the Co–C bond by 10^9-fold.[7] Theoretical study suggests that the axial coordination stabilizes the produced Co(II) species to promote the homolytic cleavage.[7b] In contrast, it is reported that the enzymatic heterolysis of the Co–C bond is ca. 10^5-fold accelerated compared to the non-catalyzed reactions.[8]

However, the mechanism of the enzymatic heterolysis has never been completely clear and the X-ray crystal structure of the heterolysis product has been unavailable.[9,10]

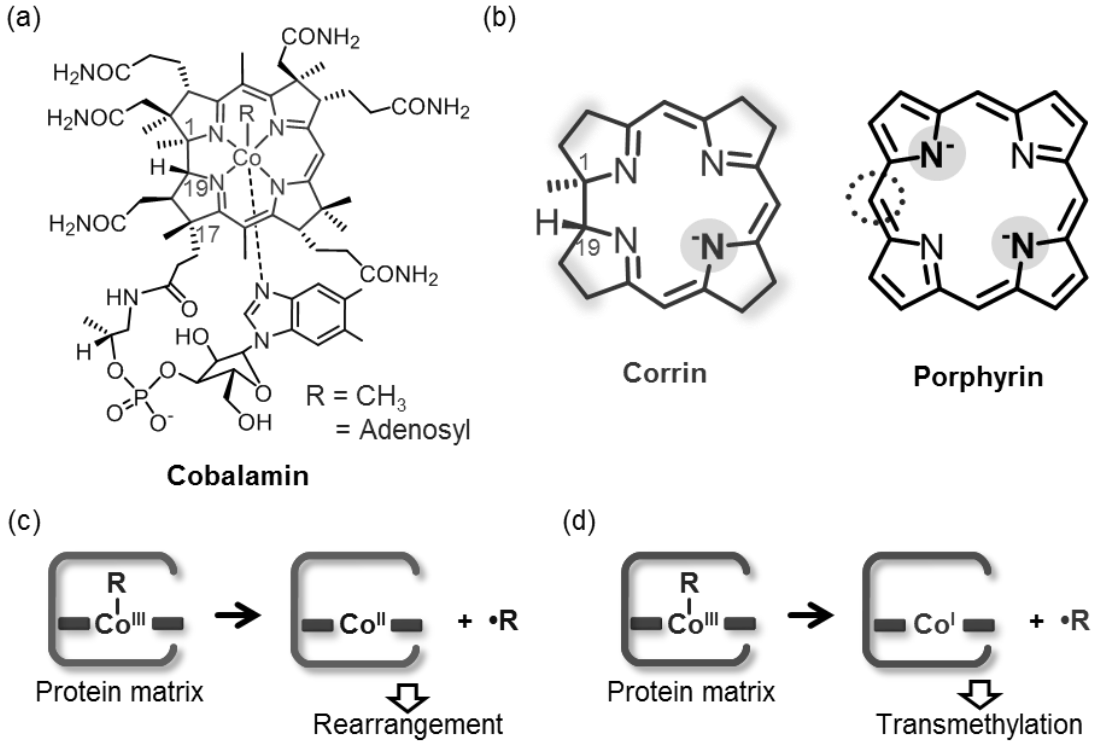

Figure 2. Chemical structure of (a) cobalamin derivatives and (b) corrin and porphyrin frameworks. (c) Homolytic and (d) heterolytic cleavages of the Co–C bonds in the cobalamin-dependent enzymes.

Methionine synthase

Cobalamin-dependent methionine synthase is widely found in Prokaryota and Eukaryota.[3,11] The enzyme is a large modular protein (ca. 146 kDa) with four distinct functional domains and one domain possesses cobalamin as a cofactor. The X-ray crystal structure of the cobalamin-binding domain shows that cobalamin interacts with a histidine residue as an axial ligand and the DMB moiety is free from the cobalt ion (Figure 3a).[12] In addition to the cobalamin-binding domain, two kinds of substrate-binding domains contain the binding sites for homocysteine and *N*-methyltetrahydrofolate, respectively.[3] Moreover, the activation domain reduces Cob(II)alamin, which is produced by an undesired oxidation reaction during the enzymatic reaction, in order to regenerate Cob(I)alamin, and subsequently the Co(I) species is methylated using *S*-adenosylmethionine as a methyl group donor to reproduce methylcobalamin.[3] The enzyme is responsible for the catalysis of transmethylation reaction, converting *N*-methyltetrahydrofolate and homocysteine to produce methionine and tetrahydrofolate. The investigation of the enzymatic reaction reveals that the enzyme promotes two kinds of methyl group transfers in the catalytic cycle: (a)

methylation of cob(I)alamin by *N*-methyltetrahydrofolate as a methyl group donor, and (b) methionine synthesis by the reaction of homocysteine with the methylcobalamin intermediate (Figure 3b).[3] However, the detailed mechanism of the transmethylations in the protein matrix and the crystal structure of the Co(I) species as an intermediate have not been understood completely.[3,6,10]

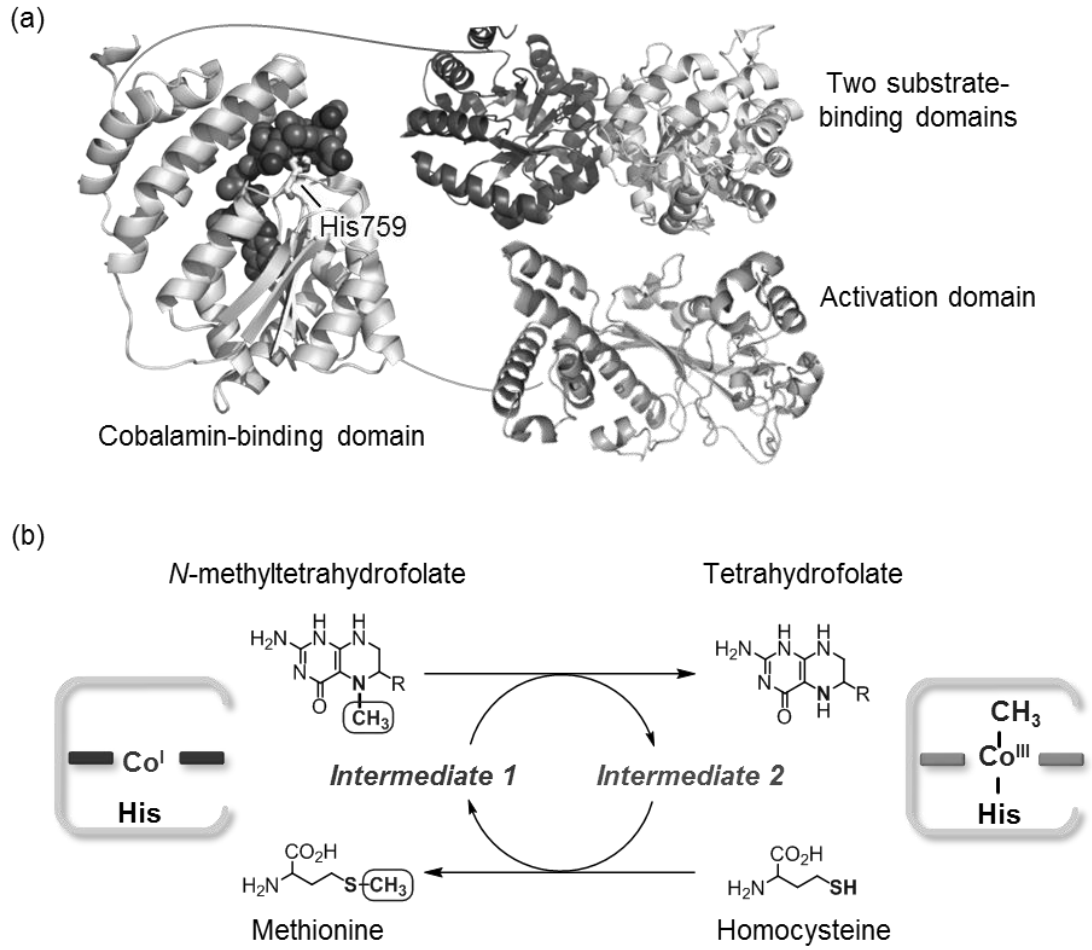

Figure 3. (a) Structures of the four domains of methionine synthase: cobalamin binding domain (PDB ID: 1BMT), two substrate-binding domains (PDB ID: 1Q8J) and activation domain (PDB ID: 1K7Y). Cobalamin is represented as sphere models. (b) Plausible catalytic cycle of the transmethylation reactions observed in methionine synthase.

Cobalamin models

As cobalamin model complexes, cobalt tetra- and di-dehydrocorrins have been prepared to understand the enzymatic reactions (Figure 4a,b).[13,14] The former has four additional double bonds at the β-position of the pyrrole rings in the framework compared to the corrin framework. The Co(II)/Co(I)-redox potential of the cobalt complex is more positive than that of cobalamin.[13] Thus, it is suggested that the Co(I) species of tetradehydrocorrin is stabler than that of cobalamin and less reactive for the formation of a Co–C bond by methyl iodide in organic solvents. In contrast, cobalt didehydrocorrin, which has two additional double bonds at the β-position of the pyrrole rings in the framework compared to the cobalamin framework,[14] has a similar Co(II)/Co(I)-redox potential to cobinamide, which is a cobalamin analog without DMB moiety (Figure 4c). The Co(I) species of cobalt didehydrocorrin is known to be more reactive for a methyl donor than that of cobalt tetradehydrocorrin. The UV-vis spectra of the Co(I) and methylated Co(III) species of didehydrocorrin are similar to those of cobinamide. The suitable model complexes of the cobalamin cofactor have been constructed,[15] however, the report of the transmethylation by the cobalamin models was quite limited.[9,16] In contrast, cobalt phthalocyanine is also a suitable model for cobalamin. The transmethylation from methylated cobalt phthalocyanine to nucleophiles occurs because the Co(I) species acts as a good leaving group.[16]

Cobalamin derivatives have been incorporated into hydrophobic environments, which mimic the protein matrices of the cobalamin-dependent enzymes.[17,18] For example, a liposome or human serum albumin (HSA) including a hydrophobic cobalamin derivative (Figure 4d) was prepared as the enzyme-inspired models (Figure 4e,f). In the former model, the alkylated hydrophobic cobalamin derivatives were noncovalently fixed in the bilayer membrane in an aqueous solution.[17] In the latter model, the alkylated hydrophobic cobalamin derivatives also inserted into the protein hydrophobic environment of HSA, which is capable of introducing hydrophobic molecules in the protein matrix.[18] Both these models demonstrate that photo-irradiation induced homolysis of the Co–C bond and then rearrangement reactions occurred in the hydrophobic environment. The models improved the radical rearrangement reactions via a homolytic cleavage of the Co–C bond of the cobalamin derivative in the hydrophobic environments. However, the model systems require activation such as the irradiation to cleave the Co–C bonds, while the natural cobalamin-dependent enzymes mediate cleavages of the Co–C bonds under the dark condition. In addition, the transmethylation reaction via heterolysis has not been reported in these models. Furthermore, the axial ligation of the cobalt complex has been unclear due to the unregulated incorporation of the cobalamin derivative in the models. Hence, construction of a cobalamin model with a well-defined coordination environment, replicating the protein matrix of the enzyme, is required to clarify the mechanism of the enzymatic transmethylation reactions and the role of the protein matrix of the complicated cobalamin-dependent enzymes.

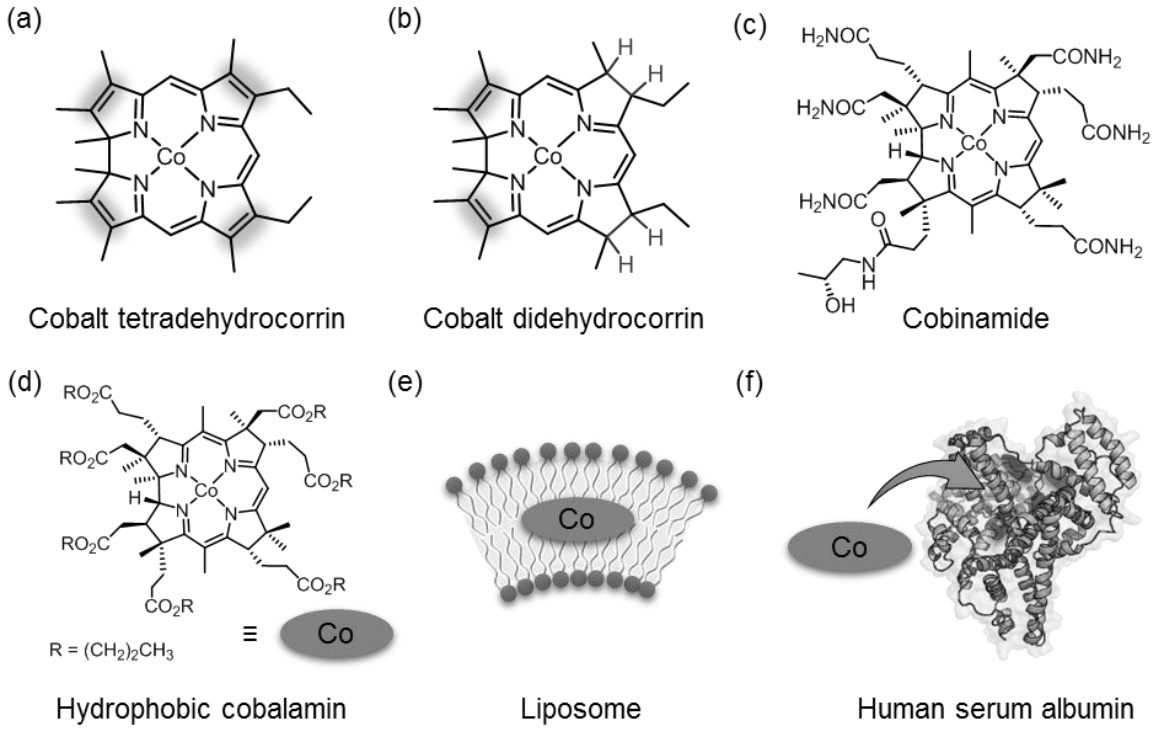

Figure 4. Chemical structures of (a) cobalt tetradehydrocorrin, (b) cobalt didehydrocorrin, (c) cobinamide and (d) hydrophobic cobalamin. Schematic representation of cobalamin models incorporated into (e) liposome and (f) human serum albumin as the hydrophobic environments.

Myoglobin reconstituted with an artificial cofactor

Myoglobin, an oxygen carrier hemoprotein (ca. 17 kDa), contains heme as a cofactor.[19] The heme cofactor is wedged in the heme pocket by the Fe–N(His93) coordination, hydrophobic contact of the heme with several nonpolar aliphatic and aromatic amino acid residues, and the formation of the salt bridge between the heme-propionate side chain and polar residues (Figure 5a).[20]

To elucidate the oxygen binding mechanism and modify its function, the replacement of the heme cofactor with an artificial cofactor has been demonstrated for myoglobin. The native heme cofactor is extracted by 2-butanone under an acidic condition to convert apomyoglobin (apoMb).[21] Under a neutralized condition, an artificial cofactor is inserted into apomyoglobin to yield reconstituted myoglobin (rMb) (Figure 5b).[22] A series of myoglobins reconstituted with artificial cofactors has been investigated by several research groups. For example, myoglobin reconstituted with manganese porphycene, a constitutional isomer of porphyrin, demonstrates catalytic hydroxylation of a C(sp^3)–H bond of ethylbenzene in the heme pocket.[23] In addition, X-ray crystallography experiments reveal that the cofactor is coordinated with the axial His93 residue in the protein matrix. Therefore, the

cofactor-substitution is a useful method for construction of an enzyme model in which the cofactor is coordinated with the axial histidine residue in the hydrophobic protein matrix.

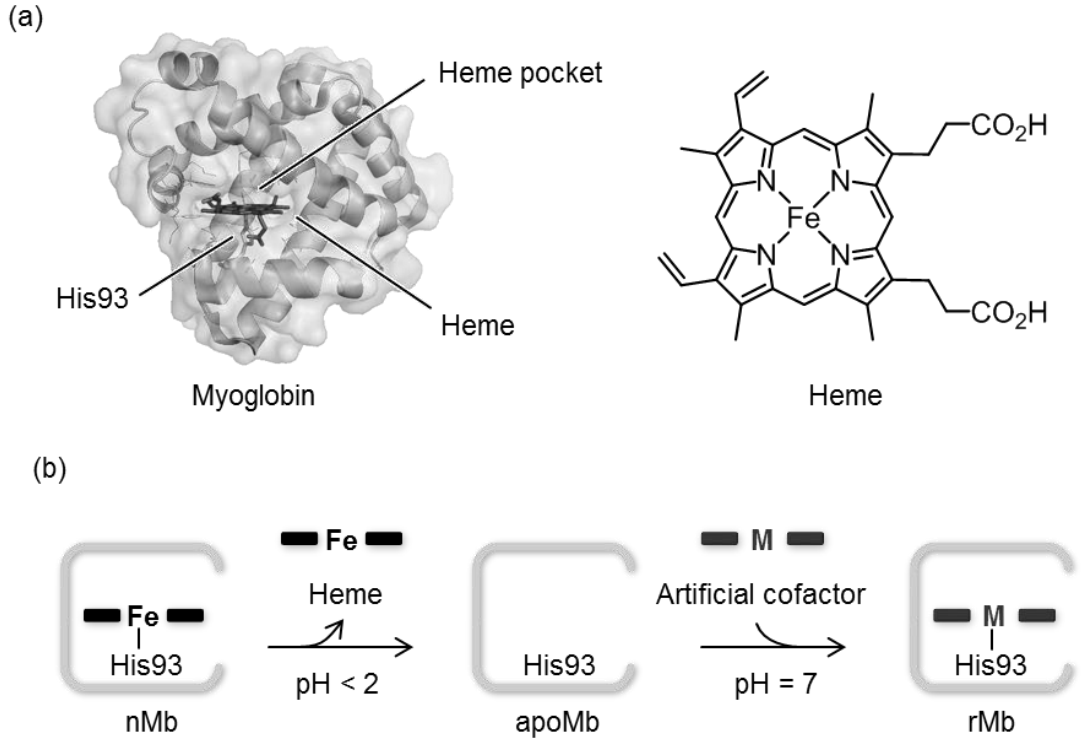

Figure 5. (a) Crystal structure of native myoglobin (PDB ID: 1YMB) and chemical structure of the heme cofactor. (b) Scheme of preparation of myoglobin reconstituted with an artificial cofactor.

Strategy for an enzyme model of methionine synthase

As an enzyme model of cobalamin dependent-methionine synthase, a cobalamin model complex with a simple protein matrix which provides a suitable coordination environment is constructed and investigated in this thesis (Figure 6).[3,12] Apomyoglobin and cobalt tetradehydrocorrin (Co(TDHC)) are employed as a suitable model complex of cobalamin and a simple protein matrix having a similar coordination environment to the cobalamin binding domain of methionine synthase, respectively.[13,22] Reconstitution of myoglobin with Co(TDHC) yields a hybrid protein, rMb(Co(TDHC)), as an enzyme model (Figure 6). The detailed investigation of rMb(Co(TDHC)) will contribute to understanding of coordination behavior of the cofactor in the protein matrix.

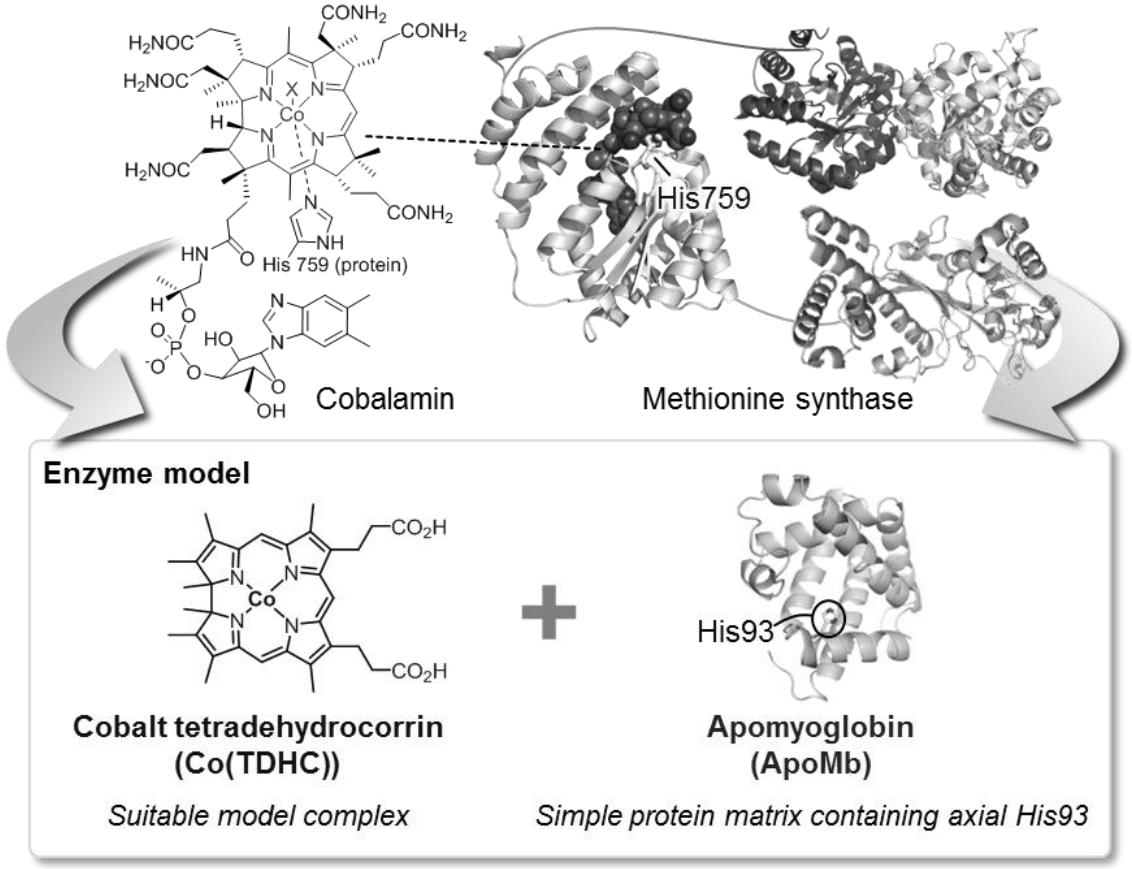

Figure 6. Strategy for construction of the methionine synthase model using cobalt tetradehydrocorrin (Co(TDHC)) as a cobalamin model complex and apomyoglobin (apoMb) as a simple protein matrix, respectively.

References and Notes

(1) G. I. Berglund, G. H. Carlsson, A. T. Smith, H. Szöke, A. Henriksen, J. Hajdu, *Nature* **2002**, *417*, 463.

(2) T. L. Poulos, B. C. Finzel, A. J. Howard, *J. Mol. Biol.* **1987**, *195*, 687.

(3) R. G. Matthews, *Acc. Chem. Res.* **2001**, *34*, 681.

(4) (a) B. Kräutler, B. Puffer, *in Handbook of Porphyrin Science*, ed. K. M. Kadish, K. M. Smith, R. Guilard, World Scientific, Singapore, 2012, ch. 117, vol. 25, pp. 131–263. (b) K. L. Brown, *Chem. Rev.* **2005**, *105*, 2075.

(5) B. Kräutler, *Helv. Chim. Acta* **1987**, *70*, 1268.

(6) K. Gruber, B. Puffer, B. Kräutler, *Chem. Soc. Rev.* **2001**, *40*, 4346.

(7) (a) K. L. Brown, *Dalton Trans.* **2006**, 1123. (b) K. L. Brown, H. M. Marques, *J. Mol. Struct.*

THEOCHEM **2005**, *714*, 209.

(8) (a) R. G. Matthews, in *Chemistry and biochemistry of B12*, ed. R. Banerjee, John Wiley & Sons. Inc., New York, 1999, ch. 27, pp. 681–706. (b) H. P. C. Hogenkamp, G. T. Bratt, A. T. Kotchevar, *Biochemistry* **1987**, *26*, 4723.

(9) (a) L. D. Zydowsky, T. M. Zydowsky, E. S. Haas, J. W. Brown, J. N. Reeve, H. G. Floss, *J. Am. Chem. Soc.* **1987**, *109*, 7922. (b) C. Wedemeyer-Exl, T. Darbre, R. Keese, *Helv. Chim. Acta* **1999**, **82**, 1173. (c) L. Pan, H. Shimakoshi, Y. Hisaeda, *Chem. Lett.* **2009**, *38*, 26. (d) L. Pan, H. Shimakoshi, T. Masuko, Y. Hisaeda, *Dalton Trans.* **2009**, 9898. (e) L. Pan, K. Tahara, T. Masuko, Y. Hisaeda, *Inorg. Chim. Acta* **2011**, *368*, 194.

(10) (a) P. Engel, G. Rytz, L. Walder, U. Vögeli, R. Scheffold, in Vitamin B12, ed. B. Zagalak, W. Friedrich, Walter de Gruyter & Co., Berlin, 1979, pp. 171–172. (b) P. Doppelt, J. Fischer, R. Weiss, *Inorg. Chem.* **1984**, *23*, 2958.

(11) (a) B. Kräutler, in *Metal Ions in Life Science*, ed. A. Sigel, H. Sigel, R. K. O. Sigel, Royal Society of Chemistry, Cambridge, 2009, ch. 1, vol. 6, pp. 1–51. (b) R. G. Matthews, in *Metal Ions in Life Science*, ed. Sigel, A., Sigel, H., Sigel, R. K. O., Royal Society of Chemistry, Cambridge, 2009, ch. 2, vol. 6, pp. 53–113.

(12) C. L. Drennan, S. Huang, J. T. Drummond, R. G. Matthews, M. L. Ludwig, *Science* **1994**, *266*, 1669.

(13) (a) Y. Murakami, K. Aoyama, *Bull. Chem. Soc. Jpn.* **1976**, *49*, 683. (b) C.-J. Liu, A. Thompson, D. Dolphin, *J. Inorg. Biochem.* **2001**, *83*, 133.

(14) Y. Murakami, Y. Aoyama, K. Tokunaga, *J. Am. Chem. Soc.* **1980**, *102,* 6736.

(15) Y. Murakami, Y. Aoyama, S. Nakanishi, *Chem. Lett.* **1977**, 991.

(16) (a) W. Galezowski, P. N. Ibrahim, E. S. Lewis, *J. Am. Chem. Soc.* **1993**, *115*, 8660. (b) W. Galezowski, E. S. Lewis, *J. Phys. Org. Chem.* **1994**, *7*, 90. (c) W. Galezowski, *Inorg. Chem.* **2005**, *44*, 5483. (d) W. Galezowski, *Inorg. Chem.* **2005**, *44*, 1530.

(17) (a) Y. Murakami, Y. Hisaeda, A. Ogawa, T. Ohno, *Chem. Lett.* **1994**, 1657. (b) Y. Murakami, J. Kikuchi, Y. Hisaeda, O. Hayashida, *Chem. Rev.* **1996**, *96,* 721.

(18) Y. Hisaeda, T. Masuko, E. Hanashima, T. Hayashi, *Sci. Technol. Adv. Mater.* **2006**, *7*, 655.

(19) B. A. Springer, S. G. Sligar, J. S. Olson, G. N. Phillips, Jr., *Chem. Rev.* **1994**, *94*, 699.

(20) S. V Evans, G. D. Brayer, *J. Mol. Biol.* **1990**, *213*, 885.

(21) F. W. J. Teale, *Biochim. Biophys. Acta* **1959**, *35*, 543

(22) T. Hayashi, in *Handbook of Porphyrin Science*, ed. K. M. Kadish, K. M. Smith, R. Guilard, World Scientific, Singapore, 2010, ch. 23, vol. 5, pp. 1–69.

(23) K. Oohora, Y. Kihira, E. Mizohata, T. Inoue, T. Hayashi, *J. Am. Chem. Soc.* **2013**, *135*, 17282.

Outline of this thesis

The author constructed an enzyme model of cobalamin-dependent methionine synthase and X-ray crystal structures of the Co(II) and Co(I) species were demonstrated (chapter 1). The formation of the Co–C bond and subsequent transmethylation were observed in the protein matrix (Chapter 2). Aqua- and cyano-Co(III) species in the heme pocket were prepared and investigated to understand the coordination behavior of the native enzyme (chapter 3).

Chapter 1: Preparation of myoglobin reconstituted with cobalt corrinoid and X-ray crystal structures of the Co(II) and Co(I) species

A conjugate between apomyoglobin and cobalt tetradehydrocorrin was prepared to replicate the coordination behavior of cobalamin in methionine synthase. X-ray crystallography experiments reveal that the tetra-coordinated Co(I) species, Co^{I}(TDHC), is formed through the cleavage of the axial Co–N(His93) ligation after the reduction of the penta-coordinated Co(II) cofactor in the heme pocket.

Chapter 2: Formation of a Co–C bond and subsequent transmethylation in myoglobin reconstituted with the cobalt corrinoid

In the heme pocket, Co^{I}(TDHC) is found to react with methyl iodide to form the methylated cobalt complex, although it is known that a similar nucleophilic reaction of a cobalt(I) tetradehydrocorrin complex does not proceed effectively in organic solvents. Furthermore, the author observed a residue- and regio-selective transmethylation from the methylated complex to the Nε2 atom of the His64 imidazole ring in myoglobin at 25 °C over a period of 48 h. The theoretical calculations provide a plausible reaction mechanism wherein the axial histidine ligation stabilizes the methylated cobalt complex and subsequent proximal histidine-flipping induces the transmethylation via heterolytic cleavage of the Co–CH_3 bond in the hybrid model.

Chapter 3: Coordination behavior of aqua- and cyano-Co(III) corrinoids with the histidine-ligation in the myoglobin matrix

Myoglobins reconstituted with aqua- and cyano-Co(III) tetradehydrocorrins were prepared as cobalamin models. X-ray crystal structure analyses clearly reveal that the cobalt complexes form a hexa-coordinated structure with axial ligation by His93 and an exogenous molecule in the heme pocket. Acid titration, ^{13}C NMR and IR data indicate that both axial bonds, Co–CN and Co–N(His), are weakened upon replacement of water with cyanide. This finding is supported by DFT calculations.

Chapter 1

Preparation of myoglobin reconstituted with cobalt corrinoid and X-ray crystal structures of the Co(II) and Co(I) species

1-1. Introduction

Methionine synthase is responsible for the essential methylation of homocysteine to yield methionine. It is known that the enzyme requires *N*5-methyltetrahydrofolate as a methyl group donor and that the methyl group transfer to homocysteine is promoted by a cobalamin cofactor, a vitamin B_{12}-like cobalt corrinoid complex.[1–4] The entire enzyme structure has a molecular weight of ca. 136 kDa and includes four domains. The complexity of this enzyme system poses significant challenges with respect to the characterization of the entire structure. The crystal structure of the cobalamin-binding domain of methionine synthase has been determined by Ludwig and co-workers, and it was found that the axial

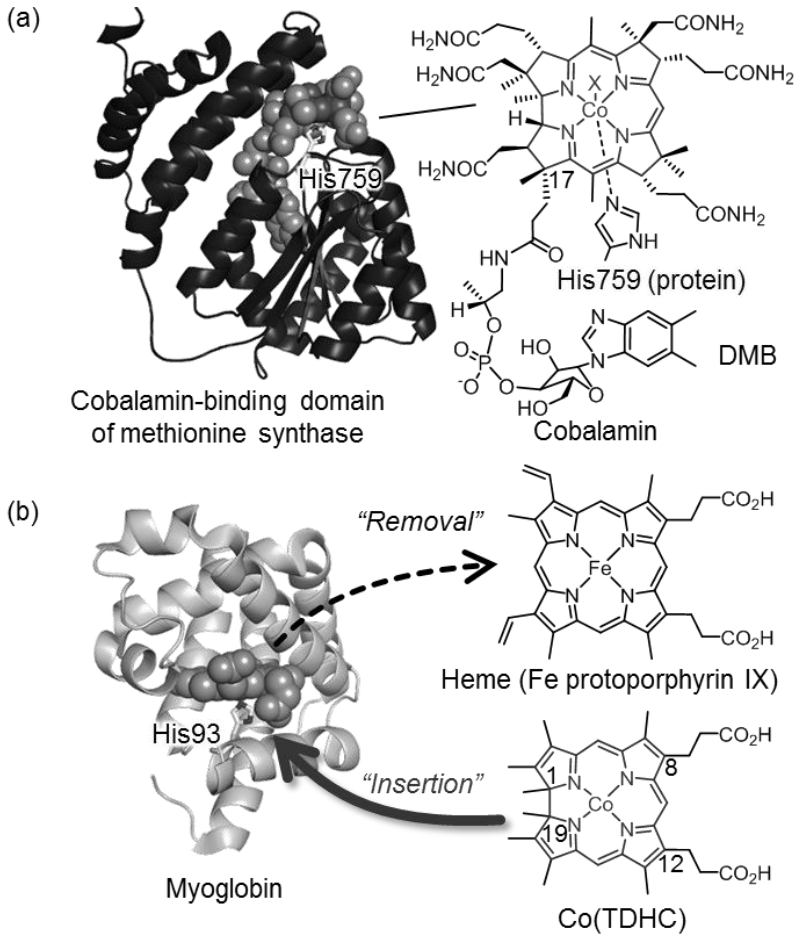

Figure 1-1. Structure of holoproteins and cofactors. (a) The crystal structure of the cobalamin-binding domain (PDB ID: 1BMT) of methionine synthase and the molecular structure of cobalamin. (b) Crystal structure of horse heart myoglobin (PDB ID: 2V1K) and molecular structures of native heme and Co^{II}(TDHC). Native heme is replaceable with Co^{II}(TDHC) as a cobalamin model.

ligand of cobalamin is a protein-derived histidine residue and not the 6,7-dimethylbenzimidazole (DMB) moiety, which is peripherally-attached at the 17-position of the cobalamin framework, a base-off/His-on state (Figure 1-1a).[5] In the catalytic cycle, two key intermediates have been proposed to exist transiently; (i) a highly nucleophilic tetra-coordinated Co(I) species known as cob(I)alamin and (ii) a methylated Co(III) species known as methylcobalamin.[1–3] However, the structure of cob(I)alamin has never been determined directly.[5,6] Herein, the author reports a hybrid model consisting of a cobalamin model complex with a suitable protein matrix to improve the our understanding of the formation of the intermediate with the axial ligand rearrangement in the protein. The hybrid model for methionine synthase was constructed as follows (Figure 1-1b): First, horse heart apomyoglobin was used as a substitute protein matrix for the cobalamin-binding domain of methionine synthase. It is a relatively small and well-known protein which provides a histidine residue as an axial ligand to the heme cofactor in the heme-binding pocket as well as the cobalamin-binding domain. Second, a cobalt tetradehydrocorrin complex was designed as an artificial cofactor to mimic the cobalamin moiety because native cobalamin consists of a tetrapyrrole macrocyclic ligand known as a corrinoid. Dolphin and co-workers synthesized a cobalt complex of 1,19-dimethyltetradehydrocorrin and detected the stable Co(I) species by UV-vis spectroscopy.[6] This inspired us to insert such a complex into the apomyoglobin heme pocket to obtain ligation by the His93 residue which coordinates to the native heme iron of myoglobin.

1-2. Results and Discussion

Preparation and characterization of the enzyme model

The cobalt corrinoid complex, Co(TDHC) (TDHC = 8,12-dicarboxyethyl-1,2,3,7,13,17,18,19-octamethyltetradehydrocorrin) (Figure 1-1b), was prepared as a model of cobalamin by cyclization of the corresponding biladiene-a,c dihydrobromide derivative in the presence of $Co(OAc)_2$ (Scheme 1-1).[7] Two methyl substituents at the C1- and C19-positions are on opposite faces of the corrinoid ring and the compound exists as two enantiomers, (1*R*,19*R*)-TDHC and (1*S*,19*S*)-TDHC, in a 1:1 ratio. The two propionate side chains introduced at the C8- and C12-positions are analogous to those of native heme and are included for the purpose of fixing the cofactor in the proper position via a hydrogen bonding network with polar amino acid residues in the heme pocket. The Co^{II}(TDHC) complex was added to apomyoglobin obtained by removal of the heme.[8] ESI-TOF MS data (Figure 1-2) and ICP analysis of the reconstituted protein, rMb(Co^{II}(TDHC)), were used to confirm that Co^{II}(TDHC) binds to the protein in a 1:1 ratio. The UV-vis spectrum of rMb(Co^{II}(TDHC)) has a sharp absorption band at 510 nm (Figure 1-3a), which is similar to that observed for the Co^{II}(TDHC) dimethyl ester in pyridine.[9] Furthermore, the EPR measurement of rMb(Co^{II}(TDHC)) indicates a typical spectrum (Figure 1-3b): the interaction of the cobalt nucleus (I = 7/2) with the unpaired electron in a

penta-coordinated low-spin d^7 configuration of Co(II) results in hyperfine splitting of the signal into an octet centered at g_z = 1.99, and the presence of a ^{14}N (I = 1) ligand attached to the axial position of the Co^{II}(TDHC) complex shows superhyperfine splitting of each component of the octet into a triplet.[5,10] This provides support for the author's proposal that the cobalt atom coordinates to the Nε2-atom of the His93 imidazole ring as an axial ligand.[11] Furthermore, the binding constant of Co^{II}(TDHC) for apomyoglobin was determined by UV-vis spectral changes in the titration experiment to be 20 μM^{-1} in 0.1 M potassium phosphate buffer (pH 7.0) at 25 ˚C (Figure 1-4), indicating that Co^{II}(TDHC) is tightly bound to form the His-on state.

Scheme 1-1. Synthetic pathway of Co^{II}(TDHC).

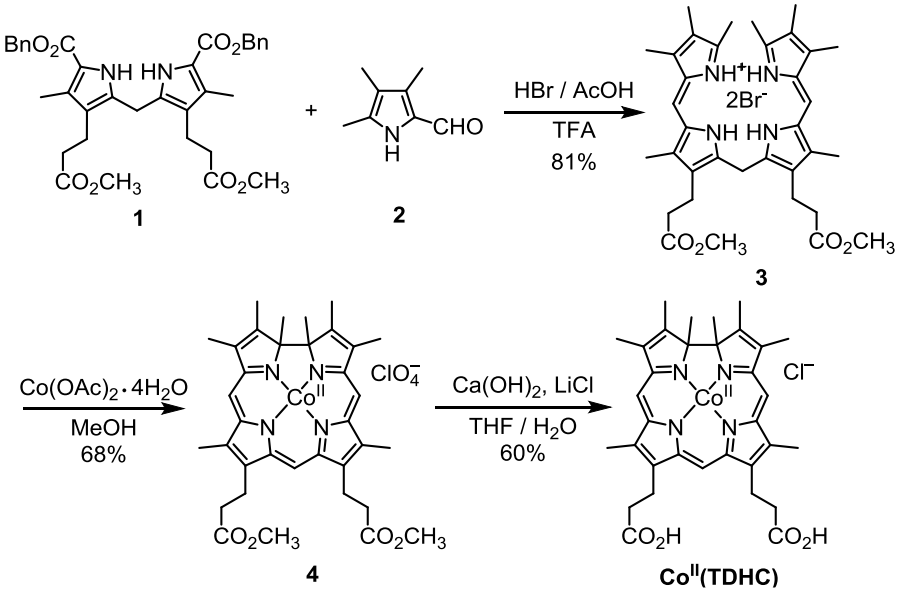

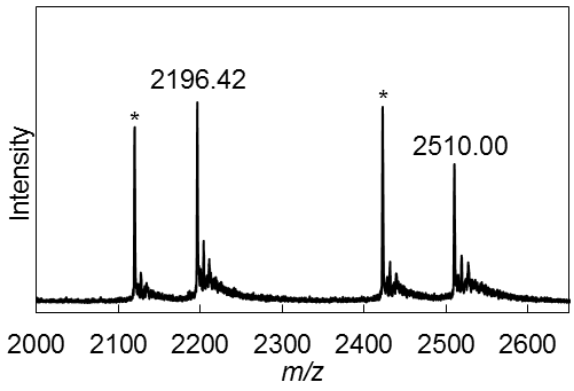

Figure 1-2. ESI-TOF MS (positive mode) spectrum of rMb(Co^{II}(TDHC)). Two characteristic peaks are consistent with the calculated mass numbers as follows. m/z (z) for rMb(Co^{II}(TDHC)): 2196.38 (8+), 2510.18 (7+). Peaks with the asterisks were assigned as multiply ionized species of apomyoglobin.

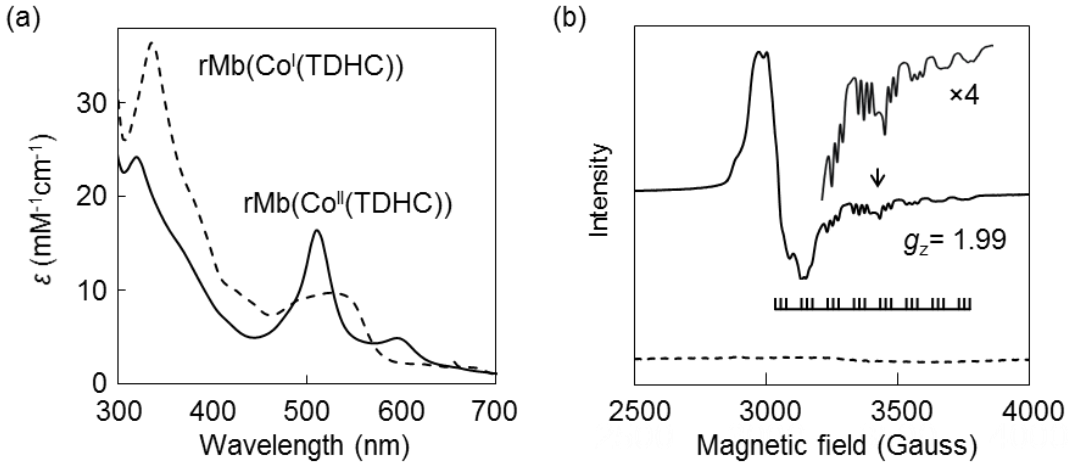

Figure 1-3. Characteristic spectra of reconstituted myoglobins: rMb(Co^{II}(TDHC)) (solid line) and rMb(Co^{I}(TDHC)) (dashed line). (a) UV-vis spectra of the reconstituted proteins in 0.1 M potassium phosphate buffer (pH 7.0) solution at 25 ˚C. (b) EPR spectra of the reconstituted proteins (0.5 mM) in 0.1 M potassium phosphate buffer (pH 7.0) solution at 10 K. The signal of $g_x = g_y$ is centered at $g = 2.23$. The coupling constants of $|A_{Coz}|$ and $|A_{Nz}|$ for rMb(Co^{II}(TDHC)) are 99.7 and 20.8 G, respectively. rMb(Co^{I}(TDHC)) is EPR-silent.

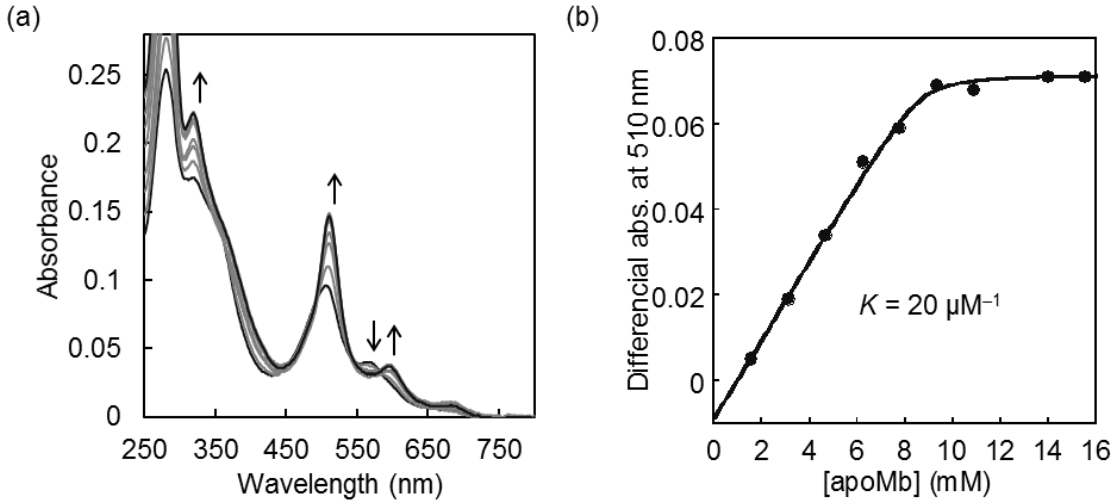

Figure 1-4. (a) UV-vis spectral changes of Co^{II}(TDHC) (8.7 μM) at various concentrations of apoMb (1.55−15.5 μM) in 0.1 M potassium phosphate buffer solution (pH 7.0) at 25 ˚C. (b) The plots of absorption at 510 nm against concentrations of apoMb with a fitting curve to determine the binding constant of Co^{II}(TDHC) for apomyoglobin (K).

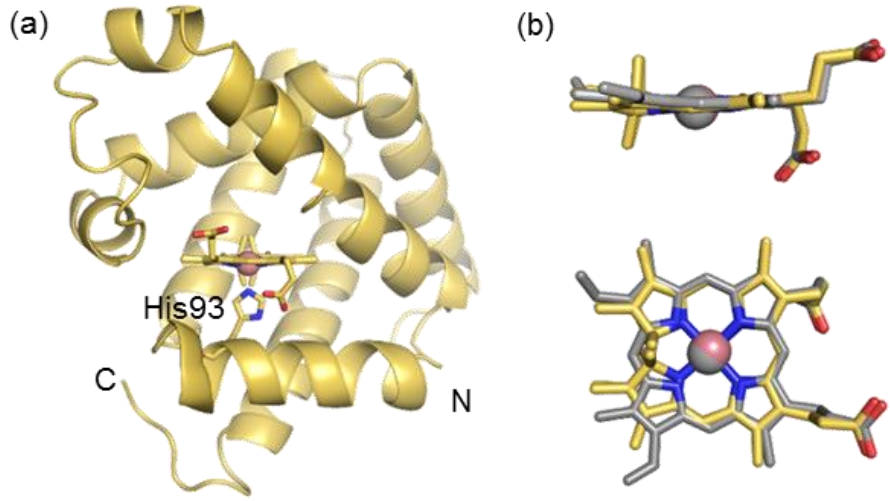

Figure 1-5. (a) Crystal structure of rMb(Co^{II}(TDHC)). The structure of the TDHC framework possesses two enantiomers with a ratio of 13:7 due to the configuration of two methyl substituents at C1- and C19-positions (Figure 1-1b). (b) Superimposed structures (top and side views) of the cofactors in rMb(Co^{II}(TDHC)) (yellow stick) and native myoglobin (PDB ID: 2V1K) (gray stick).

The crystal structure of rMb(Co^{II}(TDHC)) was obtained at a resolution of 1.30 Å and reveals that CoII(TDHC) is bound in the heme pocket with Co(II)–His93 coordination characterized by a Co–Nε2 bond length of 2.18 Å (Figure 1-5). In the crystals, the ratio of proteins, rMb(Co^{II}((1*R*,19*R*)-TDHC)) and rMb(Co^{II}((1*S*,19*S*)-TDHC)), was found to be 13:7 by the occupancy of the enantiomers because the TDHC ligand provides a mixture of two enantiomers due to introduction of two methyl substituents at the C1- and C19-positions (*vide supra*). Although the TDHC ligand, whose macrocycle is smaller than that of a porphyrin, has two methyl substituents oriented perpendicularly to the corrin plane, the position of the TDHC framework is remarkably similar to that of the porphyrin framework observed in native myoglobin. As a result, the two propionate side chains located at the C8- and C12-positions are found to participate in hydrogen bonding networks with Lys45 and Ser92/His97, respectively. These residues originally interact with the heme-propionate side chains in myoglobin. In addition, the polypeptide Cα atoms of the native myoglobin and rMb(Co^{II}(TDHC)) are superimposable with a root-mean-square deviation (RMS value) of 0.223 Å.[12] Although there are several examples of hemoproteins reconstituted with artificial porphyrinoid cofactors,[8] the present work is the first example of incorporation of a metallocorrin derivative into a hemoprotein.

Reduction of the Co(II) species

Reduction of rMb(Co^{II}(TDHC)) upon addition of dithionite under anaerobic conditions leads to UV-vis spectral changes that include clear isosbestic points over 2 s. The characteristic spectrum of the Co(I)

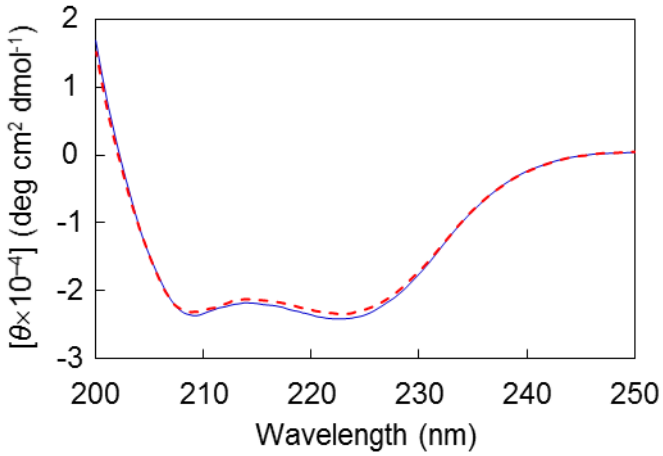

Figure 1-6. Circular dichroism (CD) spectra of rMb(Co^{II}(TDHC)) (bule solid line) and rMb(Co^{I}(TDHC)) (red dashed line), respectively. Conditions: [protein] = 0.018 mM in 0.1 M potassium phosphate buffer at pH 7.0, at 25 °C under N_2 atmosphere.

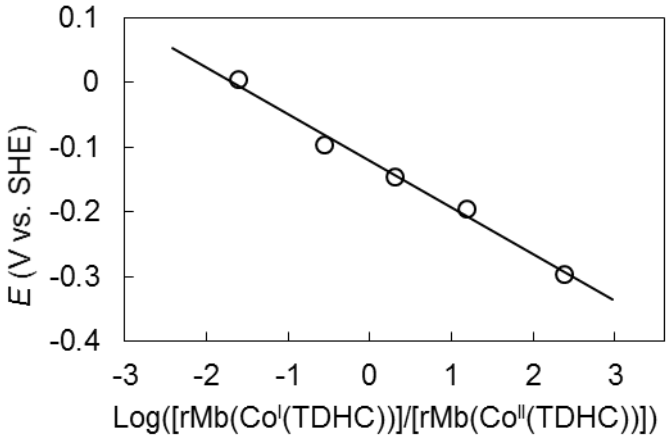

Figure 1-7. Nernst plots obtained by spectroelectrochemistry of rMb(Co(TDHC)). The plots obtained from the absorption changes at 600 nm of rMb(Co^{I}(TDHC))/rMb(Co^{II}(TDHC)) in spectroelectrochemical measurements using an optically transparent thin-layer electrode cell (optical path length of 1 mm) in a glove box. A Pt wire (counter electrode) and a Pt mesh (working electrode) were used along with an Ag|AgCl reference electrode. The potentials of these electrodes were controlled and measured with a Hokuto Denko HA-301 potentiostat/galvanostat. A solution of rMb(Co^{II}(TDHC)) (0.3 mM) was prepared in 0.1 M potassium phosphate buffer (pH 7.0) containing 2-hydroxy-1,4-naphthoquinone (0.5 M) as an electron mediator. At each applied potential, the electronic absorption spectra were monitored at 25 °C until no further spectral changes were detected.

species then appears with an absorption maximum at 530 nm (Figure 1-3a). The disappearance of the characteristic Co(II) low spin EPR signals also indicates the formation of the diamagnetic d^8 Co(I) species,

rMb(Co^{I}(TDHC)) (Figure 1-3b). At pH 7.0, the CD spectrum of rMb(Co^{I}(TDHC)) displays two prominent minima at 209 nm and 222 nm, which are typical of a-helical structures, having the consistent molar ellipticity values with those determined for rMb(Co^{II}(TDHC)) (Figure 1-6). The redox potential of rMb(Co^{II}(TDHC))/rMb(Co^{I}(TDHC)) was determined by spectroelectrochemical measurements to be –0.13 V vs. SHE at pH 7.0 (Figure 1-7), while the value of cobalamin in methionine synthase is –0.5 V.[13] This indicates that rMb(Co^{I}(TDHC)) is more thermodynamically stable than native cob(I)alamin in the protein.

Crystal structure of the Co(I) species

To understand the coordination behavior of one of the intermediates, cob(I)alamin, during the catalytic reaction, the crystals of rMb(Co^{II}(TDHC)) were directly reduced by soaking in a solution of 0.5% (w/v) dithionite, and the resulting spectral changes suggest that the Co(I) species is formed in the crystal state. The crystal structure of rMb(Co^{I}(TDHC)) was successfully determined at 1.35 Å-resolution (Figure 1-8).

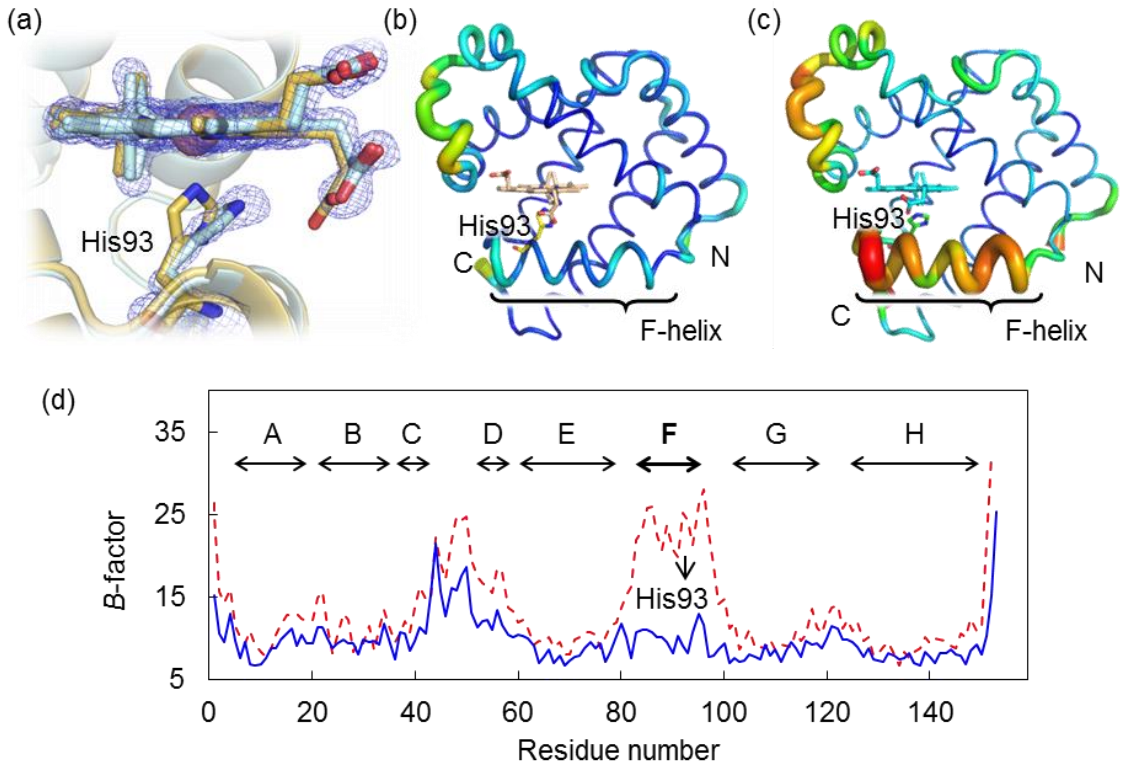

Figure 1-8. (a) Superimposition of the cofactors and the heme pocket residues of rMb(Co^{I}(TDHC)) (light blue) and rMb(Co^{II}(TDHC)) (yellow). The $2F_o - F_c$ electron density is shown as a blue grid (contoured at 1.0 σ) around the His93 residue and the cofactor of rMb(Co^{I}(TDHC)). (b) and (c) Variations in crystallographic *B*-factors represented as width of the backbone trace in rMb(Co^{II}(TDHC)) (left) and rMb(Co^{I}(TDHC)) (right), respectively. (d) *B*-factor of the reconstituted proteins. Summary of *B*-factor values of Cα atoms for rMb(Co^{II}(TDHC)) (blue solid line) and rMb(Co^{I}(TDHC)) (red dashed line).

Interestingly, the proximal His93 residue swings out upon cleavage of the Co–N(His93) coordination and gains flexibility. In fact, the decreased electron density of the His93 residue is observed in the $2F_o - F_c$ map ($\sigma = 1.0$). As a result, the distance between the Co(I) and Nε2(His93) atoms is 3.44 Å in the crystal structure of rMb(Co^{I}(TDHC)). From the crystal structure it was found that Co^{I}(TDHC) is bound in the heme pocket as a tetra-coordinate complex without axial ligands. This action then induces a steric interaction with the 12-propionate side chain, causing it to deviate from its normal position. Furthermore, in rMb(Co^{I}(TDHC)), the backbone *B*-factors of the F-helix,[14] which includes the His93 residue, are found to be remarkably large compared to those of rMb(Co^{II}(TDHC)) (Figure 1-8b–d) because of the lack of axial ligation. In contrast, the whole protein structure of rMb(Co^{I}(TDHC)) does not deviate significantly, as indicated by the RMS value of all the Ca carbons (0.204 Å). Additionally, the protein matrix of myoglobin is found to be capable of holding the tetra-coordinate cofactor in the heme pocket via hydrogen bonding and hydrophobic interactions. The CD spectrum of rMb(Co^{I}(TDHC)) provides further evidence that the α-helicity of the protein is maintained in solution even after release of the axial ligand (*vide supra*). Taken together, these results indicate that the remarkable structural changes occur locally in the proximal site upon reduction and do not exert a significant influence on the whole structure of the protein. To the best of the author's knowledge, this is the first example of a tetra-coordinate structure of a Co(I) species in a corrinoid framework.[15] It is of particular interest to monitor the unbound form of an axial ligand (His-off) in the myoglobin heme pocket in this unique situation. The author's data support the speculation that the species of methionine synthase referred to as "base-off" cobalamin only requires proximal histidine flipping in the process of oxidation/reduction of cobalamin.

1-3. Summary

In this chapter, the author has designed and prepared myoglobin reconstituted with the cobalt corrinoid complex, Co(TDHC) as a simple model for the active site of a complicated cobalamin-dependent methyltransferase. In the heme pocket of myoglobin, Co^{II}(TDHC) is tightly bound and provides a model of the baseoff/His-on state which is seen in the cobalamin binding domain of methionine synthase, and then an important intermediate, the tetra-coordinated Co(I) species, is detectable in the protein matrix.

1-4. Experimental section

Instruments

UV-vis spectral measurements were carried out with a Shimadzu UV-3150 or UV-2550 double-beam spectrophotometer, or a Shimadzu BioSpec-nano spectrometer. ESI-TOF MS analyses were performed with a Bruker Daltonics micrOTOF mass spectrometer. ^{1}H spectra were collected on a Bruker BioSpin DPX400 (400 MHz) spectrometer. The ^{1}H chemical shift values are reported in ppm relative to a residual

solvent peak. ICP-OES (inductively coupled plasma optical emission spectroscopy) was performed on a Shimadzu ICPS-8100 emission spectrometer. The EPR spectra were measured using a Bruker EMX Plus spectrophotometer at the Instrument Center of the Institute for Molecular Science (Okazaki, Japan). The equipment used for X-ray crystallographic analysis is described below. The pH measurements were made with an F-52 Horiba pH meter. Air-sensitive manipulations were performed in a UNILab glove box (MBraun, Germany).

Materials and methods

All reagents of the highest guaranteed grade available were obtained from commercial sources and were used as received unless otherwise indicated. Distilled water was demineralized using a Barnstead NANOpure DIamond^{TM} apparatus. Dibenzyl *meso*-3,3′-bis(methoxycarbonylethyl)-4,4′-dimethyldipyrromethane-5,5′-dicarboxylate **1** and 2-formyl-3,4,5-trimethylpyrrole **2** were synthesized according to a previously published method.[16,17] A standard cobalt solution for ICP-OES was purchased from Wako Pure Chemical Industries.

Preparation of cobalt(II) tetradehydrocorrin (Co^{II}(TDHC))

Dipyrromethane derivative **1** (1.4 g, 2.3 mmol) was dissolved in trifluoroacetic acid (TFA) (10 mL) under an N_2 atmosphere and then HBr/AcOH (25 wt.%, 8 mL) was added to the solution. After stirring for 8 h at room temperature, 2-formyl-3,4,5-trimethylpyrrole **2** (0.67 g, 4.8 mmol) in a methanol solution (20 mL) was added dropwise on an ice bath and stirred for 1 h at room temperature. Diethyl ether (200 mL) was added to the reaction mixture and the solution was cooled at –20 ˚C overnight. The obtained product was filtered and washed well with ether to yield a red-brown product of 1,19-dimethylbiladiene-*a,c* dihydrobromide, 8,12-bis(2′-methoxycarbonylethyl)-1,2,3,7,13,17,18,19-octamethylbiladience-*a,c* dihydrobromide **3** (1.4 g, 83%). ^{1}H NMR (400 MHz, $CDCl_3$): δ 13.31 (br, 2H), 13.25 (br, 2H), 7.11 (s, 2H), 5.22 (s, 2H), 3.45 (s, 6H), 2.83 (t, J = 8 Hz, 4H), 2.70 (s, 6H), 2.28 (s, 6H), 2.25 (s, 6H), 2.03 (t, J = 8 Hz, 4H), 2.01 (s, 6H); HRMS (ESI, positive mode, m/z): $[M–HBr_2]^+$ calcd for $C_{35}H_{45}N_4O_4$, 585.3435; found, 585.3431.

The 1,19-dimethylbiladiene-*a*,*c* compound **3** (0.50 g, 0.67 mmol) and Co(OAc)•$4H_2O$ (1.7 g, 6.7 mmol) were dissolved in methanol (500 ml) and the solution was stirred for 1 h at room temperature. After removal of the solvent, methanol (15 mL) and water (3 mL) were added to the residue. The mixture was filtered, and 2 mL of aqueous solution of $NaClO_4$•H_2O (0.86 g, 6.1 mmol) was added to the filtrate. After 12 h, the precipitates were collected by filtration and recrystallized from methanol/dichloromethane/hexane. The product of cobalt corrin derivative, 8,12-bis(2′-methoxycarbonylethyl)-1,2,3,7,13,17,18,19-octamethyltetradehydrocorrin cobalt(II) perchlorate **4**, was obtained as a dark red solid (0.34 g, 68%). HRMS (ESI, positive mode, m/z):

$[M–ClO_4]^+$ calcd for $C_{35}H_{41}N_4O_4Co$, 640.2454; found, 640.2460; UV/Vis: ε_{max} (CH_2Cl_2, nm (abs.)) 274.5 (1.1), 351 (0.92), 489 (0.74), 543.5 (0.37); UV/Vis: ε_{max} (pyridine, nm (abs.)) 506 (0.25), 585 (0.085).

The dimethyl ester of the tetradehydrocorrin cobalt complex **4** (0.10 g, 0.14 mmol), $Ca(OH)_2$ (50 mg, 0.68 mmol) and LiCl (0.40 g, 9.5 mmol) were dissolved in THF (50 mL) and water (50 mL) and then stirred at room temperature for 12 h under an N_2 atmosphere. To the solution, citric acid (1.4 g, 7.3 mmol) was added and the solution was extracted with CH_2Cl_2 (200 mL × 2). The organic phase was dried over anhydrous Na_2SO_4 and the solvent was evaporated under reduced pressure. The residue was dissolved in a minimum amount of CH_2Cl_2 and reprecipitated with hexane to yield tetradehydrocorrin cobalt complex, Co^{II}(TDHC), as a black solid (52.6 mg, 60%). HRMS (ESI, positive mode, *m*/*z*): $[M–Cl]^+$ calcd for $C_{33}H_{37}N_4O_4Co$, 612.214132; found, 612.214126; UV/Vis: ε_{max} (CH_3OH, nm (abs.)) 279.5 (1.2), 495 (0.54), 571 (0.31).

Protein crystallization

Crystallization of rMb(Co^{II}(TDHC)) was performed at 25 ºC using a hanging-drop vapor-diffusion method. The drops were prepared by mixing of 5 μL of 10 mg/mL protein in 0.1 M Tris-HCl (pH 7.4) buffer with 5 μL of a reservoir solution containing 3.4 M ammonium sulfate and 0.1 M Tris-HCl (pH 7.4). Rosette-shaped crystals grew within a week and leaflets were separated for data collection. The crystal was soaked in a cryoprotectant solution (6–12% glycerol in a reservoir solution), fished with a standard nylon loop, and flash-cooled in an N_2 gas stream at 100 K.

Crystallization of rMb(Co^{II}(TDHC)) is described bellow. The rMb(Co^{II}(TDHC)) was also crystallized by the method described above with a reservoir solution containing 3.4 M ammonium sulfate, 0.1 M Tris-HCl (pH 7.4) and 10% trehalose. The obtained crystal was soaked in the reservoir solution with 5 mg/mL sodium dithionite. A color change from dark red to pink was observed within 1 min and the crystal was then fished and flash-cooled in a stream of N_2 gas stream.

Crystal structure determination and refinement

X-ray diffraction data were collected using the synchrotron radiation sources of the beamlines at SPring-8 (Harima, Japan) or at Photon Factory (Tsukuba, Japan). Diffraction data were processed with the program *HKL2000*. The structures were determined by the molecular replacement method using the program *MOLREP* from the *CCP4* program suite. A crystal structure of horse heart myoglobin (Protein Data Bank (PDB) ID: 2V1F) was used as the search model. Refinement was carried out using the program *REFMAC*. The structures were visualized and modified using the program *COOT*. Since electron density indicated that two enantiomers of 1*R,*19*R*- and 1*S,*19*S*-TDHC are present in the heme pocket, the author assigned an approximate 1*R,*19*R*-TDHC : 1*S,*19*S*-TDHC occupancy ratio of 0.65:0.35. Data collection and refinement statistics are summarized in Table 1-1. The final atomic coordinates and

structure factor amplitudes were deposited in the Protein Data Bank (PDB). These have been assigned the following ID numbers: 3WFT for rMb(Co^{II}(TDHC)) and 3WFU for rMb(Co^{I}(TDHC)). Data collection and refinement statistics are summarized in Table 1-1.

Table 1-1. Data collection and refinement statistics for reconstituted horse heart myoglobins

	rMb(Co^{II}(TDHC))	rMb(Co^{I}(TDHC))
PDB ID	3WFT	3WFU
Data collection		
X-ray source	Photon Factory BL-17A	SPring-8 BL44XU
Detector	ADSC Quantum 315r	Rayonix MX225HE
Wavelength (Å)	1.00000	0.90000
Resolution (Å) (outer shell)	50 – 1.30 (1.35 – 1.30)	50 – 1.35 (1.40 – 1.35)
Space group	$P2_1$	$P2_1$
Unit cell parameters (Å, deg.)	a = 34.98, b = 28.99, c = 63.21, β = 106.14	a = 34.84, b = 28.72, c = 63.35, β = 105.60
No. of total / unique reflections	78,300 / 28,032	69,170 / 25,415
Completeness (%)	92.8 (90.1)	95.2 (92.2)
R_{sym}†	4.1 (22.2)	3.7 (22.1)
$I/\sigma(I)$	26.9 (4.3)	28.9 (4.0)
Refinement		
Resolution (Å)	15 – 1.30	15 – 1.35
No. of reflections	26,544	24,026
R_{cryst} / R_{free} (%)	12.6 / 18.3	14.3 / 19.7
Mean B-factor (Å^2)	13.6	17.3
No. of non-H atoms	1,490	1,427
Rmsd from ideal		
Bond lengths (Å) / angles (deg.)	0.026 / 3.065	0.026 / 3.000
PDB ID	3WFT	3WFU

† $R_{sym} = \Sigma_{hkl}\Sigma_i |I_i(hkl) - \langle I(hkl)\rangle| / \Sigma_{hkl}\Sigma_i I_i(hkl)$, where $I_i(hkl)$ is the value of the ith measurement of the intensity of a reflection, $\langle I(hkl)\rangle$ is the mean value of the intensity of that reflection and the summation is over all measurements.

References and notes

(1) B. Kräutler, *in Metal Ions in Life Science*, ed. A. Sigel, H. Sigel, R. K. O. Sigel, RSC, Cambridge, 2009, ch. 1, vol. 6, pp. 1–51.

(2) R. G. Matthews, *in Metal Ions in Life Science*, ed. A. Sigel, H. Sigel, R. K. O. Sigel, RSC, Cambridge, 2009, ch. 2, vol. 6, pp. 53–113.

(3) B. Kräutler, B. Puffer, *in Handbook of Porphyrin Science*, ed. K. M. Kadish, K. M. Smith, R. Guilard, World Scientific, Singapore, 2012, ch. 117, vol. 25, pp. 131–263.

(4) (a) K. L. Brown, *Chem. Rev.* **2005**, *105*, 2075. (b) R. Banerjee, C. Gherasim, D. Padovani, *Curr. Opin. Chem. Biol.* **2009**, *13*, 484. (c) K. Gruber, B. Puffer, B. Kräutler, *Chem. Soc. Rev.* **2001**, *40*, 4346. (d) R. G. Matthews, *Acc. Chem. Res.* **2001**, *34*, 681. (e) Y. Kung, N. Ando, T. I. Doukov, L. C. Blasiak, G. Bender, J. Seravalli, S. W. Ragsdale, C. L. Drennan, *Nature* **2012**, *484*, 265. (f) C. H. Hagemeier, M. Kruër, R. K. Thauer, E. Warkentin, U. Ermler, *Proc. Natl. Acad. Sci. U. S. A.* **2006**, *103*, 18917.

(5) C. L. Drennan, S. Huang, J. T. Drummond, R. G. Matthews, M. L. Ludwig, *Science* **1994**, *266*, 1669.

(6) C.-J. Liu, A. Thompson, D. Dolphin, *J. Inorg. Biochem.* **2001**, *83*, 133.

(7) D. Dolphin, R. L. N. Harris, J. L. Huppatz, A. W. Johnson, I. T. Kay, *J. Chem. Soc. C* **1966**, 30.

(8) T. Hayashi, *in Handbook of Porphyrin Science*, ed. K. M. Kadish, K. M. Smith, R. Guilard, World Scientific, Singapore, 2010, ch. 23, vol. 5, pp. 1–69.

(9) Y. Murakami, Y. Aoyama, *Bull. Chem. Soc. Jpn.* **1976**, *43*, 683.

(10) (a) S. A. Cockle, H. A. O. Hill, J.M. Pratt and R. J. P.Williams, *Biochim. Biophys. Acta* **1969**, *177*, 686. (b) Y. Murakami, Y. Hisaeda, A. Kajihara, *Bull. Chem. Soc. Jpn.* **1983**, *56*, 3642.

(11) N. S. Hush, I. S. Woolsey, *J. Chem. Soc., Dalton Trans.* **1974**, 24.

(12) H.-P. Hersleth, T. Uchida, A. K. Rohr, T. Teschner, V. Schünemann, T. Kitagawa, A. X. Trautwein, C. H. Görbitz, K. K. Andersson, *J. Biol. Chem.* **2007**, *282*, 23372.

(13) R. V. Banerjee, S. R. Harder, S. W. Ragsdale, R. G. Matthews, *Biochemistry* **1990**, *29*, 1129.

(14) (a) P. Picotti, A. Marabotti, A. Negro, V. Musi, B. Spolaore, M. Zambonin, A. Fontana, *Protein Sci.* **2004**, *13*, 1572. (b) C. Nishimura, H. J. Dyson and P. E. Wright, *J. Mol. Biol.* **2011**, *411*, 248.

(15) (a) P. Engel, G. Rytz, L. Walder, U. Vögeli and R. Scheffold, in Vitamin B12, ed. B. Zagalak, W. Friedrich, Walter de Gruyter & Co., Berlin, 1979, pp. 171–172. (b) P. Doppelt, J. Fischer, R. Weiss, *Inorg. Chem.* **1984**, *23*, 2958.

(16) T. Matsuo, A. Hayashi, M. Abe, T. Matsuda, Y. Hisaeda, T. Hayashi, *J. Am. Chem. Soc.* **2009**, *131*, 15124.

(17) K. L. Swanson, K. M. Snow, D. Jeyakumar, K. M. Smith, *Tetrahedron* **1991**, *47*, 685.

Chapter 2
Formation of a Co–C bond and subsequent transmethylation in myoglobin reconstituted with the cobalt corrinoid

2-1. Introduction

Cobalamin-dependent methionine synthase mediates an essential methylation of homocysteine to form methionine.[1−11] In the catalytic cycle, the enzyme promotes two kinds of methyl group transfers: (i) methylation of cob(I)alamin by *N*5-methyl tetrahydrofolate as a methyl group donor, and (ii) methionine synthesis from homocysteine with the methylcobalamin intermediate. Compared to the non-catalyzed reactions, both reactions are ca. 10^5-fold accelerated by the catalytic activity of the enzyme.[12,13] Elucidation of the mechanisms of these enzymatic reactions is challenging because of the complicated enzyme structures and the dynamic conformational changes occurring during activation of the cofactor and substrates.[2,8,14−24] In this context, cobalt complexes have been investigated as enzyme models with the objective of understanding how the organometallic Co–C bond is formed and homolytically cleaved in several cobalamin-dependent enzymes.[25−38] However, the examples of model reactions of heterolytic Co–C bond cleavage, which is seen in methionine synthase, are quite limited[30,31] because alkylated cobalt(III) complexes including methylcobalamin are generally less reactive with nucleophiles.[25−29,32]

Cobalt tetra- and di-dehydrocorrins have been synthesized as representative cobalamin models with tetrapyrrole macrocyclic ligands.[36−38] It is known that the former has a relatively positive Co(II)/(I)-redox potential and the Co(I) species does not have sufficient nucleophilicity to promote attack by alkyl halides in organic solvents.[36,37] The latter is found to have a relatively negative Co(II)/(I)-redox potential, and successive reactions of the obtained R–Co species with a nucleophile have not been reported.[38] In contrast to these models, it is known that the transmethylation from methylated cobalt phthalocyanine to nucleophiles occurs. This is rationalized by the expectation that Co(I) species would be a good leaving group.[32−35] However, there are few appropriate enzyme models for investigation of the role of the protein matrix, which is expected to stabilize the reaction intermediates and initiate the S_N2-like transmethylation.[1−9,25−38]

The author has developed myoglobin reconstituted with cobalt tetradehydrocorrin Co(TDHC) as a His-on methionine synthase model (Figure 2-1), which was prepared and a tetra-coordinated Co(I) species was detected in the protein matrix.[39] Here, in an effort to replicate the reaction mechanism of methionine synthase, the author demonstrates the spontaneous key reactions promoted by the enzyme and by the reconstituted protein, rMb(Co(TDHC)): (i) the formation of the methylated Co(III) species from the supernucleophilic Co(I) species and (ii) subsequent intraprotein transmethylation in the myoglobin heme pocket (Scheme 2-1).[39]

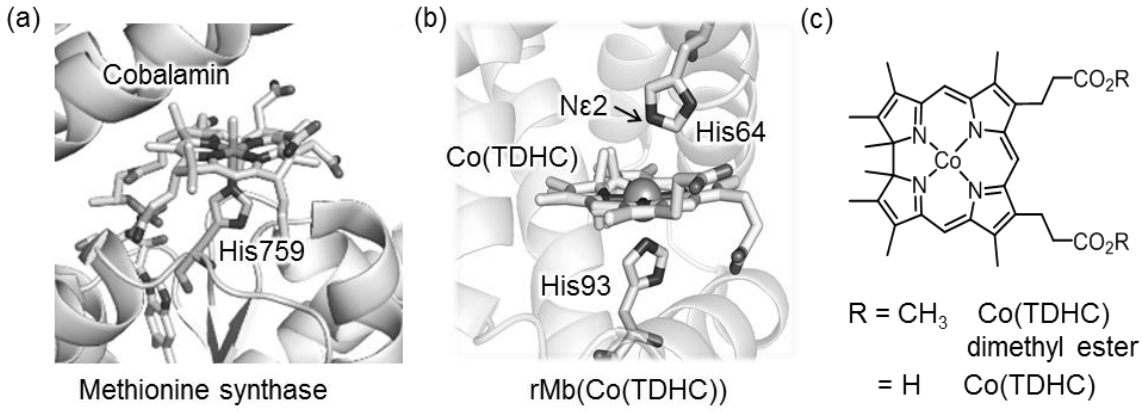

Figure 2-1. Crystal structure of (a) cobalamin-binding domain of methionine synthase (PDB ID: 1BMT) and (b) rMb(Co^{II}(TDHC)) (PDB ID: 3WFT). (c) Chemical structures of Co(TDHC) dimethyl ester and Co(TDHC).

Scheme 2-1. Model reactions of the transmethylations by methionine synthase in the myoglobin matrix

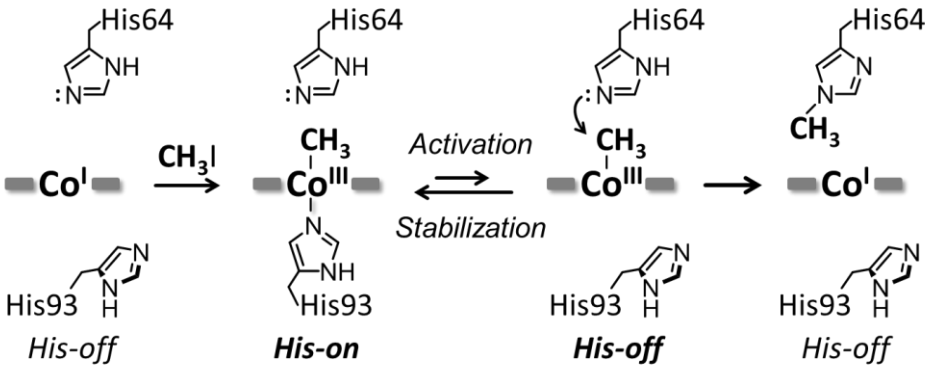

2-2. Results and discussion

The reaction of Co(I) species with methyl iodide in the reconstituted protein

Addition of methyl iodide to a solution of rMb(Co^{I}(TDHC)) leads to a new absorption maxima at 425 nm and 445 nm with disappearance of the 530-nm absorption within 2 h (Figure 2-2a) despite the continued absence of EPR signals (Figure 2-2b). The resulting species is photoactive and gradually converts to the Co(II) species upon irradiation with a Xe-lamp under aerobic conditions. The process is found to be accelerated upon the addition of 4-hydroxy-TEMPO (4-hydroxy-2,2,6,6-tetramethylpiperidine-1-oxyl, free radical) as a radical quencher (Figure 2-3). These findings generally support the fact that the Co(I) species reacts with methyl iodide to form the Co–C bond under anaerobic conditions.[38,40–42] In this

reaction, a nucleophilic pathway is more plausible than a radical pathway which requires an electron transfer from the Co(I) species to methyl iodide, because rMb(Co(TDHC)) has the relevantly positive Co(I)/Co(II)-redox potential (E = −0.13 V vs. NHE).[39,43,44]

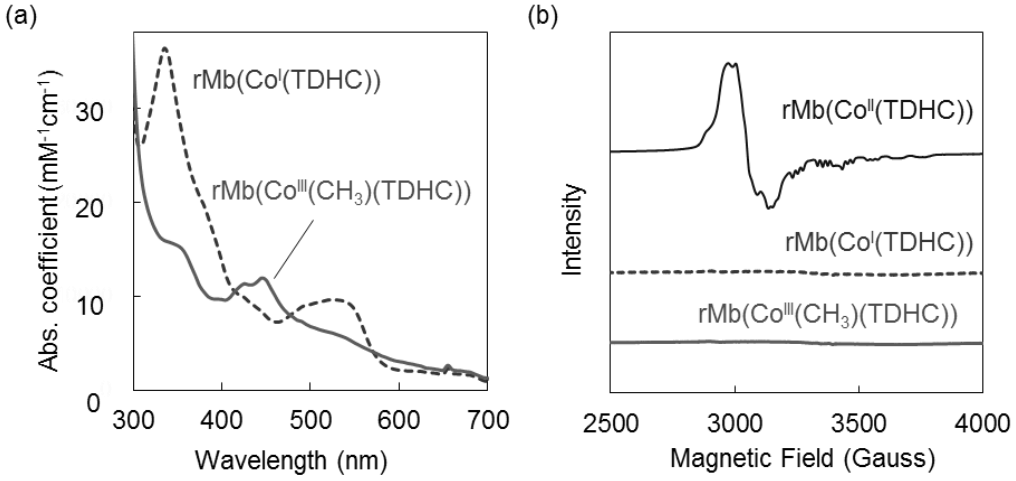

Figure 2-2. (a) UV-vis spectra of rMb(Co^{I}(TDHC)) and rMb(Co^{III}(CH$_3$)(TDHC)) in 0.1 M potassium phosphate buffer (pH 7.0) at 25 °C. (b) EPR spectra of rMb(Co^{II}(TDHC)), rMb(Co^{I}(TDHC)) and rMb(Co^{III}(CH$_3$)(TDHC)) in 0.1 M potassium phosphate buffer (pH 7.0) at 10 K.

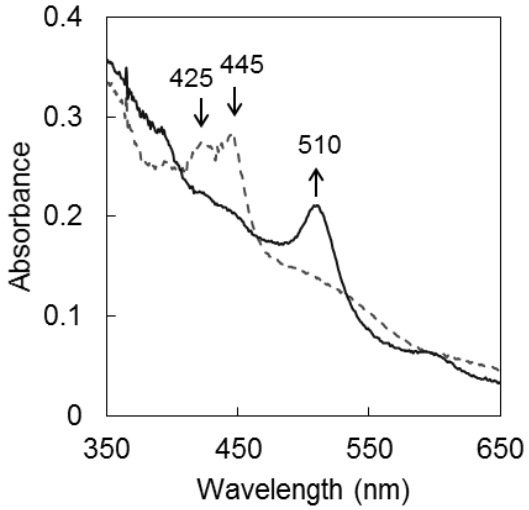

Figure 2-3. The spectral changes of rMb(Co^{III}(CH$_3$)(TDHC)) species induced by photo-irradiation over 90 sec in the aqueous solution containing 4-hydroxy-TEMPO as a radical quencher. Solid line and dashed line represents the initial and final stages of the photoreaction, respectively. The aqueous solution was irradiated by a 500 W xenon arc lamp filtered with cut-off filters. The illuminance of the irradiated light from 420 nm to 800 nm monitored by a luminometer was 1.8 × 10^5 lux. Conditions: [protein] = 0.024 mM and [4-hydroxy-TEMPO] = 0.038 mM in 0.1 M potassium phosphate buffer (pH 7.0) at 25 °C under N_2 atmosphere.

The CD spectrum of the new species also suggests formation of the Co–C bond in the protein. In the visible region, the positive Cotton effect is observed (Figure 2-4). This effect is also observed in native myoglobin and reconstituted myoglobins.[45,46] Moreover, the CD spectrum in the far-UV region is completely consistent with the spectrum of rMb(Co^{I}(TDHC)) (Figure 2-5). This rules out dissociation of the methylated cofactor from the heme pocket.

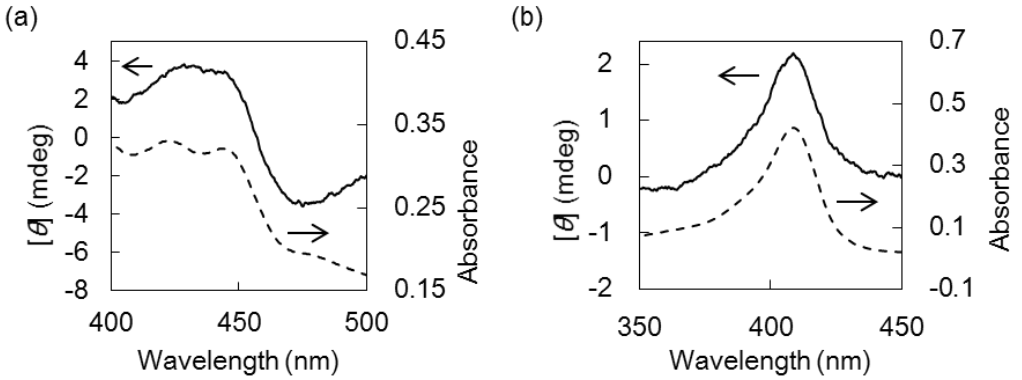

Figure 2-4. Circular dichroism (CD) and UV-vis spectra of (a) rMb($Co^{III}(CH_3)$(TDHC)) and (b) native myoglobin in the visible region. Solid and dashed lines represent CD and UV-vis spectra, respectively. Conditions: (a) [rMb($Co^{III}(CH_3)$(TDHC))] = 0.023 mM in 0.1 M potassium phosphate buffer (pH 7.0) at 25 ºC under N_2 atmosphere, (b) [native myoglobin] = 0.0020 mM in the same buffer at 25 °C.

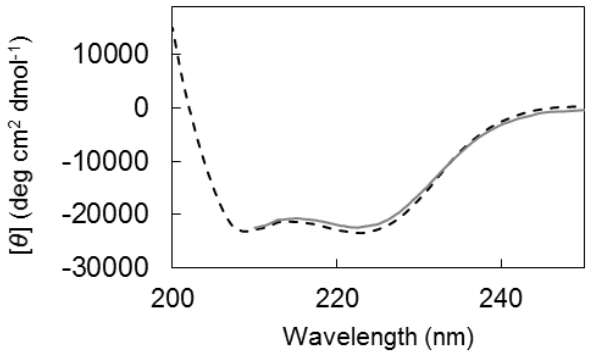

Figure 2-5. CD spectra of rMb(Co^{I}(TDHC)) (dashed line) and rMb($Co^{III}(CH_3)$(TDHC)) (solid line). Conditions: [protein] = 0.018 mM in 0.1 M potassium phosphate buffer (pH 7.0) at 25 °C under N_2 atmosphere. In the case of rMb($Co^{III}(CH_3)$(TDHC)), the region of the spectrum below 210 nm is omitted due to the strong absorption of excess methyl iodide in this region.

The ESI-TOF mass spectrum of the species in the negative ion mode confirms the generation of the methylated cobalt corrinoid complex in the protein, rMb($Co^{III}(CH_3)$(TDHC)) (Figure 2-6).[47] Figure 2-6b indicates the characteristic peak at m/z = 2510.10, which is consistent with the mass number of the 7–

charge state for rMb($Co^{III}(CH_3)$(TDHC)) (calculated m/z = 2510.02). These findings indicate that the nucleophilic Co(I) species reacts with methyl iodide to yield the $Co^{III}(CH_3)$(TDHC) complex in the heme pocket of myoglobin.

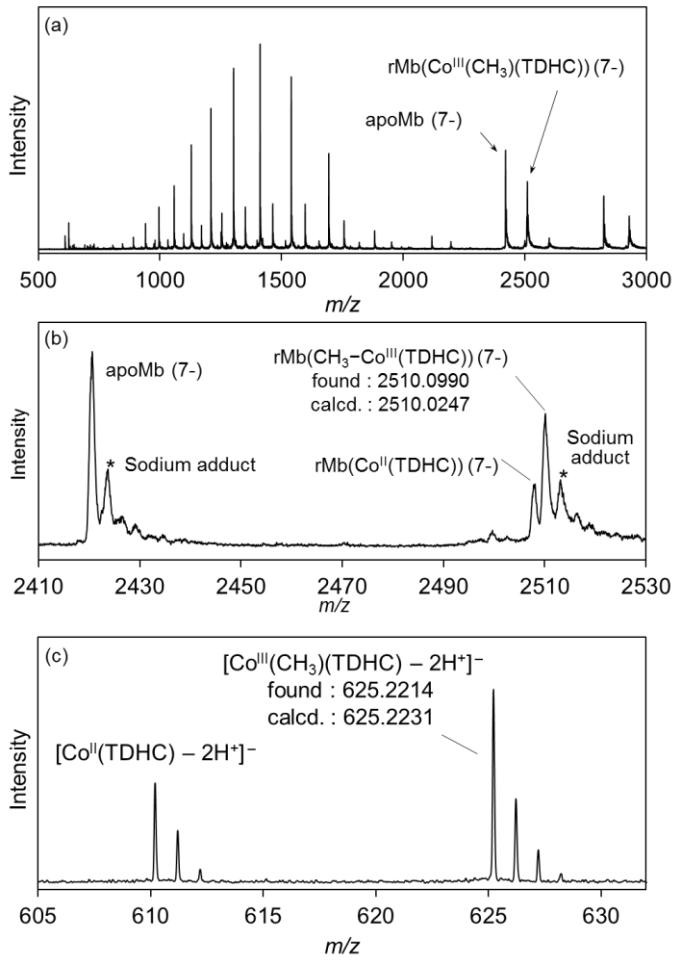

Figure 2-6. ESI mass spectrum (negative mode) of rMb($Co^{III}(CH_3)$(TDHC)), prepared upon addition of methyl iodide to rMb(Co^{I}(TDHC)) at 4 °C in 0.1 M ammonium acetate buffer (pH 6.7). (a) the raw spectrum, and (b) and (c) the expanded spectrum. The voltage difference between the gas capillary exit and the 1st skimmer is 20 V. The desolvation temperature is 180 ˚C. The asterisks identify sodium adducts of the apoprotein and rMb($Co^{III}(CH_3)$(TDHC)).

In contrast to rMb(Co^{I}(TDHC)), no spectral change of Co^{I}(TDHC) dimethyl ester (Figure 2-1c) was observed in CH_2Cl_2 upon the addition of methyl iodide, regardless of the presence of imidazole (1 mM, 40 eq.) as an axial ligand (Figure 2-7). The time-course plots of spectral changes at 525 nm clearly indicate that the Co(I) complex in the protein[39] is more reactive with methyl iodide than the Co(I) complex in CH_2Cl_2.

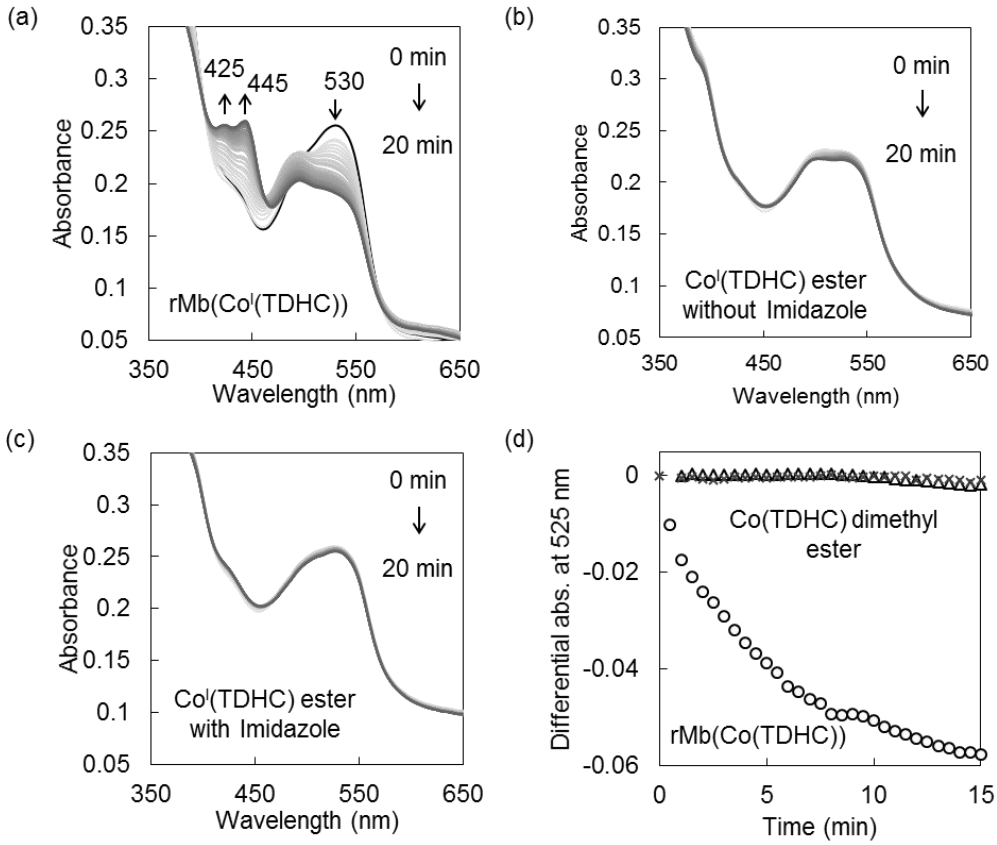

Figure 2-7. UV-vis spectral changes of the Co(I) species after addition of methyl iodide until 20 min at 25 °C. (a) rMb(Co^{I}(TDHC)) in 0.1 M potassium phosphate buffer solution (pH 7); (b) Co^{I}(TDHC) dimethyl ester in CH_2Cl_2; (c) Co^{I}(TDHC) dimethyl ester in CH_2Cl_2 containing imidazole. Conditions: [Co(I) species] = 25 μM, [CH_3I] = 16 mM, [Imidazole] = 1 mM. (d) Time courses of the spectral changes of rMb(Co^{I}(TDHC)) at 525 nm (circle, ○), Co^{I}(TDHC) ester in CH_2Cl_2 (rhombus, ×) and the Co(I) complex in CH_2Cl_2 containing imidazole (triangle, △) at 25 °C. Conditions: [Co(I) species] = 25 μM, [CH_3I] = 16 mM, [imidazole] = 1 mM.

Bond-dissociation energy of methylated complexes

As discussed above, the protein environment is essential for the formation of the methylated Co(III) complex, which indicates that the Co−C bond is stabilized in the heme pocket. To explain the stabilization of methylated Co(III) complexes by axial coordination of imidazole,[48] the author computed the heterolytic bond-dissociation energy (BDE)[49,50] with density functional theory (DFT) calculations (Table 2-1 and Figure 2-8). As listed in Table 2-1, the BDE of the methylated Co(III) complexes can be increased by the coordination of imidazole. The BDEs of the Co–N(Im) bonds for the methylated Co(TDHC') and Co(corrin) complexes[49] were computed to be 14.2 and 15.9 kcal/mol, respectively, which indicates that the cobalt complexes are significantly stabilized by the coordination of imidazole.[51] In

contrast, the homolytic BDE of $Co^{III}(CH_3)$(TDHC') is higher than that of $Co^{III}(CH_3)$(Im)(TDHC') because the homolytic cleavage of the Co–C bond does not bring about the Co–N bond dissociation and stabilization of the Co(II) species induced by the axial ligation is greater than that of the CH_3−Co(III) species (Table 2-2). Thus, it appears that the stability of the methylated Co(III) species is derived from His93 ligation in the myoglobin matrix.[52]

Table 2-1. DFT-computed heterolytic bond-dissociation energy (BDE) and stabilization energy provided by imidazole ligation in the gas phase (kcal/mol)

cobalt	BDE of the Co–C bond (kcal/mol)		Stabilization by Im-coordination[c] (kcal/mol)
complex	$Co^{III}(CH_3)(Im)(L_{eq})$[a]	$Co^{III}(CH_3)(L_{eq})$[b]	$Co^{III}(CH_3)(Im)(L_{eq})$
Co(TDHC')	151.0	136.8	14.2
Co(corrin)	169.6	153.7	15.9

[a]The value of the heterolytic BDE for the imidazole-coordinated Co−CH_3 complex consists of the dissociation of the Co−CH_3 and Co−N(Im) bonds which provides the three fragments: methyl cation, imidazole and a corresponding tetra-coordinated Co(I) complex. [b]The value of the heterolytic BDE for the Co−CH_3 bond. [c]The stabilization energy is evaluated by the BDE value of the Co−N(Im) bond in the methylated Co(III) complex with the imidazole ligation.

Table 2-2. DFT-computed homolytic bond-dissociation energy (BDE) of the Co–C bond and stabilization energy induced by coordination of imidazole in the gas phase[a]

cobalt	BDE of the Co–C bond (kcal/mol)		Stabilization by Im-coordination[d] (kcal/mol)	
complex	$Co^{III}(CH_3)(Im)(L_{eq})$[b]	$Co^{III}(CH_3)(L_{eq})$[c]	$Co^{III}(CH_3)(Im)(L_{eq})$	$Co^{II}(Im)(L_{eq})$
Co(TDHC')	32.5	41.8	14.3	23.6
Co(corrin)	36.4	42.3	15.9	21.8

[a]L_{eq} is equatorial corrinoid ligand. [b]The methylated complex is split into two fragments, a methyl radical and a corresponding penta-coordinated Co(II) complex with imidazole as an axial ligand. [c]The BDE of the Co−CH_3 bond of the methylated complex (penta-coordination) was determined. [d]The stabilization energy was evaluated by the BDE value of the Co−N(Im) bond in the each imidazole-coordinated complex. The energy diagram for the homolytic dissociation is illustrated below.

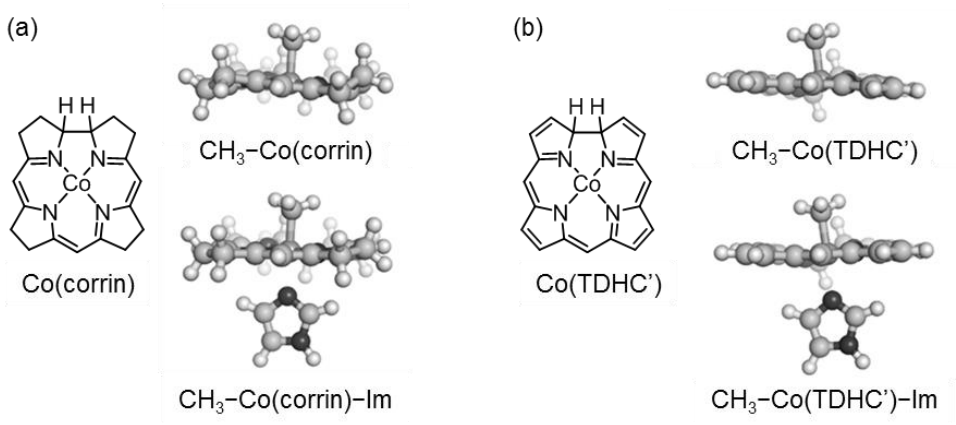

Figure 2-8. Structure of (a) Co(corrin) and (b) Co(TDHC') optimized by DFT calculations.

Intraprotein transmethylation from the $Co^{III}(CH_3)$(TDHC) complex

The author found that the deconvoluted peak intensity of the apoprotein at 16950.5, detected by ESI-TOF MS, gradually decreases after addition of methyl iodide to the protein solution of rMb(Co^{I}(TDHC)), and then a new peak at 16964.2 appears. Surprisingly, the in-source decay mode of MALDI-TOF MS shows an increase of the sole His64 mass number by +14 over 24 h (Figure 2-9). The fragment including the His64 residue, HGTVVLTALGGILK, was obtained by trypsin digestion and characterized by ESI-TOF MS and NMR spectroscopy (see Figure 2-10). In the ^{1}H and ^{13}C NMR spectra, the characteristic peaks at 4.05 ppm and 36.31 ppm are respectively assigned to the hydrogen and carbon of the methyl group that was transferred to the His64 residue. These values are completely consistent with those of the authentic sample, Nε2-methylated histidine as shown in Figure 2-10.[53] The NMR study provides a strong indication that the methylation reaction selectively occurs at the Nε2-position of the His64 imidazole ring. In a control experiment, it was found that addition of a large amount of methyl iodide (ca. 640 equiv.) to native myoglobin and to myoglobin reconstituted with cobalt protoporphyrin IX leads to non-selectively monomethylated protein on the surface in both cases with 50% conversion over 24 h and failure to produce the methylated His64 residue. These results indicate that the Nε2 atom of the His64 imidazole nucleophilically attacks the activated methyl group bound to the cobalt atom prior to residue- and regio-selective transfer of the methyl group within the heme pocket of myoglobin.

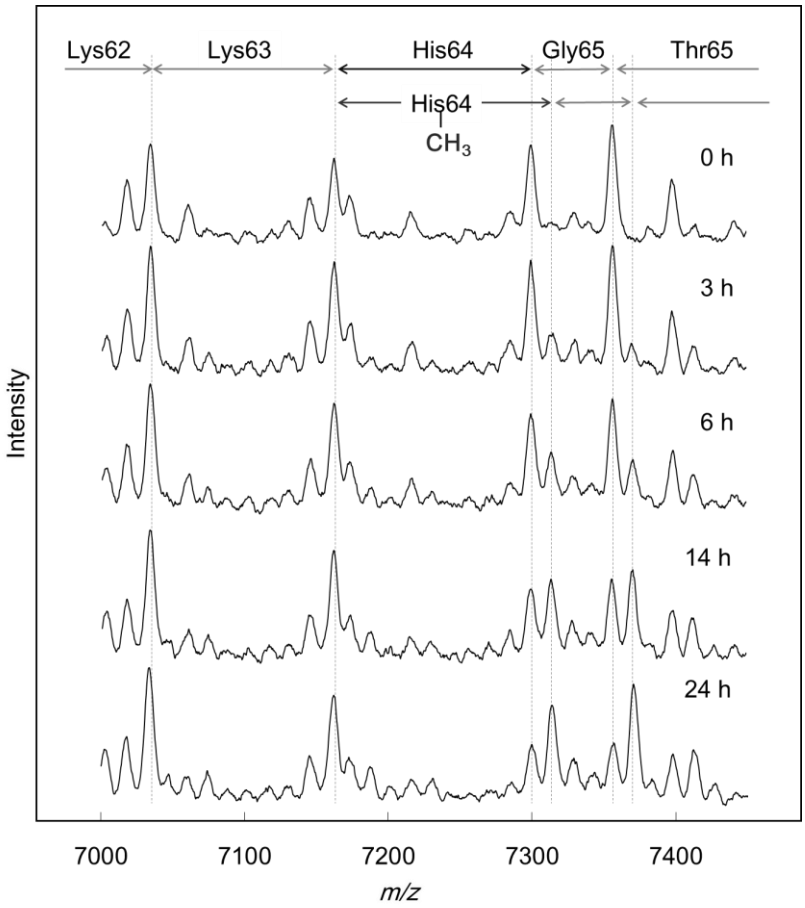

Figure 2-9. MALDI-TOF MS (in-source decay mode) spectra of rMb($Co^{III}(CH_3)$(TDHC)) treated with methyl iodide after the reaction for 0, 3, 6, 14 and 24 h.

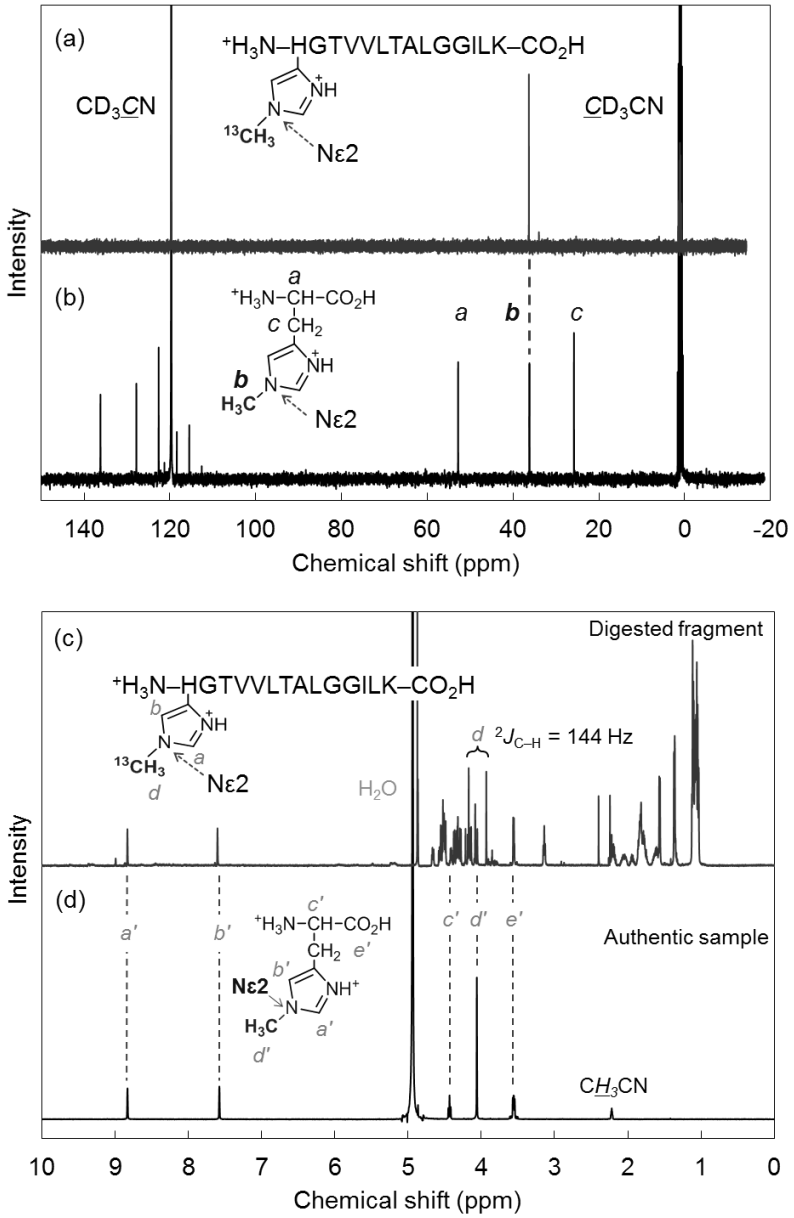

Figure 2-10. (a) ^{13}C NMR (150 MHz, D_2O/CD_3CN (9:1)) spectrum of the H($^{13}CH_3$)GTVVLTALGGILK fragment after trypsin digestion of rMb($Co^{III}(CH_3)$(TDHC)). The fragment was protonated because the eluent (H_2O/CH_3CN) containing 0.1% TFA was used for the HPLC purification. The chemical shift of the ^{13}C-enriched methyl group was determined to be 36.31 ppm. (b) ^{13}C NMR (100 MHz, D_2O/CD_3CN (9:1) containing 1% TFA) spectrum of Nε2-methylated histidine as an authentic sample.[53] (The chemical shift of the methyl group bounded to the Nε2 position was determined to be 36.20 ppm.) Each ^{13}C signal was assigned using the HMQC technique. (c) ^{1}H NMR (600 MHz, D_2O/CD_3CN (9:1)) spectrum of the peptide of H($^{13}CH_3$)GTVVLTALGGILK and (d) ^{1}H NMR (400 MHz, D_2O/CD_3CN (9:1) containing 1% TFA) spectrum of Nε2-methylated histidine as an authentic sample.

Kinetic study of the intraprotein transmethylation

The first-order rate constant of the transmethylation is determined to be 0.062 h^{-1} for rMb(Co(TDHC)) by conversion of the digested fragments evaluated by HPLC, while the transmethylation does not occur in native myoglobin under the same conditions (Figure 2-11). In contrast, methylcobalamin does not provide any spectral changes owing to the transmethylation in 0.1 M phosphate buffer (pH 7.0) in the presence of histidine over 12 h. These findings may be explained by the proximity effect and the low heterolytic BDE of $Co^{III}(CH_3)$(TDHC')(Im) (151.0 kcal/mol) in contrast to the cobalamin model (169.6 kcal/mol) (Table 2-1).

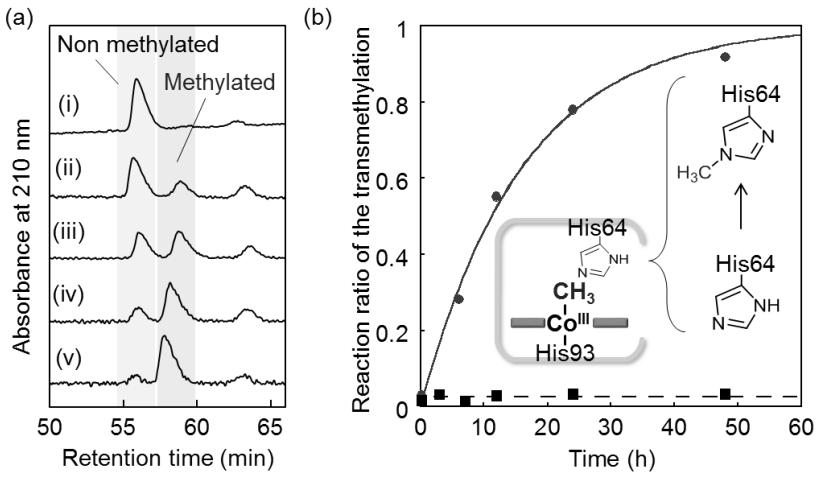

Figure 2-11. (a) HPLC traces for the digested peptide fragment (HGTVVLTALGGILK) of rMb(Co(TDHC)) after reaction with methyl iodide in 0.1 M potassium phosphate buffer (pH 7.0) at 25 °C for 0, 6, 12, 24, 48 h (i−v). (b) Time courses of the conversion of His64 to methylated His64. Gray circle (●) and black tetragon (■) plots represent the data for rMb(Co(TDHC)) and native myoglobin, respectively. Conditions: [protein] = 25 μM, [sodium dithionite] = 0.6 mM, [CH_3I] = 16 mM.

Theoretical calculation of the transmethylation in myoglobin

To investigate the mechanism of transmethylation in the protein matrix, nucleophilic stepwise and concerted pathways were considered in DFT computations as shown in Figure 2-12.[23,54] A base-off methylated Co(III) complex is produced in the stepwise mechanism. In the calculations, the author used a simplified active site model, in which the two carbon atoms corresponding to the α-carbons of the His64 and His93 residues and the two β-carbons of TDHC pyrroles conjugating each of the propionate side chains are fixed at the position of the crystal structure of rMb(Co^{II}(TDHC)) (Figure 2-13a).[49,55] As shown in Figure 2-13b and Figure 2-14, the axial imidazole is readily displaced from the methylated Co(III) complex with an activation barrier of 4.9 kcal/mol to produce a penta-coordinated

$Co^{III}(CH_3)$(TDHC') intermediate (RC→TS1→Int). As discussed above, the Co–C bond is weakened in Int, and therefore, the activation barrier of 13.6 kcal/mol in the stepwise pathway is lower than that of the concerted pathway (20.2 kcal/mol). These theoretical results demonstrate that the stepwise pathway via the base-off methylated Co(III) complex activated by His93 flipping in rMb(Co(TDHC)) is more plausible than the concerted reaction. The author found that the barriers for the methyl transfer are reduced and the final product is significantly stabilized by the dielectric effect of the protein environment. This is because the cobalt complexes are highly polarized in the course of the methyl transfer. In the crystal structure, the Nδ1 atom of the His64 is hydrogen-bonded to a water molecule,[39] and therefore, the barriers can be further reduced by the partial or full deprotonation of the methylated histidine.[23]

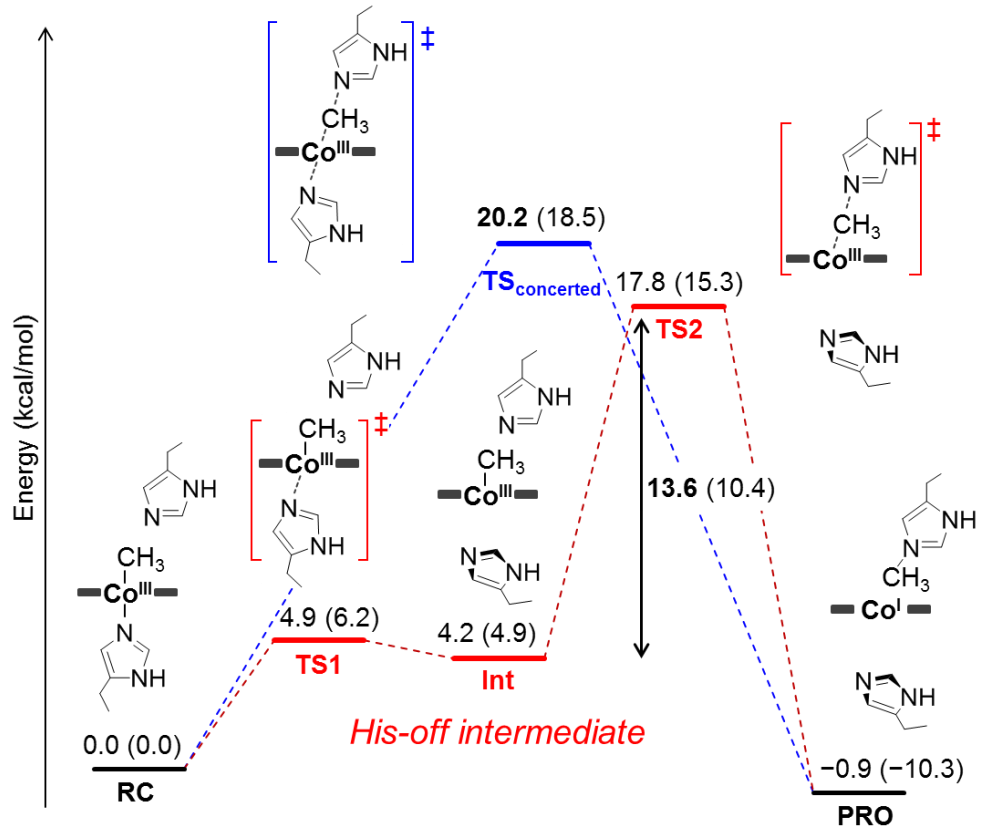

Figure 2-12. Energy diagrams for the stepwise reaction (red line) and the concerted reaction (blue line) for the transmethylation by Co(TDHC'). Energy values in the gas phase relative to $Co^{III}(CH_3)$(TDHC')(Im) are indicated. The relative energies in parentheses include the effect of a dielectric constant of 4.0.

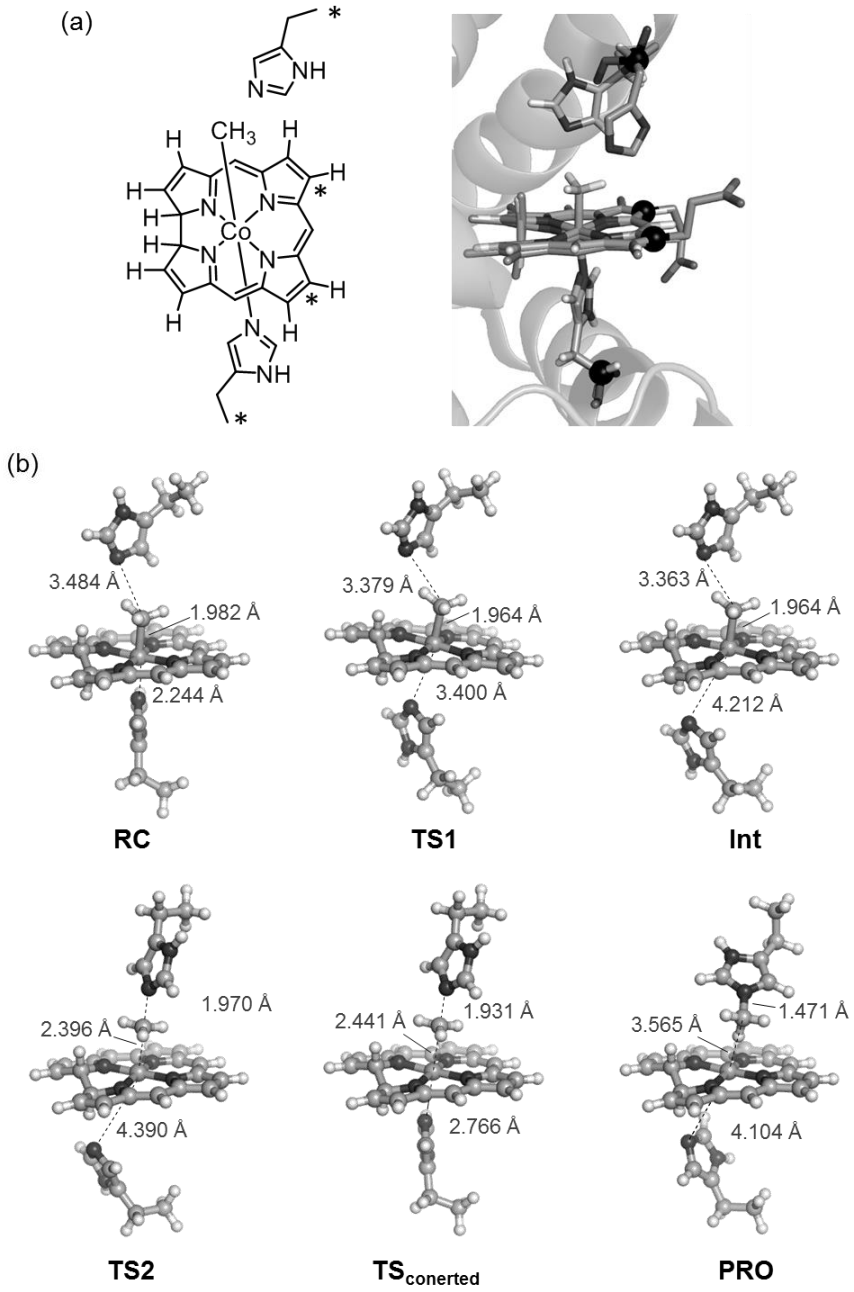

Figure 2-13. Optimized structures of key species in each transmethylation pathway: reaction complex (RC), transition state (TS1, TS2, $TS_{concerted}$), intermediate (Int) and product (PRO) in Figure 2-12. The stepwise and concerted pathways consist of RC → TS1 → Int → TS2 → PRO and RC → $TS_{concerted}$ → PRO, respectively.

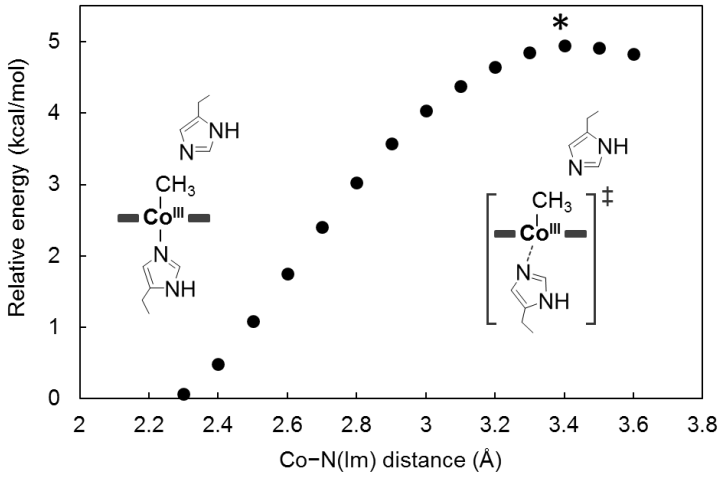

Figure 2-14. Energy barrier for the deligation of imidazole from the $Co^{III}(CH_3)$(TDHC') estimated by the DFT calculations. The maximum point marked with asterisk is identified as a transition state in the stepwise pathway.

2-3. Summary

The author demonstrated the reactivity of the methionine synthase model conjugated between cobalt tetradehydrocorrin and apomyoglobin. The heme pocket of myoglobin is found to enhance the nucleophilicity of the Co(I) species and provide a methylated Co(III) species stabilized by the ligation. Furthermore, the residue- and regio-selective transmethylation of the Nε2 atom of the His64 residue was observed at 25 ˚C. In support of the experimental results, the author's theoretical calculations indicate that His-on/off switching regulates the reactivity of the methylated Co(III) species for both the formation and the transmethylation.

2-4. Experimental

Instruments

UV-vis spectral measurements were carried out with a Shimadzu UV-3150 or UV-2550 double-beam spectrophotometer, or a Shimadzu BioSpec-nano spectrometer. ESI-TOF MS and MALDI-TOF MS analyses were performed with a Bruker Daltonics micrOTOF mass spectrometer and a Bruker autoflex III smartbeam mass spectrometer, respectively. ^{1}H and ^{13}C NMR spectra were collected on a Bruker BioSpin DPX400 (400 MHz) or a Varian Unity Inova 600 MHz NMR spectrometer. The ^{1}H and ^{13}C NMR chemical shift values are reported in ppm relative to a residual solvent peak. ICP-OES (inductively coupled plasma optical emission spectroscopy) was performed on a Shimadzu ICPS-7510 emission spectrometer. EPR spectra were measured using a Bruker EMX Plus spectrophotometer at the Instrument

Center of the Institute for Molecular Science (Okazaki, Japan). CD spectra were recorded at 25 °C on a JASCO spectropolarimeter (Model J-820). The pH measurements were made with an F-52 Horiba pH meter. Air-sensitive manipulations were performed in a UNILab glove box (MBraun, Germany). A 500 W xenon arc lamp (Ushio Optical Modulex, SX-U1501XQ) filtered with cut-off filters (Asahi Spectra, Super cold filter 5C0751 and HOYA CANDEO OPTONICS, Sharp cut filter L42) was used for photo-irradiation experiments. The illuminance of the irradiated light from 420 nm to 800 nm was monitored by a luminometer (MINOLTA, Illuminance meter T-10P).

Materials and methods

All reagents of the highest guaranteed grade available were obtained from commercial sources and were used as received unless otherwise indicated. Distilled water was demineralized using a Barnstead NANOpure DIamond^{TM} or Millipore Integral3 apparatus. Syntheses of tetradehydrocorrin dimethyl ester cobalt complex, Co(TDHC) dimethyl ester, and tetradehydrocorrin cobalt complex, Co(TDHC) were reported in the author's previous work.[39] Native horse heart myoglobin (Sigma Aldrich) was purified with a cation exchange CM-52 cellulose column. The apoprotein was prepared according to Teale's method.[56,57] The reconstituted protein, rMb(Co^{II}(TDHC)), was obtained by the conventional method.[39] A cobalt standard solution for ICP-OES was purchased from Wako Pure Chemical Industries.

Reduction of rMb(Co^{II}(TDHC)) and following methylation

The following procedures were performed in a glove box (O_2 < 0.1 ppm). A solution of sodium dithionite (10 mg/mL, 10 μL, 0.57 μmol) in 0.1 M potassium phosphate buffer (pH 7.0) was added to 1 mL of rMb(Co^{II}(TDHC)) solution (25 μM) in the same buffer at 25°C. A solution of rMb(Co^{I}(TDHC)) was immediately obtained.[39] To the solution, methyl iodide (1 μL, 16 μmol) was added to yield an organometallic species, rMb(Co^{III}(CH_3)(TDHC)), within 2 h. The reaction was monitored by performing UV-vis spectral measurements at 25 °C.

EPR measurements

The measurements of EPR spectra were carried out at the X-band (9.35 GHz) microwave frequency with 100 kHz field modulation and 10 G of modulation amplitude. During EPR measurements, the sample temperature was maintained at 10 K by an Oxford Instruments ESR900 cryostat equipped with a turbo pump to lower the vapor pressure of the liquid He. Each protein solution (0.5 mM) in 0.1 M potassium phosphate buffer (pH 7.0) was placed in a 5 mm tube. The sample was quickly frozen in a cold pentane bath chilled with liquid N_2.

Preparation of rMb($Co^{III}(CH_3)$(TDHC)) for the ESI mass spectrometry experiment.

The sample solution was prepared in degassed water prior to use in a nitrogen-purged glove box (O_2 < 0.1 ppm). To a solution of rMb(Co^{II}(TDHC)) (0.1 mM, 0.5 mL, 50 nmol) in 0.1 M ammonium acetate buffer (pH 6.7), sodium dithionite (57 mM, 1.6 mL, 91 nmol) and saturated CH_3I (99 mM, 25 μL, 2.5 μmol) in the same buffer were added and the solution was allowed to stand for 1 h at 4 °C.

Identification of a methylated amino acid residue in the protein

Site-specific methylation in the protein was confirmed by the in-source decay mode on a Bruker autoflex III smartbeam mass spectrometer (MALDI-TOF MS). As a matrix solution, 1,5-diaminonaphthalene was saturated in a mixture of CH_3CN and 0.1% TFA aqueous solution (1/1 v/v). After the methyl transfer reaction, the protein solution was purified by HiTrap Desalting (5 mL, GE Healthcare). To 1 μL of the concentrated protein solution (0.1 mM) was added 5.0 μL of the matrix solution, and then 1 μL of the mixed solution was placed on a sample plate. The solvent was evaporated under ambient conditions. All mass spectra were acquired in positive ion mode.

For the NMR study, the methylated protein was prepared by ^{13}C-enriched methyl iodide. The concentrated protein solution (0.25 mM, 1 mL) was passed through a HiTrap Desalting column (GE Healthcare) equilibrated with 50 mM Tris-HCl buffer (pH 8.0) containing 6 M guanidine HCl. After denaturation of the protein by incubation of the collected solution at 95 °C for 20 min, the buffer was exchanged to 50 mM Tris-HCl buffer (pH 7.6) containing 1 mM $CaCl_2$ using the same gel filtration column. To the solution, Sequencing Grade Modified Trypsin (Promega) (0.5 mg/mL, 20 μL) was added and the mixture was incubated at 37 °C for 24 h. The peptide fragment containing methylated His64, H($^{13}CH_3$)GTVVLTALGGILK, was isolated by HPLC with a YMC-Pack Pro C18 column (water/acetonitrile co-solvent containing 0.1% TFA). Purification was performed at a flow rate of 8 mL/min with a linear gradient of two eluents for 60 min. The isolated peptide was characterized by ESI-TOF MS: found m/z = 1392.854, calculated m/z = 1392.857 (z = 1+). ^1H and ^{13}C NMR spectra of the isolated peptide fragment in 10% acetonitrile-d_3 in D_2O solution were obtained on 600 MHz NMR instrument at 25 °C.

HPLC analysis for the kinetics of the transmethylation

The transmethylations reactions of native myoglobin and rMb(Co(TDHC)) were evaluated by HPLC analysis.

Native myoglobin: The solution of native myoglobin (25 μM, 3 mL) in 0.1 M potassium phosphate buffer solution (pH 7.0) was reduced with 30 μL of 10 mg/mL sodium dithionite (54.8 mM) in the same buffer solution and then methyl iodide (3 μL) was added. At desired reaction times (0, 3, 7, 12, 24, 48 h),

the protein solution (25 μM, 0.5 mL) was passed through a PD MiniTrap G-25 column (GE Healthcare) equilibrated with 50 mM Tris-HCl buffer (pH 8) containing 6 M guanidine HCl at 4 ºC. The buffer was exchanged to 50 mM Tris-HCl buffer (pH 7.6) containing 1 mM $CaCl_2$ using the same gel filtration column and the solution was concentrated to 50 μL using an Amicon Ultra-4 Centrifugal Filter (10 kDa) (GE Healthcare). To the solution, Sequencing Grade Modified Trypsin (Promega) (0.05 mg/mL, 1 μL) was added and the mixture was incubated at 37 ºC overnight.

rMb(Co^{II}(TDHC)): The protein (25 μM, 5 mL) in 0.1 M potassium phosphate buffer solution (pH 7.0) was reduced with 50 μL of 10 mg/mL sodium dithionite (54.8 mM) in the same buffer solution and then methyl iodide (5 μL) was added. At desired reaction times (0, 6, 12, 24, 48 h), each protein solution (12.5 μM, 1 mL) was dissolved in 4 mL of 17 mM Tris-HCl buffer (pH 8) containing 1 M guanidine HCl at 4 ºC. After concentration to 0.5 mL, the protein solution was passed through the same gel filtration column equilibrated with 17 mM Tris-HCl buffer (pH 7.5) containing 1 M guanidine HCl at 4 ºC. The buffer was exchanged to 50 mM Tris-HCl buffer (pH 7.6) containing 1 mM $CaCl_2$ and concentrated until 50 μL using the same centrifugal filter. To each solution, Sequencing Grade Modified Trypsin (Promega) (0.5 mg/mL, 1 μL) was added and the mixture was incubated at 37 ºC for 2 h.

The solutions containing the peptide fragments were analyzed by HPLC with a YMC-Pack Pro C18 column. The analysis was performed at a flow rate of 1 mL/min of 75% or 78% water/acetonitrile co-solvent containing 0.1% TFA for 40 or 70 min in a column oven at 60 ˚C, respectively. Each fraction was characterized by ESI-TOF-MS.

The fractions of the peaks located at about 56 and 58 min were assigned to the peptide containing non-methylated His64, HGTVVLTALGGILK, and the peptide containing methylated His64, H(CH_3)GTVVLTALGGILK, by ESI-TOF MS. Found m/z = 1378.813 (56 min) and 1392.829 (58 min), calculated m/z = 1378.841 (z = 1+) and 1392.857 (z = 1+). The concentration of the methylated peptide was determined from the ratio of peak areas of methylated and non-methylated peptides.

Computational chemistry

The author used the Becke–Perdew (BP86)[58,59] method implemented in the Gaussian 09 program. For all atoms, the 6-31G(d) basis set was used. This level of theory BP86/6-31G(d) serves as an appropriate platform for addressing the structural, electronic, and spectroscopic properties of cobalamin cofactors.[60–66] All calculations were carried out in the gas phase unless otherwise noted. To explore the realistic reaction pathways, the author used a truncated model of Co(TDHC) where all peripheral side chains of TDHC were replaced with hydrogens. The positions of four atoms marked with asterisk * in Figure 2-13 are constrained at the coordinate of the crystal structure (PDB ID: 3WFT) to retain the structure of the active site. All of the transition states were characterized by an imaginary frequency mode that

corresponds to the motion along the reaction coordinate under consideration. The dielectric effect of protein environment on the transmethylation reaction was estimated at the BP86/SV(P) level of theory by using the conductor-like screening model[67] (COSMO) implemented in the TURBOMOLE program. The dielectric constant was chosen to be 4, which is a standard value that has been used in previous studies.[23]

References and notes

(1) B. Kräutler, in *Metal Ions in Life Science*, ed. A. Sigel, H. Sigel, R. K. O. Sigel, Royal Society of Chemistry, Cambridge, 2009, ch. 1, vol. 6, pp. 1–51.

(2) R. G. Matthews, in *Metal Ions in Life Science*, ed. Sigel, A., Sigel, H., Sigel, R. K. O., Royal Society of Chemistry, Cambridge, 2009, ch. 2, vol. 6, pp. 53–113.

(3) B. Kräutler, B. Puffer in *Handbook of Porphyrin Science*, ed. K. M. Kadish, K. M. Smith, R. Guilard, World Scientific, Singapore, 2012, ch. 117, vol. 25, pp. 131–263.

(4) B. Kräutler, S. Ostermann in *The Porphyrin handbook*, ed. K. M. Kadish, K. M. Smith, R. Guilard, Academic Press, San Diego**,** 2003, ch. 68, vol. 11, pp. 229–276.

(5) K. L. Brown, *Chem. Rev*. **2005**, *105*, 2075.

(6) R. Banerjee, C. Gherasim, D. Padovani, *Curr. Opin. Chem. Biol*. **2009**, *13*, 484.

(7) K. Gruber, B. Puffer, B. Kräutler, *Chem. Soc. Rev*. **2001**, *40*, 4346.

(8) R. G. Matthews, *Acc. Chem. Res*. **2001**, *34*, 681.

(9) Y. Kung, N. Ando, T. I. Doukov, L. C. Blasiak, G. Bender, J. Seravalli, S. W. Ragsdale, C. L. Drennan, *Nature* **2012**, *484*, 265.

(10) F. Zelder, *Chem. Commun.* **2015**, *51*, 14004.

(11) C. L. Drennan, S. Huang, J. T. Drummond, R. G. Matthews, M. L. Ludwig, *Science* **1994**, *266*, 1669.

(12) R. G. Matthews, in *Chemistry and biochemistry of B12*, ed. R. Banerjee, John Wiley & Sons. Inc., New York, 1999, ch. 27, pp. 681–706.

(13) H. P. C. Hogenkamp, G. T. Bratt, A. T. Kotchevar, *Biochemistry* **1987**, *26*, 4723.

(14) C. W. Goulding, D. Postigo, R. G. Matthews, *Biochemistry* **1997**, *36*, 8082.

(15) J. S. Dorweiler, R. G. Finke, R. G. Matthews, *Biochemistry* **2003**, *42*, 14653.

(16) V. Bandarian, M. L. Ludwig, R. G. Matthews, *Proc. Natl. Acad. Sci. U. S. A.* **2003**, *100*, 8156.

(17) N. Kumar, P. M. Kozlowski, *J. Phys. Chem. B* **2013**, *117*, 16044.

(18) M. Alfonso-Prieto, X. Biarne, M. Kumar, C. Rovira, *J. Phys. Chem. B* **2010**, *114*, 12965.

(19) N. Kumar, M. Alfonso-Prieto, C. Rovira, P. Lodowski, M. Jaworska, P. M. Kozlowski, *J. Chem. Theory Comput.* **2011**, *7*, 1541.

(20) K. Kornobis, K. Ruud, P. M. Kozlowski, *J. Phys. Chem. A* **2013**, *117*, 863.

(21) M. Koutmos, S. Datta, K. A. Pattridge, J. L. Smith, R. G. Matthews, *Proc. Natl. Acad. Sci. U. S. A.* **2009**, *106*, 18527.

(22) S. Datta, M. Koutmos, K. A. Pattridge, M. L. Ludwig, R. G. Matthews, *Proc. Natl. Acad. Sci. U. S. A.* **2008**, *105*, 4115.

(23) S.-L. Chen, M. R. A. Blomberg, P. E. M. Siegbahn, *J. Phys. Chem. B* **2011**, *115*, 4066.

(24) P. M. Kozlowski, T. Kamachi, M. Kumar, K. Yoshizawa, *J. Biol. Inorg. Chem.*, **2012**, *17*, 611–619.

(25) L. D. Zydowsky, T. M. Zydowsky, E. S. Haas, J. W. Brown, J. N. Reeve, H. G. Floss, *J. Am. Chem. Soc.* **1987**, *109*, 7922.

(26) C. Wedemeyer-Exl, T. Darbre, R. Keese, *Helv. Chim. Acta* **1999**, *82*, 1173.

(27) L. Pan, H. Shimakoshi, Y. Hisaeda, *Chem. Lett.* **2009**, *38*, 26.

(28) L. Pan, H. Shimakoshi, T. Masuko, Y. Hisaeda, *Dalton Trans.* **2009**, 9898.

(29) L. Pan, K. Tahara, T. Masuko, Y. Hisaeda, *Inorg. Chim. Acta* **2011**, *368*, 194.

(30) K. L. Brown, *Dalton Trans.*, **2006**, 1123.

(31) Y. Hisaeda, T. Masuko, E. Hanashima, T. Hayashi, *Sci. Technol. Adv. Mater.* **2006**, *7*, 655.

(32) W. Galezowski, P. N. Ibrahim, E. S. Lewis, *J. Am. Chem. Soc.* **1993**, *115*, 8660.

(33) W. Galezowski, E. S. Lewis, *J. Phys. Org. Chem.* **1994**, *7*, 90.

(34) W. Galezowski, *Inorg. Chem.* **2005**, *44*, 5483.

(35) W. Galezowski, *Inorg. Chem.* **2005**, *44*, 1530.

(36) Y. Murakami, K. Aoyama, *Bull. Chem. Soc. Jpn.* **1976**, *49*, 683.

(37) C.-J. Liu, A. Thompson, D. Dolphin, *J. Inorg. Biochem*. **2001**, *83*, 133.

(38) Y. Murakami, Y. Aoyama, K. Tokunaga, *J. Am. Chem. Soc.* **1980**, *102,* 6736.

(39) T. Hayashi, Y. Morita, E. Mizohata, K. Oohora, J. Ohbayashi, T. Inoue, Y. Hisaeda, *Chem. Commun.* **2014**, *50*, 12560.

(40) M. J. Kendrick, W. Al-Akhdar, *Inorg. Chem.* **1987**, *26*, 3971.

(41) D. Dolphin, A. W. Johnson, R. Rodrigo, *Ann. N. Y. Acad. Sci.* **1964**, *112*, 590.

(42) H. Chen, H. Yan, L. Luo, X. Cui, W. Tang, *J. Inorg. Biochem.* **1997**, *66*, 219.

(43) D. Lexa, J. M. Saveant, *J. Am. Chem. Soc.* **1976**, *98*, 2652.

(44) D. Occhialini, J. S. Kristensen, K. Daasbjerg, H. Lund, *Acta Chem. Scand.* **1992**, *46*, 474.

(45) C. Li, K. Nishiyama, I. Taniguchi, *Electrochim. Acta* **2000**, *45*, 2883.

(46) M. Nagai, Y. Nagai, K. Imai, S. Neya, *Chirality* **2014**, *442*, 438.

(47) Furthermore, two additional peaks were observed at 625.221 and 2420.608, corresponding to $Co^{III}(CH_3)$(TDHC) and apoprotein, respectively, which are mainly derived from dissociation of the methylated cobalt complex from the protein matrix by CID (collision-induced dissociation) under the harsh ionization conditions.

(48) B. Kräutler, *Helv. Chim. Acta* **1987**, *70*, 1268.

(49) As truncated models of Co(TDHC) and cobalamin, the author used TDHC' and corrin where all of the peripheral side chains were replaced with hydrogen atoms for DFT calculations.

(50) The heterolytic cleavage of the Co–C bond inevitably brings about the Co–N bond dissociation since Co(I) favours four-coordinate square planar geometry. Thus, the BDE_{Im} and $BDE_{Im\text{-}free}$ for the Im-coordinated Co(III) complex and the Im-free Co(III) complex (penta-coordination), respectively, are defined by the following equations:

$$BDE_{Im} = E(\mathrm{Co(I)}) + E(^{+}\mathrm{CH_3}) + E(\mathrm{Im}) - E(\mathrm{CH_3{-}Co(III){-}Im})$$

$$BDE_{Im\text{-}free} = E(\mathrm{Co(I)}) + E(^{+}\mathrm{CH_3}) - E(\mathrm{CH_3Co(III)})$$

where E(X) is the energy of the optimized structure of X.

(51) In aqueous solution, the stabilization energy of the CH_3–Co(III) complex by the imidazole ligation would not be large because of the exchange of a water molecule as a sixth ligand with the imidazole moiety. Indeed, an energy difference between CH_3−Co(corrin)−OH_2 and CH_3−Co(corrin)−Im was estimated at the BP86/SV(P) level of theory to be −4.2 kcal/mol. The value includes the effect of a dielectric constant of 74.8, which is a standard value of aqueous solution. The computed energy difference is in a good agreement with the experimentally determined equilibrium constant for the ligand exchange of the water molecule with imidazole ($K = 4.52 \times 10^2$, $\Delta G = -RT\ln(K) = -3.6$ kcal/mol).[68] In contrast, the Co–C bond formation is smoothly promoted in the protein environment since the solvent water molecules is not accessible to the proximal site and the histidine residue occupies at the coordination site of the cobalt atom.

(52) In contrast to the His93 residue in the myoglobin matrix, imidazole does not serve as a suitable axial ligand because the addition of imidazole (1 mM) to the Co^{II}(TDHC) aqueous solution (0.05 mM) does not produce spectral changes. The binding constant of Co^{II}(TDHC) for apomyoglobin was determined by UV-vis spectral changes in the titration experiment to be 20 μM^{-1} in 0.1 M potassium phosphate buffer (pH 7.0) at 25 ˚C.[29]

(53) The chemical shifts of methyl groups of Nε2-methylated histidine and of Nδ1-methylated histidine were determined to be 36.20 ppm and 33.89 ppm, respectively, in D_2O/CD_3CN co-solvent (9:1, v/v) containing 1% TFA at 25 ˚C.

(54) In this study, the author focus on the two pathways because activation barrier for reductive elimination pathway is much higher than that for the concerted pathway.[24] In methionine synthase, a radical mechanism is one of the considerable pathways of the transmethylation from methylcobalamin to deprotonated homocysteine.[18,69] However, the nucleophilic mechanism is more likely than a radical mechanism in the author's system because the radical mechanism requires the significantly uphill electron transfer (ET) from His64 to the methylated complex to form a diradical species. The relative energy of the intermediate generated by ET was estimated to be 102.9 kcal/mol at the BP86/6-31G(d) level of theory by following equation.

$$\Delta E = E([Co^{III}(CH_3)(TDHC')]^{\bullet}) + E([Im]^{\bullet+}) - E([Co^{III}(CH_3)(TDHC')]^{+}) - E([Im])$$

where $[Co^{III}(CH_3)(TDHC')]^{\bullet}$ and $[Im]^{\bullet+}$ are one electron-reduced methylated complex and imidazole radical cation, respectively. The energy difference is significantly larger than the energy barrier of the stepwise pathway, indicating that the nucleophilic mechanism is more plausible than the radical mechanism.

(55) The truncated model of Co(TDHC) and 4-ethylimidazole as a model of distal and proximal histidine residues, His64 and His93, were used for DFT calculations.

(56) F. W. J. Teale, *Biochim. Biophys. Acta* **1959**, *35*, 543.

(57) T. Hayashi, in Handbook of Porphyrin Science, ed. K. M.Kadish, K. M. Smith, R. Guilard, World Scientific, Singapore, 2010, ch. 23, vol. 5, pp. 1–69.

(58) A. D. Becke, *J. Chem. Phys.* **1986**, *84*, 4524.

(59) J. P. Perdew *Phys. Rev. B* **1986**, *33*, 8822.

(60) K. P. Jensen, U. Ryde, *J. Phys. Chem. A* **2003**, *107*, 7539.

(61) C. Rovira, X. Biarnés, K. Kunc, *Inorg. Chem.* **2004**, *43*, 6628.

(62) C. Rovira, P. M. Kozlowski, *J. Phys. Chem. B* **2007**, *111*, 3251.

(63) N. Dölker, A. Morreale, F. Maseras, *J. Biol. Inorg. Chem.* **2005**, *10*, 509.

(64) J. Kuta, S. Patchkovskii, M. Z. Zgierski, P. M. Kozlowski, *J. Comput. Chem.* **2006**, *27*, 1429.

(65) P. M. Kozlowski, T. Kamachi, T. Toraya, K. Yoshizawa, *Angew. Chem. Int. Ed.* **2007**, *46*, 980.

(66) P. M. Kozlowski, T. Kamachi, T. Toraya, K. Yoshizawa, *J. Biol. Inorg. Chem.* **2011**, *17*, 293.

(67) A. Klamt, G. Schüürmann, *J. Chem. Soc., Perkin Trans. 2* **1993**, 799.

(68) G. C. Hayward, H. A. Hill, J. M. Pratt, N. J. Vanston, R. J. Williams, *J. Chem. Soc. Perkin 1* **1965**, 6485.

(69) N. Kumar, M. Jaworska, P. Lodowski, M. Kumar, P. M. Kozlowski, *J. Phys. Chem. B*, **2011**, *115* 6722.

Chapter 3
Coordination behavior of aqua- and cyano-Co(III) corrinoids with histidine-ligation in the myoglobin matrix

3-1. Introduction

Methionine is responsible for catalysis of a transmethylation reaction and it is noted that the reaction via the heterolytic cleavage of the Co–CH_3 bond of methylcobalamin is accelerated by ca. 10^5-fold within the enzyme compared to the non-enzymatic reaction.[1,2b,d,3] To understand the enzymatic reaction mechanism, it is essential to consider the effects on the electronic and structural properties of the corrin framework as well as the axial ligand.[4–11] To evaluate the chemical properties of the corrin framework, two characteristic cobalt corrinoids, di- and tetradehydrocorrin cobalt complexes, have been reported as models of cobalamin.[4] Furthermore, several substituted cobalamins with substitution at the 10-position of the corrinoid and cobalt corrole derivatives have been also synthesized to investigate the framework-effect using theoretical and experimental methods.[5,6] In addition to the framework-effect, various cobalamin derivatives were synthesized to investigate the axial-ligation effect, particularly the relationship between the Co–C and Co–N(DMB) bond lengths.[1d,5b,7] A bulky axial ligand such as DMB is known to cause elongation of the Co–C bond due to upward folding of the corrin ring.[1d,8] This axial ligation generally promotes homolytic cleavage of the Co–C bond as a result of electronic stabilization of the produced Co(II) species.[1d,8] In contrast, there are few appropriate cobalamin models which replicate the DMB-off/His-on ligation which occurs in the reaction cycle of methionine synthase, where the methyl group bound to the cobalt atom is transferred to homocysteine via the heterolytic Co–C bond cleavage.[9,12] To evaluate the effect of the histidine ligation, it is of interest to construct a conjugate model between a cobalt complex and a protein matrix.[10,11,13]

Myoglobin reconstituted with tetradehydrocorrin cobalt complex, rMb(Co(TDHC)), was prepared to replicate the cobalamin-binding domain of methionine synthase.[10] Furthermore, it has been found that the Co(I) species reacts with methyl iodide to form the Co–CH_3 bond and the subsequent intraprotein transmethylation occurs in the heme pocket.[4,11] In these transmethylation events as a model reaction of methyltransferase, the theoretical study suggests that ligation and de-ligation of the axial histidine residue in the myoglobin matrix has important roles for the formation and activation of the CH_3–Co(III) species, respectively. However, an X-ray crystal structure of the methylated complex has not been available because the organometallic Co(III) species is more unstable than methylcobalamin[11] and rapidly decomposes when subjected to X-ray irradiation.[14] Here, the author reports the structures and physicochemical properties of relatively stable aqua- and cyano-Co(III) complexes of myoglobin, rMb($Co^{III}(OH_2)$(TDHC)) and rMb(Co^{III}(CN)(TDHC), respectively, as models of methylcobalamin in the

enzyme matrix (Scheme 3-1).

Scheme 3-1. Reaction scheme for oxidation of rMb(Co^{II}(TDHC)) and subsequent ligand exchange with a cyanide ion.

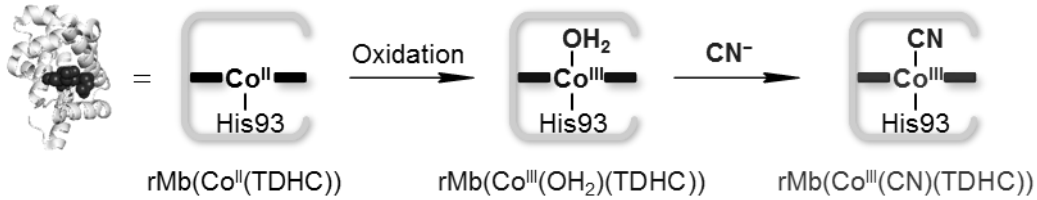

3-2. Results and discussion

Preparation of rMb(Co^{III}(OH_2)(TDHC) by oxidation of rMb(Co^{II}(TDHC))

Addition of $K_3[Fe(CN)_6]$ to a solution of rMb(Co^{II}(TDHC)) in 0.1 M phosphate buffer at pH 7.0 leads to a new set of absorption maxima (λ_{max}) at 657 nm and 687 nm with disappearance of the 510-nm absorption (Figure 3-1a). These new absorption bands have been attributed to an intermolecular charge transfer transition for the cobalt–axial ligand bond of the Co^{III}(TDHC) species.[4d] As a reference experiment, the author also monitored the UV-vis spectral change of the bare Co^{III}(TDHC) complex in the same buffer containing $K_3[Fe(CN)_6]$ upon addition of imidazole (Im) as an axial ligand. The obtained spectrum of the Im-ligated Co^{III}(TDHC) species is generally consistent with that of Co^{III}(TDHC) in the protein (Table 3-1), indicating that Co^{II}(TDHC) is oxidized by $K_3[Fe(CN)_6]$ to form the Co(III) species, rMb(Co^{III}(OH_2)(TDHC)), coordinated by the His93 residue in the heme pocket of myoglobin at pH 7.0.

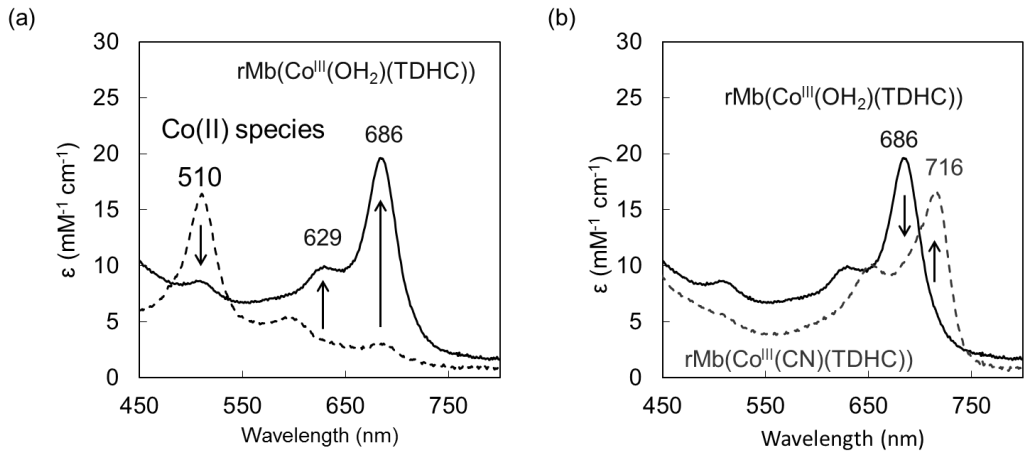

Figure 3-1. (a) UV-vis spectra of rMb(Co^{II}(TDHC)) (dashed line) and rMb(Co^{III}(OH_2)(TDHC)) (solid line) in 0.1 M potassium phosphate buffer at pH 7.0 at 25 ˚C. (b) UV-vis spectral changes of rMb(Co^{III}(OH_2)(TDHC)) upon addition of cyanide in the same buffer.

Table 3-1. UV-vis spectral absorption data in 0.1 M potassium phosphate buffer at pH 7.0 at 25 ºC

protein or complex	λ_{max} (nm) [ε^a (mM^{-1} cm^{-1})]
rMb($Co^{III}(OH_2)$(TDHC))	629 [10.0], 686 [19.6]
rMb(Co^{III}(CN)(TDHC))	652 [10.2], 716 [16.7]
rMb(Co^{II}(TDHC))[b]	510 [16.4]
Co^{III}(TDHC)L_2 [c]	629 [11.0]
Co^{III}(TDHC)L_2 + Im[d]	629 [9.1], 677 [11.7]
$Co^{III}(CN)_2$(TDHC)	671 [8.0], 740 [11.6]

[a]The molar coefficient was determined from ICP-OES measurements. [b]Ref. 10. [c]L = H_2O or OH^-.
[d]Co^{III}(TDHC) (5.2 μM) in 0.1 M phosphate buffer containing 1 mM of Im.

Increasing the pH value of the oxidized protein solution induces spectral changes with isosbestic points (Figure 3-2a), which are derived from deprotonation of a water molecule coordinated to the cobalt atom in the reconstituted myoglobin (eq 1).

$$\text{rMb}(Co^{III}(OH_2)(\text{TDHC})) \rightleftharpoons \text{rMb}(Co^{III}(OH)(\text{TDHC}) + H^+ \qquad (1)$$

A pK_a value of 7.5 for the coordinated water molecule in rMb(Co(OH_2)(TDHC)) was determined from data obtained in a pH titration experiment (Figure 3-2b). This pK_a value is similar to that of base-on aquacobalamin (pK_a = 7.8) and higher than that of base-off diaquacobalamin (pK_a = 6.0), where the base-on and base-off transitions represent the transitions of the intramolecular DMB-ligated and H_2O-ligated forms in the cobalamin molecule, respectively.[15] This finding suggests that the His93 residue coordinates to Co^{III}(TDHC) in myoglobin (His-on) under conditions of neutral pH.

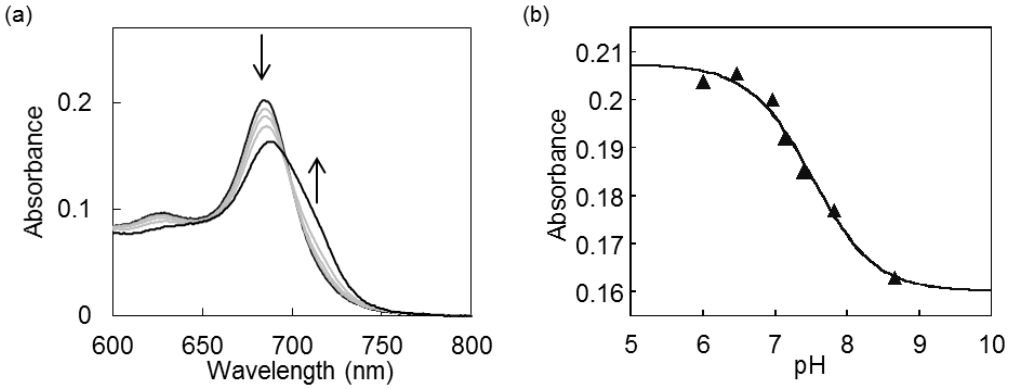

Figure 3-2. (a) UV-vis spectral changes occurring with increasing pH (pH 7–9) at 25 ºC. (b) The pH titration curve of the absorbance at 686 nm, which is the absorption maximum of rMb($Co^{III}(OH_2)$(TDHC)).

Ligand exchange to obtain the cyano-Co(III) complex

The coordinated water molecule in rMb($Co^{III}(OH_2)$(TDHC)) is exchangeable with a cyanide ion upon addition of a solution of KCN, giving red shifted absorption maxima at 652 nm and 716 nm (Figure 3-1b and Table 3-1). These maxima are different from those of the bare $Co^{III}(CN)_2$(TDHC) complex, which are consistent with those of the reported Co(III) tetradehydrocorrin dicyano-complex in CH_2Cl_2.[4d] These results support the formation of a monocyano-adduct of Co^{III}(TDHC) with the His93 coordination in the heme pocket of myoglobin, rMb(Co^{III}(CN)(TDHC)), as characterized by ESI-TOF MS. The affinity of the cyanide for rMb($Co^{III}(OH_2)$(TDHC)) was determined by relaxation analysis[16] and indicated a K value of 8.9×10^5 M^{-1} at pH 7.0, which is lower than that of CNCbl ($\geq 10^{12}$ M^{-1}).[15]

Interestingly, rMb(Co^{III}(CN)(TDHC)) can also be obtained by autoxidation of the Co(II) species in the reconstituted protein upon addition of an excess amount of cyanide (10 eq) under aerobic conditions, whereas similar oxidation does not occur in the absence of cyanide. The oxidation appears to be initiated by coordination of cyanide to the Co(II) species, which would lead to a negative shift of the Co(II)/Co(III)-redox potential of Co(TDHC).

Crystal structures of rMb(Co^{III}(OH)(TDHC)) and rMb(Co^{III}(CN)(TDHC))

The crystal of myoglobin with the Co(III) species was obtained by soaking the crystal of rMb(Co^{II}(TDHC))[10] in a reservoir solution containing $K_3[Fe(CN)_6]$ (15.2 mM) at pH 7.4. At this pH, approximately half of the coordinated water molecules in rMb($Co^{III}(OH_2)$(TDHC)) are deprotonated to rMb(Co^{III}(OH)(TDHC)) at room temperature (*vide supra*). In addition, the pH value of the reservoir solution containing 0.1 M Tris-HCl buffer is found to increase at low temperature, suggesting that the water molecule coordinated to Co^{III}(TDHC) will be deprotonated to form rMb(Co^{III}(OH)(TDHC)) under the conditions used for data collection at 100 K.

The color of the rMb(Co^{III}(OH)(TDHC)) crystal changes from green to deep red after X-ray irradiation, indicating that the Co(III) species is reduced to the Co(II) species by the generated photo-electron and/or hydroxyl radical in the protein.[14] The X-ray crystal structure of the reconstituted protein was determined and refined at 1.20 Å resolution (Figure 3-3a). The cofactor is bound in the heme pocket by Co–N(His93) ligation.

The electron density map clearly shows two oxygen atoms above the cobalt atom of Co(TDHC). Each oxygen occupancy is assigned to be 50% and the distances of Co–O1 and Co–O2 are 1.86 Å and 3.01 Å, respectively (Figure 3-4a). These results suggest that under X-ray irradiation, the hexa-coordinated Co^{III}(OH)(TDHC)–His93 complex is partially reduced to form the penta-coordinated Co^{II}(TDHC)–His93 complex in the heme pocket. After cleavage of the Co–OH bond of rMb(Co^{III}(OH)(TDHC)), it appears that the released hydroxide accepts the proton bound to the Nε2 atom of the His64 residue (Figure 3-4b).

The produced water molecule is located in the heme pocket and participates in hydrogen bonding with the Nε2 atom of the His64 residue with an O2–Nε2 distance of 2.60 Å. Furthermore, the crystal structure reveals that the Co–O bond length of rMb(Co^{III}(OH)(TDHC)) is shorter than the Fe–O bond length of native met-aquo myoglobin and the Co–O bond length of myoglobin reconstituted with cobalt protoporphyrin IX, rMb(Co^{III}(OH_2)(PP)). Furthermore, the Co–O bond length of rMb(Co^{III}(OH)(TDHC)) is much shorter than that of aquacobalamin, H_2OCbl,[17a] and is also shorter than that of hydroxocobalamin, OHCbl, (Table 3-2).[7c] The relatively short Co–O bond length indicates that the water molecule coordinated to the cobalt atom is deprotonated to form the hydroxide ion observed in the crystal structure (Table 3-2).

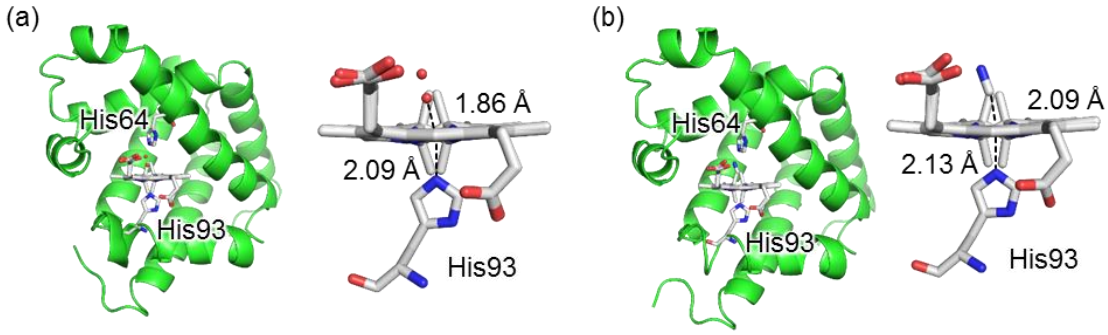

Figure 3-3. Crystal structures of (a) rMb(Co^{III}(OH)(TDHC)) and (b) rMb(Co^{III}(CN)(TDHC)). The whole protein structure (each left), and the structure of cofactor with axial ligand (each right) are shown. Each cofactor consists of two enantiomers, (1*R*,19 *R*)-TDHC and (1*S*,19*S*)-TDHC, with a ratio of 65:35 due to two chiral centers at the C1- and C19-positions of the corrinoid framework.

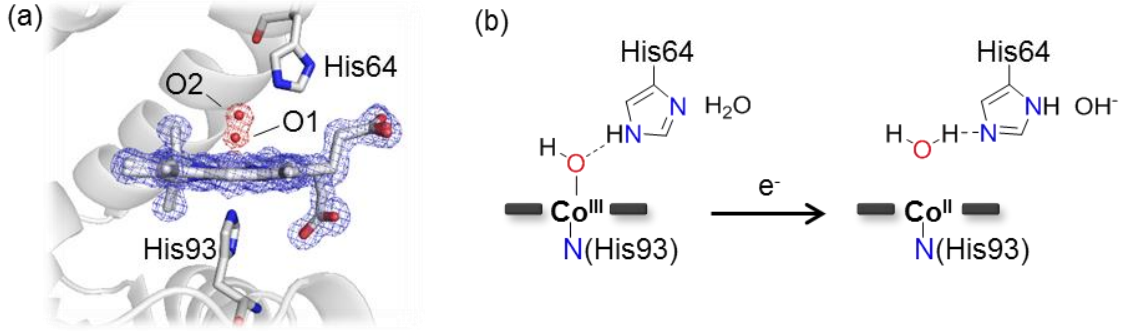

Figure 3-4. (a) Electron density map of the cofactor of rMb(Co^{III}(OH)(TDHC)). The $2F_o - F_c$ electron density is shown as a blue mesh for the cofactor and a red mesh for the oxygen atoms above the cobalt atom (contoured at 1.0 σ). (b) Plausible scheme for the reduction of rMb(Co^{III}(OH)(TDHC)) to rMb(Co^{II}(TDHC)) upon X-ray irradiation.

Table 3-2. Bond lengths of axial coordination for Co(TDHC)s or cobalamins

protein or complex	M–X[a] (Å)	M–N(axial ligand) (Å) [b]
rMb(Co^{III}(OH)(TDHC))[c]	1.86	2.09
rMb(Co^{III}(CN)(TDHC))[c]	2.09	2.13
rMb(Co^{II}(TDHC))[d]	–	2.17
nMb(Fe^{III}(OH_2)(PP))[e]	2.29	2.26
rMb(Co^{III}(OH_2)(PP))[f]	2.46	2.15
H_2OCbl[g]	1.95	1.93
OHCbl[h]	1.92	1.99
CNCbl[i]	1.89	2.04
CNCbl–Im[j]	1.86	1.97
Cob(II)alamin[k]	–	2.13

[a]X is the 6th ligand: X = OH^-, CN^- or H_2O. [b]Distance between the Co–N(His93) and Co–N(DMB) bonds for myoglobin and cobalamin, respectively. [c]This work. [d]Ref. 10. PDB ID: 3WFT. [e]Ref. 17b. PDB ID: 1YMb. [f]Ref. 17c. PDB ID: 2O5T. [g]Aquacobalamin. Ref. 17a. [h]Hydroxocobalamin. Ref. 7c. [i]Cyanocobalamin (CNCbl). Ref. 7a. [j]DMB of CNCbl was substituted with Im. Ref. 7e. [k]Penta-coordinated Co(II)species of cobalamin. Ref. 7d.

The author also determined the X-ray crystal structure of rMb(Co^{III}(CN)(TDHC)) at 1.40 Å resolution (Figure 3-3b). In this case, the X-ray irradiation-induced reduction was not observed. The crystal structure shows the hexa-coordinated Co^{III}(CN)(TDHC) complex bound in the heme pocket by Co–N(His93) ligation. To the best of the author's knowledge, this is the first known instance of determination of 3D-structures of a hexa-coordinated Co(III) tetradehydrocorrin complex with two different ligands at the axial positions.[4d]

Table 3-2 provides a comparison of several bond distances between axial ligands and metal cofactors. The Co–N(His93) bonds of the reconstituted myoglobins are longer than the Co–N(DMB) bonds of the corresponding cobalamins, although the substitution of DMB of cyanocobalamin (CNCbl) with Im is known to provide a shorter Co–N bond.[7e,18] The oxidation of rMb(Co^{II}(TDHC)) provides a shorter Co–N(His93) bond in rMb(Co^{III}(OH)(TDHC)), which is consistent with the fact that the bond length of OHCbl is shorter than that of Cob(II)alamin. Furthermore, the replacement of hydroxide in rMb(Co^{III}(OH)(TDHC)) with cyanide elongates the Co–N(His93) bond in rMb(Co^{III}(CN)(TDHC)). This also occurs during the conversion from OHCbl to CNCbl. Next, comparing the structures of the three cyano-Co(III) complexes listed in Table 3-2, the author found that the Co–N(axial ligand) bond elongates with increasing length of the Co–CN bonds in the order of CNCbl-Im < CNCbl < rMb(Co^{III}(CN)(TDHC)).

These cyano-Co(III) complexes exhibit an inverse trans effect-like property on both axial bond lengths.[7]

Moreover, the polypeptide Cα atoms of rMb(Co^{III}(OH)(TDHC)) and rMb(Co^{III}(CN)(TDHC)) are superimposable on those of nMb with root-mean-square (RMS) deviation values of 0.225 Å and 0.264 Å, respectively. The oxidation of rMb(Co^{II}(TDHC)) and the subsequent ligand exchange from hydroxide to cyanide do not have a significant influence on structural changes of the protein matrix, although the reduction of the Co(II) species provides a His-off state via flipping of the His93 residue with a significantly high *B*-factor.[10] However, the ligation of cyanide provides slightly higher *B*-factor values of the His93 residue of rMb(Co^{III}(CN)(TDHC)) than those of rMb(Co^{III}(OH)(TDHC)) and rMb(Co^{II}(TDHC)) (Figure 3-5). This suggests that the Co–N(His93) bond slightly weakens upon binding of cyanide.

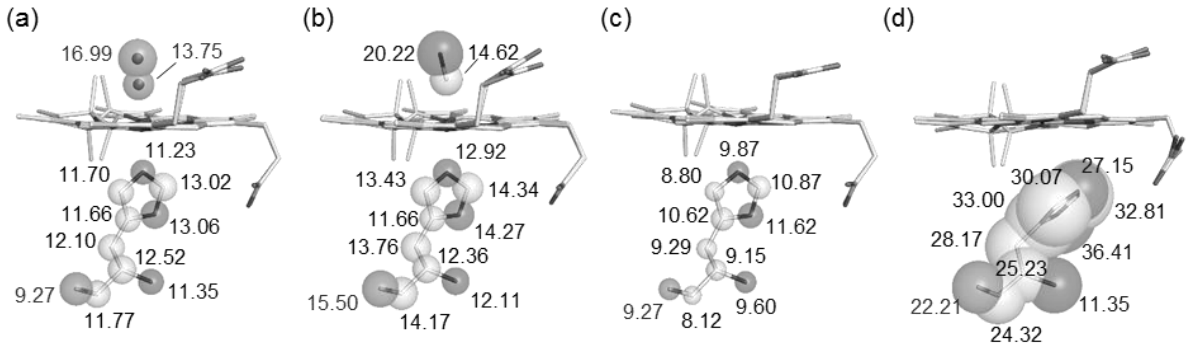

Figure 3-5. Variations in crystallographic *B*-factors of the axial ligands of the reconstituted proteins are represented as both the value and sphere size of each atom: (a) rMb(Co^{III}(OH)(TDHC)), (b) rMb(Co^{III}(CN)(TDHC)), (c) rMb(Co^{II}(TDHC))[11] and (d) rMb(Co^{I}(TDHC))[11].

NMR spectroscopy

The ^{13}C NMR spectra of rMb(Co^{III}(CN)(TDHC)) are shown in Figure 3-6, in which Figure 3-6a was obtained from a sample with ^{13}C-enriched KCN. The differential spectrum (Figure 3-6a – Figure 3-6b) gives two peaks at 108.4 ppm and 110.6 ppm assigned as ^{13}C-enriched cyanide bound to the cobalt ion in the protein matrix (Figure 3-6c), because of the mixture of the two cofactor enantiomers in the asymmetric protein matrix (*vide supra*). A ratio of the areas of these peaks was determined to be 6:4 (Figure 3-6d), which is similar to the ratio estimated by crystallography.

Chemical shifts of the cyanide peak in cyano-cobalt corrinoids are listed in Table 3-3. In comparison with dicyanocobalamin, $(CN)_2$Cbl, CNCbl(base-on) and $Co(CN)_2$(TDHC), the ^{13}C-cyanide peak of rMb(Co^{III}(CN)(TDHC)) undergoes an up-field shift. The similar up-field shift of the cyanide peak is seen in CNCbl(base-off). Taken together, these findings suggest that the weaker σ-donation from the cyanide ion to the cobalt ion relative to CNCbl(base-on) is due to the longer Co–CN bond of

rMb(Co^{III}(CN)(TDHC)) than that of CNCbl.

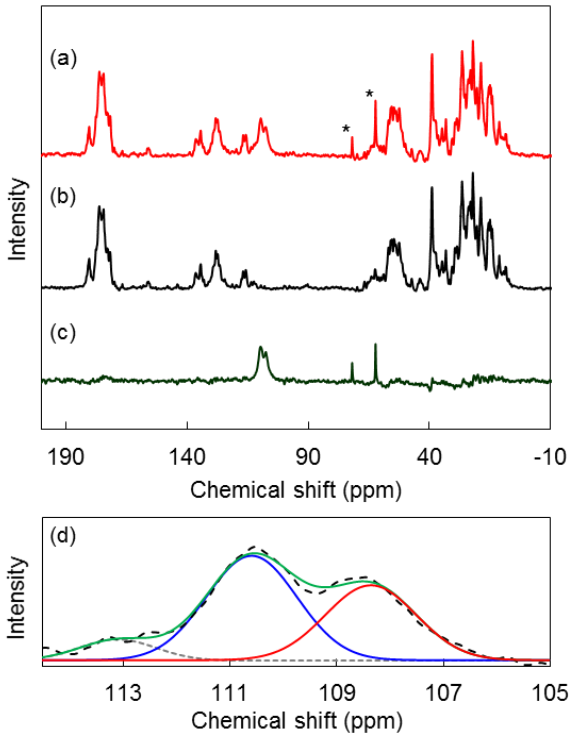

Figure 3-6. ^{13}C NMR (150 MHz) spectra of rMb(Co^{III}(CN)(TDHC)) prepared with (a) ^{13}C-enriched and (b) non-enriched KCN in 0.1 M potassium phosphate buffer at pH 7.0 containing 10% D_2O. The asterisks identify the peaks of glycerin at 63.17 ppm and 71.90 ppm as a reference. (c) The differential spectrum of a – b. (d) Expanded NMR spectrum of rMb(Co^{III}(^{13}CN)(TDHC)) (dash line) with simulated spectra of the peaks at 108.4 ppm, 110.6 ppm and 112.3 ppm (gray dashed line), and the sum of the simulated spectra (in green solid line) for the determination of the ratio of the areas.

Table 3-3. ^{13}C-NMR chemical shifts of cyano-cobalt corrinoids

protein or complex	δ (ppm)
rMb(Co^{III}(CN)(TDHC))[a]	108.4 110.6
CNCbl(base-on)[b]	121.4
CNCbl(base-off)[b]	111.8
$Co(CN)_2$(TDHC)[a]	112.7
$(CN)_2$Cbl[b,c]	140.2

[a]This work. [b]Ref. 19. [c]Dicyanocobalamin.

IR spectroscopy

IR spectra of rMb(Co^{III}(^{13}CN)(TDHC)) and rMb(Co^{III}(^{12}CN)(TDHC)) are shown in Figure 3-7. The ^{13}CN/^{12}CN-differential spectrum clearly shows the typical isotope shift.[20] The stretching frequency of the cyanide ion in rMb(Co^{III}(^{12}CN)(TDHC)) which is assigned at 2151 cm^{-1} is higher than that of both the mono- and di-cyanocobalamins and $Co(CN)_2$(TDHC) (Table 3-4). The higher stretching frequency of the cyanide ion in rMb(Co^{III}(CN)(TDHC)) is due to weak π-back donation from the cobalt atom to the cyanide ion,[21] indicating that the Co–CN bond is weakened relative to that of CNCbl. These findings are supported by the observation that the Co–CN bond in rMb(Co^{III}(CN)(TDHC)) is longer than that of CNCbl, as revealed by X-ray crystallography (*vide supra*).

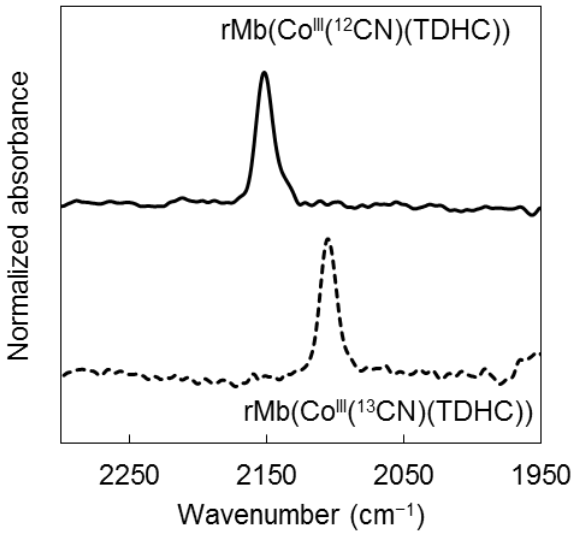

Figure 3-7. IR spectra of rMb(Co^{III}(CN)(TDHC)) prepared with K^{13}CN and K^{12}CN. Conditions: [protein] = 6 mM in 0.1 M potassium phosphate buffer at pH 7.0 at 25 ˚C.

Table 3-4. Cyanide stretching frequencies in cyanocorrinoids

protein or complex	wavenumber (cm^{-1})
rMb(Co^{III}(CN)(TDHC))[a]	2151
$Co(CN)_2$(TDHC)[b]	2128
CNCbl[c]	2137
$(CN)_2$Cbl[c,d]	2119

[a]This work. [b]Ref. 21a. [c]Ref. 21b. [d]Dicyanocobalamin.

Determination of p$K_{1/2}$ values for reconstituted myoglobins

The p$K_{1/2}$ value for each reconstituted protein, which represents the pH value corresponding to a 50% loss of a cofactor from the myoglobin matrix via the cleavage of the metal–N(His93) bond, was determined by fitting the titration curve (Figure 3-8 and Table 3-5). From the UV-vis spectral changes of rMb($Co^{III}(OH_2)$(TDHC)) and rMb(Co^{II}(TDHC)) which occur when the pH decreases, the p$K_{1/2}$ values were determined to be 3.2 and 5.5, respectively. rMb($Co^{III}(OH_2)$(TDHC)) has the lower p$K_{1/2}$ value than rMb(Co^{II}(TDHC)), indicating that the oxidation of the Co(II) species enhances the Co–N(His93) bond strength because the Co(III) species has higher Lewis acidity than the Co(II) and Fe(III) species. In contrast, the p$K_{1/2}$ value of rMb(Co^{III}(CN)(TDHC)) is 2.3 pH units higher than that of rMb($Co^{III}(OH_2)$(TDHC)) (Figure 3-8c), while the p$K_{1/2}$ values of nMb($Fe^{III}(OH_2)$(PP)) and nMb(Fe^{III}(CN)(PP)) are slightly different (0.3 pH units). Table 3-5 also demonstrates that in the case of cobalamins, an increase in the electron-donating ability of an axial ligand increases the p$K_{base\text{-}off}$ values (see the legend under Table 3-5),[7f,15] indicating that the strong electron donating cyanide ligand weakens the Co–N(His93) bond of rMb(Co^{III}(CN)(TDHC)). This finding is supported by the IR and X-ray structure data which indicate elongation of the Co–N(His93) bond.

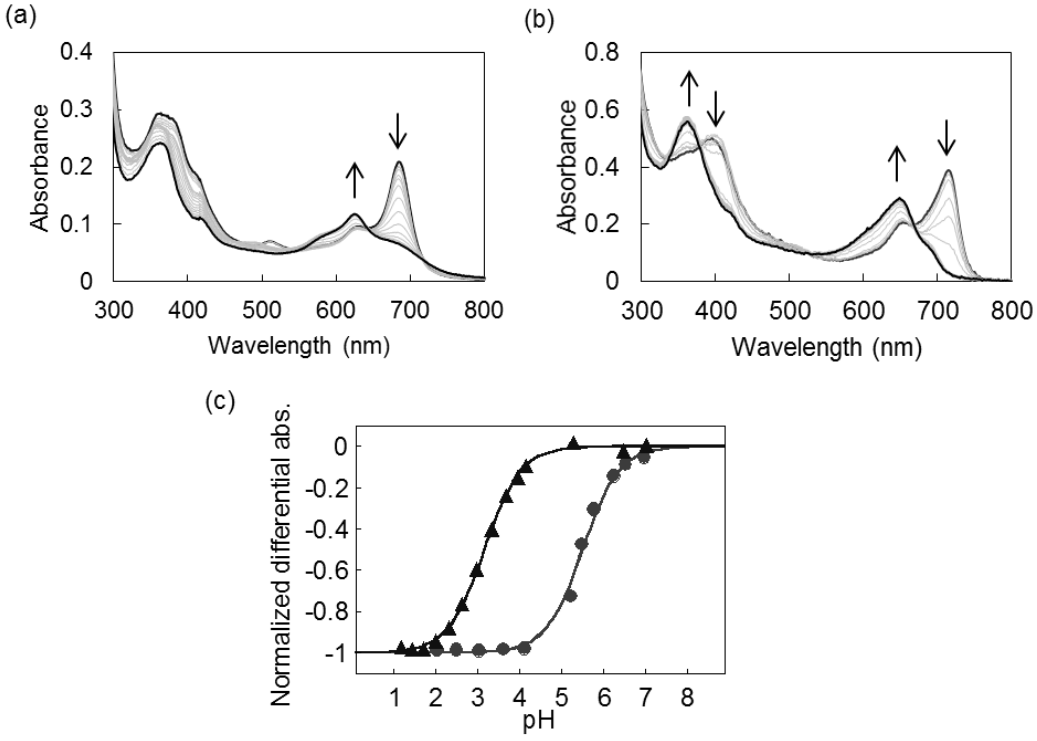

Figure 3-8. UV-vis spectral changes of (a) rMb($Co^{III}(OH_2)$(TDHC)) and (b) rMb(Co^{III}(CN)(TDHC)) occurring with decreasing pH at 25 ºC. (c) The pH titration curves of the absorbance at 686 nm for rMb($Co^{III}(OH_2)$(TDHC)) (triangle, ▲) and at 716 nm for rMb(Co^{III}(CN)(TDHC)) (circle, ●).

Table 3-5. The p$K_{1/2}$ values for reconstituted and native myoglobins and the p$K_{base\text{-}off}$ values for cobalamins

protein or complex	p$K_{1/2}$ or p$K_{base\text{-}off}$
rMb($Co^{III}(OH_2)$(TDHC))[a]	3.2
rMb(Co^{III}(CN)(TDHC))[a]	5.5
rMb(Co^{II}(TDHC))[a]	5.0
nMb($Fe^{III}(OH_2)$(PP))[a]	5.0
nMb(Fe^{III}(CN)(PP))[b]	5.3
H_2OCbl[c,d]	–2.4
CNCbl[c]	0.1
methylcobalamin[c]	2.5

[a]This work. [b]Ref. 22. [c]Ref. 16. [d]Aquacobalamin.

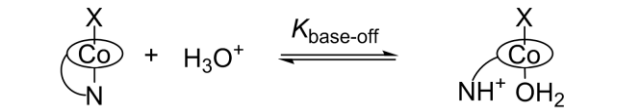

X is the 6th ligand: X = OH^-, CN^- or CH_3^-.

Theoretical calculations for the Co(III) species of the TDHC and corrin frameworks

To characterize the weakening of the Co–N(His93) bond of the Co(III) species by axial coordination of cyanide, the author computed the BDE with density functional theory (DFT) calculations (Table 3-6). As truncated models of Co(TDHC) and cobalamin, the author used Co(TDHC') and Co(corrin), where all of the peripheral side chains are replaced with hydrogen atoms for the DFT calculations (Figure 3-9). Im was used as a simplified model of the axial His93 residue. The BDEs of the Co–N(Im) bonds of $Co^{III}(OH_2)$(Im)(TDHC') and Co^{III}(CN)(Im)(TDHC') were calculated to be 47.9 kcal/mol and 20.5 kcal/mol, respectively, indicating that ligation of cyanide ion decreases the BDE of the Co–N(Im) bond. This is also supported by the higher p$K_{1/2}$ value of rMb(Co^{III}(CN)(TDHC)) (Table 3-5). Furthermore, it is noted that the methylation of Co(Im)(TDHC') significantly reduces the BDE value of the Co–N(Im) bond (14.3 kcal/mol).

The data listed in Table 3-6 indicate that the Co–N(Im) bond of Co(Im)(TDHC')(X) lengthens as the BDE value of the Co–N(Im) bond decreases. The elongation of the bond length of the Co–N(Im) which occurs upon binding of cyanide binding is supported by the X-ray crystal structure data (Figure 3-10).[7,23,24] In the case of rMb($Co^{III}(CH_3)$(TDHC)), similar elongation of the bond length of the Co–N(His93) would lead to the de-ligation of His93, which promotes the transmethylation in the

myoglobin matrix.[11] Such ligation and de-ligation events should be also significant for methylcobalamin in the native enzyme to regulate the reactivity.

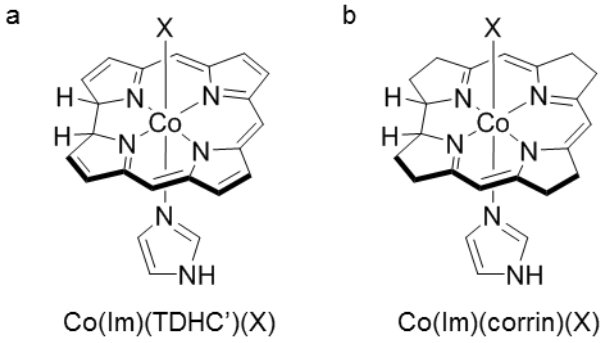

Figure 3-9. Chemical structures of the imidazole-coordinated (a) Co(TDHC')(X) and (b) Co(corrin)(X) as models of Co(TDHC) and cobalamin, respectively. X = X = OH_2, CN^- or CH_3^-.

Table 3-6. Bond-dissociation energy (BDE) of the Co–N(Im) bond and bond lengths of Co–X and Co–N(Im) bonds in Co^{III}(TDHC')(Im)(X).[a,b]

cobalt complex	BDE of Co–N(Im) (kcal/mol)	bond length (Å)	
		Co–X[b]	Co–N(Im)
$Co^{III}(OH_2)$(Im)(TDHC')[c]	47.9	2.08	1.90
Co^{III}(CN)(Im)(TDHC')[c]	20.5	1.85	2.08
$Co^{III}(CH_3)$(Im)(TDHC')[d]	14.3	1.98	2.21

[a]at the BP86/6-31G(d) level of theory. [b]X is the 6th ligand: X = OH_2, CN^- or CH_3^-. [c]This work. [d]Ref. 11.

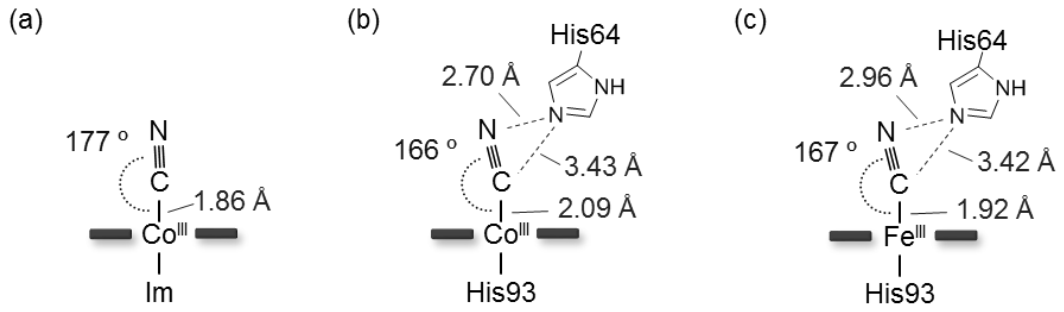

Figure 3-10. Schematic representations for (a) DFT-optimized structure of Co^{III}(CN)(Im)(TDHC'), and crystal structures of (b) rMb(Co^{III}(CN)(TDHC)) and (c) cyano-nMb (PDB ID: 2JHO).

3-3. Summary

The author demonstrates that myoglobins reconstituted with aqua- and cyano-cobalt tetradehydrocorrins are appropriate for investigation as simplified cobalamin models. It is of particular interest to evaluate the binding characteristics of axial ligands for Co(III) corrinoids. ^{13}C NMR and IR studies of rMb(Co^{III}(CN)(TDHC)) indicate that the cyanide weakly interacts with Co^{III}(TDHC). The σ-donation from the cyanide ion to Co^{III}(TDHC) is relatively weaker than that of cyanide-binding cobalamin. Furthermore, the large p$K_{1/2}$ value of rMb(Co^{III}(CN)(TDHC)) suggests that cyanide binding weakens the Co–N(His93) bond strength. In addition, the X-ray crystal structure analysis reveals that the Co–N(His93) bond length is slightly elongated. The DFT calculations also clearly support the unique axial ligation; the Co–N(Im) bond is elongated and the BDE of Co–N(Im) is significantly decreased upon replacement of H_2O with cyanide as an axial ligand. Given these findings, it appears that the cyanide-binding species in Co(TDHC) is a transient structural model of methylcobalamin which promotes methyl group transfer to homocysteine in methionine synthase.

3-4. Experimental section

Instruments

UV-vis spectral measurements were carried out with a Shimadzu UV-3150 or UV-2550 double-beam spectrophotometer, or a Shimadzu BioSpec-nano spectrometer. ^{13}C NMR spectra were collected on an Avance III (600 MHz) NMR spectrometer. IR spectra were recorded with a JASCO FT/IR-6200 spectrometer using the SL-2 demountable cell unit (optical path-length = 0.025 mm, Pier Optics Co., Ltd., Japan) with CaF_2 windows. ICP-OES (inductively coupled plasma optical emission spectroscopy) was performed with a Shimadzu ICPS-7510 emission spectrometer. The pH measurements were made with an F-52 Horiba pH meter.

Materials and methods.

All reagents of the highest guaranteed grade available were obtained from commercial sources and were used as received unless otherwise indicated. Distilled water was demineralized using a Barnstead NANOpure DIamond™ or Millipore Integral3 apparatus. Synthesis of cobalt tetradehydrocorrin, Co(TDHC), was described in the author's previous report.[10] Native horse heart myoglobin, nMb, (Sigma Aldrich) was purified with a cation exchange CM-52 cellulose column. The apoprotein was prepared according to Teale's method.[25] The reconstituted protein, rMb(Co^{II}(TDHC)), was obtained by the conventional method.[10] A co balt standard solution for ICP-OES was purchased from Wako Pure Chemical Industries.

Preparation of rMb($Co^{III}(OH_2)$(TDHC))

Into a solution of rMb(Co^{II}(TDHC))[10] (50 μM, 5 mL, 0.25 μmol) in 0.1 M potassium phosphate buffer at pH 7.0 was added a solution of $K_3[Fe(CN)_6]$ (0.1 M, 0.25 mL, 25 μmol, 100 eq). After equilibrating at 4 ºC under aerobic conditions for 2 h, the protein was purified using a HiTrap desalting column (5 mL, GE Healthcare) with 0.1 M potassium phosphate buffer at pH 7.0. The protein solution was stored in the dark at –80 ºC. UV-vis spectral data of the protein are shown in Table 3-1.

Preparation of rMb(Co^{III}(CN)(TDHC))

Into a solution of rMb(Co^{II}(TDHC)) (50 μM, 5 mL, 0.25 μmol) in 0.1 M potassium phosphate buffer at pH 7.0 were added a solution of $K_3[Fe(CN)_6]$ (0.1 M, 50 μL, 5 μmol, 20 eq) and a solution of KCN (50 mM, 50 μL, 2.5 μmol, 10 eq). After equilibrating at 4 ºC under aerobic conditions for 12 h, the protein was purified using a HiTrap desalting column (5 mL, GE Healthcare) with 0.1 M potassium phosphate buffer at pH 7.0. The protein solution was stored in the dark at –80 ºC. UV-vis spectral data of the protein are shown in Table 3-1. ESI-TOF MS (negative mode, *m*/*z*): $[M–7H^+]^{7–}$ calcd for $C_{803}H_{1241}CoN_{215}O_{222}S_2$, 2511.59; found, 2511.62.

UV-vis spectral measurements of Co(TDHC) complexes without the protein matrix as control experiments

Into a solution of Co^{II}(TDHC) (10 μM, 20 mL, 0.2 μmol) in 0.1 M potassium phosphate buffer at pH 7.0 was added a solution of $K_3[Fe(CN)_6]$ (0.1 M, 0.2 mL, 20 μmol, 100 eq). After equilibrating at 4 ºC under aerobic conditions for 2 h, the oxidized Co(III) species, Co^{III}(TDHC)L_2 (L = H_2O or $OH^–$), was obtained. Subsequently, into the solution of Co^{III}(TDHC)L_2 (10 μM, 5 mL, 0.05 μmol) was added a solution of imidazole (0.5 M, 10 μL, 5 μmol, 100 eq) to yield the imidazole-ligated species. Into the solution of Co^{III}(TDHC)L_2 (10 μM, 5 mL, 0.05 μmol) was added a solution of KCN (50 mM, 50 μL, 2.5 μmol, 50 eq) to yield the dicyano species, $Co^{III}(CN)_2$(TDHC). The UV-vis spectrum of each species was recorded at 25 ˚C without any purification. The UV-vis spectral data are summarized in Table 3-1.

Autoxidation of rMb(Co^{II}(TDHC)) in the presence of KCN

Into a solution of rMb(Co^{II}(TDHC)) (50 μM, 1 mL, 0.05 μmol) in 0.1 M potassium phosphate buffer at pH 7.0 was added a solution of KCN (50 mM, 10 μL, 0.5 μmol, 10 eq). After equilibrating at 4 ºC under aerobic conditions for 12 h, the UV-vis spectrum of the solution was monitored.

Determination of pK_a and p$K_{1/2}$ values

UV-vis spectra of rMb($Co^{III}(OH_2)$(TDHC)), rMb(Co^{III}(CN)(TDHC)), rMb(Co^{II}(TDHC)) and nMb (10–40 μM) in 0.1 M potassium phosphate buffer at 25 °C were measured under conditions of varying pH values which were adjusted by incremental addition of aqueous solutions of 1–12 M HCl or 10 M NaOH. The pH values of the solution were recorded before and after each spectroscopic measurement. The pK_a and p$K_{1/2}$ values were determined from the data which are fitted to the following Henderson-Hasselbach equation (eq 2) for a one proton transfer process,[26]

$$Z = \frac{A_{acid} + A_{neutral} \times 10^{(pH - pK)}}{1 + 10^{(pH - pK)}} \qquad (2)$$

where Z is absorbance at a certain pH; and A_{acid} and $A_{neutral}$ are absorbances of the acid and neutral forms, respectively.

Protein crystallization

Crystallization of rMb(Co^{II}(TDHC)) was performed at 25 ºC using the hanging-drop vapor-diffusion method.[10] The protein drops were prepared by mixing of 5 μL of the protein solution (10 mg/mL) in 0.1 M Tris-HCl buffer at pH 7.4 with 5 μL of a reservoir solution at pH 7.4 containing 3.4 M ammonium sulfate, 0.1 M Tris-HCl and 10% trehalose. The obtained crystals were soaked in the reservoir solution containing $K_3[Fe(CN)_6]$ (15.2 mM) to prepare the crystals of the aqua-Co(III) species. A color change from dark red to green was observed within 10 days and the crystal was then fished and flash-cooled in a stream of N_2 gas at 100 K. To prepare the crystals of the cyano-Co(III) species, the crystals of rMb(Co^{II}(TDHC)) were soaked in the reservoir solution containing 5 mM KCN and 117 mM $K_3[Fe(CN)_6]$. A color change from dark red to green was observed within 20 min and the crystal was then fished and flash-cooled in a stream of N_2 gas.

Crystal structure determination and refinement

X-ray diffraction data were collected at beamline BL44XU of SPring-8 (Harima, Japan). The data were processed with the program *HKL2000*.[27a] The structures were determined by the molecular replacement method using the program *PHASER*[27b] from the *CCP4* program suite.[27c] A crystal structure of horse heart myoglobin (Protein Data Bank (PDB) ID: 3WFT) was used as the search model. Refinement was carried out using the program *REFMAC*.[27d] The structures were visualized and modified using the program *COOT*.[27e] Since the electron density of Co(TDHC) indicates that two enantiomers (1*R*,19*R*)- and (1*S*,19*S*)-TDHCs of Co(TDHC) exist in the heme pocket, the author assigned approximate *RR*:*SS* occupancy with a ratio of 35:65 in both proteins. Data collection and refinement statistics are

summarized in Table 3-7.

Table 3-7. Data collection and refinement statistics for the reconstituted myoglobins

	rMb(Co^{III}(OH)(TDHC))	rMb(Co^{III}(CN)(TDHC))
PDB ID	5AZR	5AZQ
Data collection		
X-ray source	SPring-8 BL44XU	SPring-8 BL44XU
Detector	Rayonix MX225HE	Rayonix MX225HE
Wavelength (Å)	0.90000	0.90000
Resolution (Å) (outer shell)	50 – 1.20 (1.24 – 1.20)	50 – 1.40 (1.45 – 1.40)
Space group	$P2_1$	$P2_1$
Unit cell parameters (Å, deg.)	a = 34.79, b = 28.84, c = 63.32, β = 106.17	a = 34.77, b = 28.81, c = 63.26, β = 105.64
Total reflections	136,063	85,185
Unique reflections	37,167	23,585
Completeness (%)	97.6 (97.5)	97.8 (95.5)
R_{sym}[a]	5.8 (42.8)	5.6 (37.6)
$I/\sigma(I)$	20.4 (3.1)	22.6 (2.4)
Refinement		
Resolution (Å)	50 – 1.20	50 – 1.40
No. of reflections	35,357	22,308
R_{cryst} / R_{free} (%)	12.1 / 16.8	12.8 / 18.9
Mean B-factor (Å^2)	17.3	18.8
No. of non-H atoms	1,476	1,456
Bond lengths (Å) / angles (deg.)	0.033 / 3.248	0.027 / 3.070

[a] $R_{sym} = \Sigma_{hkl}\Sigma_i |I_i(hkl) - \langle I(hkl)\rangle| / \Sigma_{hkl}\Sigma_i I_i(hkl)$, where $I_i(hkl)$ is the value of the ith measurement of the intensity of a reflection, $\langle I(hkl)\rangle$ is the mean value of the intensity of that reflection and the summation is over all measurements.

NMR measurements of rMb(Co^{III}(CN)(TDHC))

Into a solution of rMb(Co^{II}(TDHC)) (0.55 mM, 3 mL, 1.65 μmol) in 0.1 M potassium phosphate buffer at

pH 7.0 was added a solution of normal or ^{13}C-enriched KCN (0.1 M, 33 μL, 3.3 μmol, 2 eq) and then the mixture was equilibrated at 4 ºC under aerobic conditions for 30 min. After concentration to 0.8 mL using an Amicon Ultra-4 centrifugal filter (10 kDa) (GE Healthcare), the protein solution was passed through a HiTrap desalting column (GE Healthcare) equilibrated with 0.1 M potassium phosphate buffer at pH 7.0. After addition of D_2O (final concentration of D_2O: 10%v/v), the solution was concentrated to 0.4 mL and transferred to an NMR microtube (Shigemi Co., Ltd., Hachioji, Japan). The ^{13}C NMR measurements of the proteins were carried out at 5 ˚C over 2 days (65536 scans). As the control experiments of the reconstituted proteins, $Co^{III}(^{13}CN)_2$(TDHC) was prepared by autoxidation of Co^{II}(TDHC) (2 mM) in the same buffer containing K^{13}CN (4 mM) under aerobic conditions.

FT-IR measurements of rMb(Co^{III}(CN)(TDHC))

Each solution containing ^{13}C-enriched or normal cyanide bound to the cobalt complex (ca. 6 mM) in 0.1 M potassium phosphate buffer at pH 7.0 was prepared. A series of FT-IR spectra were accumulated (50 scans) at 25 ºC with 4.0 cm^{-1} resolution.

Relaxation analysis of cyanide binding

In general, it is difficult to determine the affinity of cyanide for aqua-Co(III) complexes, because the ligand-exchange process is too slow to detect by conventional titrimetric measurements at 25 °C, pH 7.0 in the presence of KCN (10 μM).[16] Thus, the binding constant of cyanide was determined by a relaxation analysis.[16] Into a solution of rMb($Co^{III}(OH_2)$(TDHC)) (10 μM) in 0.1 M potassium phosphate buffer at pH 7.0 was added a solution of 0.20 M or 0.10 M KCN in the same buffer to the desired final concentrations of KCN (0.10, 0.50, 1.0, 1.5 and 2.0 mM) and then UV-vis spectra were recorded at 25 ºC for 20 min. The concentrations of the cyanide ion were determined using the following Henderson-Hasselbach equation (eq 3)

$$\mathrm{p}H = \mathrm{p}K_a - \log\left(\frac{[\mathrm{HCN}]}{[\mathrm{CN}^-]}\right) = \mathrm{p}K_a - \log\left(\frac{C_0 - [\mathrm{CN}^-]}{[\mathrm{CN}^-]}\right) \qquad (3)$$

where the pH and pK_a values are 7.0 and 9.2[28] at 25 ˚C, respectively; C_0 is the initial concentration of KCN. The spectral changes occurring over 20 min upon addition of KCN were observed. The transient relaxation kinetics are represented by the following equation (eq 4),

$$\mathrm{rMb}(\mathrm{Co^{III}}(\mathrm{H_2O})(\mathrm{TDHC})) + \mathrm{L} \underset{k_{\mathrm{off}}}{\overset{k_{\mathrm{on}}}{\rightleftharpoons}} \mathrm{rMb}(\mathrm{Co^{III}}(\mathrm{L})(\mathrm{TDHC})) \qquad (4)$$

where L denotes an exogenous ligand; k_{on} and k_{off} are rate constants for the association and dissociation of

L, respectively. The observed rate constant $k_{obs.}$ is given by following equation (eq 5).[16]

$$k_{obs.} = k_{off} + k_{on}[L] \quad (5)$$

The binding constant of cyanide for rMb($Co^{III}(H_2O)$(TDHC)) was determined by following equation (eq. 6),

$$K = k_{on}/k_{off} \quad (6)$$

Computational chemistry

The author used the Becke–Perdew (BP86)[29] method implemented in the Gaussian 09 program. For all atoms, the 6-31G(d) basis set was used. This level of theory BP86/6-31G(d) serves as an appropriate platform to address the structural, electronic, and spectroscopic properties of cobalamin cofactors.[30] All calculations were carried out in the gas phase. As truncated models of Co(TDHC) and cobalamin, the author used Co(TDHC') and Co(corrin), respectively, where all of the peripheral side chains in TDHC and corrin are replaced with hydrogen atoms for DFT calculations.[11] The bond dissociation energies (BDEs) of the Co–N(Im) bonds of the Im-coordinated Co(III) complexes are defined by the following equation (eq 7),

$$BDE = E(Co^{III}(L)) + E(Im) - E(Co^{III}(Im)(L)) \quad (7)$$

where E(X) is the energy of the optimized structure of X; L and Im are exogenous axial ligand and imidazole, respectively; and Co^{III}(L) and Co^{III}(Im)(L) are Im-free and Im-coordinated Co(III) complexes which are coordinated by L, respectively.

References and notes

(1) (a) B. Kräutler, Organometallic Chemistry of B_{12} Coenzyme. In *Metal Ions in Life Science;* A. Sigel, H. Sigel, R. K. O. Sigel, Eds.; RSC: Cambridge, 2009; Vol. 6, pp 1–51. (b) B. Kräutler, B. Puffer, Vitamin B_{12}-Derivatives: Organometallic Catalysts, Cofactors and Ligands of Bio-Macromolecules. In *Handbook of Porphyrin Science;* K. M. Kadish, K. M. Smith, R. Guilard, Eds.; World Scientific: Singapore, 2012; Vol. 25, pp 131–263. (c) B. Kräutler, S. Ostermann, Structure, Reactions, and Functions of B_{12} and B_{12}-Proteins. In *The Porphyrin handbook;* K. M. Kadish, K. M. Smith, R. Guilard, Eds.; Academic Press: San Diego, 2003, Vol. 11, pp 229–276. (d) K. L. Brown, *Chem. Rev*. **2005**, *105*, 2075. (e) R. Banerjee, C. Gherasim, D. Padovani, *Curr. Opin. Chem. Biol*. **2009**, *13*, 484. (f) K. Gruber, B. Puffer, B. Kräutler, *Chem. Soc. Rev*. **2001**, *40*, 4346. (g) F. Zelder, *Chem. Commun*. **2015**, *51*, 14004.

(2) (a) C. L. Drennan, S. Huang, J. T. Drummond, R. G. Matthews, M. L. Ludwig, *Science* **1994**, *266*,

1669. (b) R. G. Matthews, *Acc. Chem. Res.* **2001**, *34*, 681. (c) R. G. Matthews, Cobalamin- and Corrinoid-Dependent Enzyme. In *Metal Ions in Life Science;* A. Sigel, H. Sigel, R. K. O. Sigel, Eds.; RSC: Cambridge, 2009; Vol. 6, pp 53–113. (d) R. G. Matthews, Cobalamin-dependent Methionine Synthase. In *Chemistry and biochemistry of B_{12};* R. Banerjee, Eds.; John Wiley & Sons. Inc.: New York, 1999; pp 681–706.

(3) H. P. C. Hogenkamp, G. T. Bratt, A. T. Kotchevar, *Biochemistry*, **1987**, *26*, 4723.

(4) (a) Y. Murakami, Y. Aoyama, K. Tokunaga, *J. Am. Chem. Soc.* **1980**, *102,* 6736. (b) Y. Murakami, K. Aoyama, *Bull. Chem. Soc. Jpn.* **1976**, *49*, 683. (c) Y. Murakami, Vitamin B_{12} Models with Macrocyclic Ligands. In *Biomimetic Chemistry;* M. J. Comstock, Advances in Chemistry Series 191; American Chemical Society: Washington, DC, 1980; pp 179–199. (d) C.-J. Liu, A. Thompson, D. Dolphin, *J. Inorg. Biochem*. **2001**, *83*, 133. (e) M. Dommaschk, V. Thoms, C. Schütt, C. Näther, R. Puttreddy, K. Rissanen, R. Herges, *Inorg. Chem.* **2015**, *54*, 9390.

(5) (a) P. P. Govender, I. Navizet, C. B. Perry, H. M. Marques, *Chem. Phys. Lett.* **2012**, *550*, 150. (b) D. M. March, N. Demitri, S. Geremia, N. Hickey, L. Randaccio, *J. Inorg. Biochem.* **2012**, *116*, 215. (c) I. Navizet, C. B. Perry, P. P. Govender, H. M. Marques, *J. Phys. Chem. B* **2012**, *116*, 8836. (d) P. P. Govender, I. Navizet, C. B. Perry, H. M. Marques, *J. Phys. Chem. A* **2013**, *117*, 3057.

(6) (a) K. L. Brown, S. F. Cheng, X. Zou, J. D. Zubkowski, E. J. Valente, L. Knapton, H. M. Marques, *Inorg. Chem.* **1997**, *36*, 3666. (b) H. M. Marques, L. Knapton, X. Zou, K. L. Brown, *J. Chem. Soc., Dalton Trans.* **2002**, 3195. (c) C. F. Zipp, J. P. Michael, M. A. Fernandes, S. Mathura, C. B. Perry, I. Navizet, P. P. Govender, H. M. Marques, *Inorg. Chem.* **2014**, *53*, 4418. (d) C. F. Zipp, J. P. Michael, M. A. Fernandes, M. Nowakowska, H. W. Dirr, H. M. Marques, *Inorg. Chem. Commun.* **2015**, *57*, 15.

(7) (a) L. Randaccio, M. Furlan, S. Geremia, M. Šlouf, I. Srnova, D. Toffoli, *Inorg. Chem.* **2000**, *39*, 3403. (b) L. Hannibal, C. A. Smith, J. A. Smith, A. Axhemi, A. Miller, S. Wang, N. E. Brasch, D. W. Jacobsen, *Inorg. Chem.* **2009**, *48*, 6615. (c) L. Ouyang, P. Rulis, W.-Y. Ching, M. Slouf, G. Nardin, L. Randaccio, *Spectrochim. Acta, Part A* **2005**, *61*, 1647. (d) B. Kräutler, W. Keller, C. Kratky, *J. Am. Chem. Soc.* **1989**, *111*, 8936. (e) B. Kräutler, R. Konrat, E. Stupperich, G. Färber, K. Gruber, C. Kratky, *Inorg. Chem.* **1994**, *33*, 4128. (f) L. Randaccio, G. Brancatelli, N. Demitri, R. Dreos, N. Hickey, P. Siega, S. Geremia, *Inorg. Chem.* **2013**, *52*, 13392. (g) C. Steffen, K. Thomas, U. Huniar, A. Hellweg, O. Rubner, A. Schroer, *J. Comput. Chem.* **2010**, *31*, 2967.

(8) (a) K. L. Brown, H. M. Marques, *J. Inorg. Biochem.* **2001**, *83*, 121. (b) K. L. Brown, H. M. Marques, *J. Mol. Struct. THEOCHEM* **2005**, *714*, 209. (c) K. L. Brown, *Dalton Trans.* **2006**, 1123. (d) K. S. Conrad, C. D. Jordan, K. L. Brown, T. C. Brunold, *Inorg. Chem.* **2015**, *54*, 3736.

(9) (a) W. Galezowski, P. N. Ibrahim, E. S. Lewis, *J. Am. Chem. Soc.* **1993**, *115*, 8660. (b) W. Galezowski, E. S. Lewis, *J. Phys. Org. Chem.* **1994**, *7*, 90. (c) W. Galezowski, *Inorg. Chem.* **2005**,

44, 5483. (d) W. Galezowski, *Inorg. Chem.* **2005**, *44*, 1530.

(10) T. Hayashi, Y. Morita, E. Mizohata, K. Oohora, J. Ohbayashi, T. Inoue, Y. Hisaeda, *Chem. Commun.* **2014**, *50*, 12560.

(11) Y. Morita, K. Oohora, A. Sawada, K. Doitomi, J. Ohbayashi, T. Kamachi, K. Yoshizawa, Y. Hisaeda, T. Hayashi, *Dalton Trans.* **2016,** *45*, 3277.

(12) (a) J. W. Brown, J. N. Reeve, H. G. Floss, *J. Am. Chem. Soc.* **1987**, *109*, 7922. (b) C. Wedemeyer-Exl, T. Darbre, R. Keese, *Helv. Chim. Acta* **1999**, *82*, 1173. (c) L. Pan, H. Shimakoshi, Y. Hisaeda, *Chem. Lett.* **2009**, *38*, 26. (d) L. Pan, H. Shimakoshi, T. Masuko, Y. Hisaeda, *Dalton Trans.* **2009**, 9898. (e) L. Pan, K. Tahara, T. Masuko, Y. Hisaeda, *Inorg. Chim. Acta* **2011**, *368*, 194.

(13) (a) Y. Hisaeda, T. Masuko, E. Hanashima, T. Hayashi, *Sci. Technol. Adv. Mater.* **2006**, *7*, 655. (b) Y. Murakami, J. Kikuchi, Y. Hisaeda, O. Hayashida, *Chem. Rev.* **1996**, *96*, 721.

(14) (a) O. Carugo, K. D. Carugo, *Trends Biochem. Sci.* **2005**, *30*, 213. (b) S. MacEdo, M. Pechlaner, W. Schmid, M. Weik, K. Sato, C. Dennison, K. Djinović-Carugo, *J. Synchrotron Radiat.* **2009**, *16*, 191.

(15) G. C. Hayward, H. A. Hill, J. M. Pratt, N. J. Vanston, R. J. Williams, *J. Chem. Soc. Perkin 1* **1965**, 6485.

(16) S. Neya, M. Suzuki, T. Hoshino, A. T. Kawaguchi, *Inorg. Chem.* **2013**, *52*, 7387.

(17) (a) C. Kratky, G. Färber, K. Gruber, K. Wilson, Z. Dauter, H. F. Nolting, R. Konrat, B. Kräutler, *J. Am. Chem. Soc.* **1995**, *117*, 4654. (b) S. V. Evans, G. D. Brayer *J. Mol. Biol.* **1990,** *213*, 885. (c) Z. N. Zahran, L. Chooback, D. M. Copeland, A. H. West, G. B. Richter-Addo, *J. Inorg. Biochem.* **2008**, *102*, 216. (d) A. Arcovito, M. Benfatto, M. Cianci, S. S. Hasnain, K. Nienhaus, G. U. Nienhaus, C. Savino, R. W. Strange, B. Vallone, S. L. Della, *Proc. Natl. Acad. Sci. U. S. A.* **2007**, *104*, 6211.

(18) The elongated Co–N(His93) bond might be influenced by the characteristics of the TDHC framework and/or structural perturbations of the histidine residue in the protein.

(19) (a) K. L. Brown, NMR spectroscopy of B_{12}. In *Chemistry and Biochemistry of B_{12};* R. Banerjee, Ed.; J. Wiley & Sons: New York, 1999; pp 197–237. (b) K. L. Brown, M. Hakimi, *J. Inorg. Chem.* **1984**, *23*, 1756.

(20) The ratio of the wavenumber (ν_{13CN}/ν_{12CN} = 0.98) is consistent with the inverse ratio of the reduced mass (μ_{12CN}/μ_{13CN} = 0.98).

(21) (a) Y. Murakami, Y. Aoyama, S. Nakanishi, *Inorg. Nucl. Chem. Lett.* **1976**, *12*, 809. (b) J. M. Pratt, The Roles of Co, Corrin, and Protein. I. Co-Ligand Bonding and the Trans Effect. In *Chemistry and Biochemistry of B_{12};* R. Banerjee, Eds.; J. Wiley & Sons: New York, 1999; pp 73–112. (c) K. S. Reddy, T. Yonetani, A. Tsuneshige, B. Chance, B. Kushkuley, S. S. Stavrov, J. M. Vanderkooi, *Biochemistry* **1996**, *35*, 5562.

(22) R. Krishnamoorthi, G. N. LaMar, *Eur. J. Biochem.* **1984**, *138*, 135.

(23) (a) T.Andruniow, M. Z. Zgierski, P. M. Kozlowski, *J. Am. Chem. Soc.* **2001**, *123*, 2679. (b) S. M. Chemaly, M. Florczak, H. Dirr, H. M. Marques, *Inorg. Chem.* **2011**, 8719.

(24) The computed Co–CN bond length of Co^{III}(CN)(Im)(TDHC') is clearly shorter than that observed for the crystal structure of rMb(Co^{III}(CN)(TDHC)). The cyanide ion is vertically coordinated to the cobalt atom in the optimized structure of Co^{III}(CN)(Im)(TDHC') with a Co–C–N angle of 177˚ (Figure S8a). In contrast, the observed bond angle of rMb(Co^{III}(CN)(TDHC)) is similar to the Fe–C–N angle of cyano-nMb (Figure S8b,c).[23d] The bent structure of the cyanide ion in myoglobin is known to be due to steric hindrance between the cyanide ion and the His64 residue.

(25) (a) F. W. J. Teale, *Biochim. Biophys. Acta* **1959**, *35*, 543. (b) T. Hayashi, Hemoproteins Reconstituted with Artificially Created Heme. In *Handbook of Porphyrin Science;* K. M. Kadish, Smith, R. Guilard, Eds.; World Scientific: Singapore, 2010; Vol. 5, pp. 1–69.

(26) T. Matsuo, H. Dejima, S. Hirota, D. Murata, H. Sato, T. Ikegami, H. Hori, Y. Hisaeda, T. Hayashi, *J. Am. Chem. Soc.* **2004**, *126*, 16007.

(27) (a) Z. Otwinowski, W. Minor, *Methods Enzymol.* **1997**, *276*, 307. (b) A. J. McCoy, R. W. Grosse-Kunstleve, P. D. Adams, M. D. Winn, L. C. Storoni, R. J. Read, *J. Appl. Cryst.* **2007**, *40*, 658. (c) M. D. Winn, C. C. Ballard, K. D. Cowtan, E. J. Dodson, P. Emsley, P. R. Evans, R. M. Keegan, E. B. Krissinel, A. G. W. Leslie, A. McCoy, S. J. McNicholas, G. N. Murshudov, N. S. Pannu, E. A. Potterton, H. R. Powell, R. J. Read, A. Vagin, K. S. Wilson, *Acta Crystallogr., Sect. D: Biol. Crystallogr.* **2011**, *67* 235. (d) G. N. Murshudov, P. Skubák, A. A. Lebedev, N. S. Pannu, R. A. Steiner, R. A. Nicholls, M. D. Winn, F. Long, A. A. Vagin, *Acta Crystallogr., Sect. D: Biol. Crystallogr.* **2011**, *67,* 355. (e) P. Emsley, B. Lohkamp, W. G. Scott, K. Cowtan, *Acta Crystallogr., Sect. D: Biol. Crystallogr.* **2010**, *66* 486.

(28) R. M. Izatt, J. J. Christensen, R. T. Pack, R. Bench, *Inorg. Chem.* **1962**, *1*, 828.

(29) (a) A. D. Becke *J. Chem. Phys.* **1986**, *84*, 4524. (b) J. P. Perdew, *Phys. Rev. B,* **1986**, *33*, 8822.

(30) (a) K. P. Jensen, U. Ryde, *J. Phys. Chem. A* **2003**, *107*, 7539. (b) C. Rovira, X. Biarnés, K. Kunc. *Inorg. Chem.* **2004**, *43*, 6628. (c) C. Rovira, P. M. Kozlowski, *J. Phys. Chem. B* **2007**, *111*, 3251. (d) N. Dölker, A. Morreale, F. Maseras, *J. Biol. Inorg. Chem.* **2005**, *10*, 509. (e) J. Kuta, S. Patchkovskii, M. Z. Zgierski, P. M. Kozlowski, *J. Comput. Chem.* **2006**, *27*, 1429. (f) P. M. Kozlowski, T. Kamachi, T. Toraya, K. Yoshizawa, *Angew. Chem. Int. Ed.* **2007**, *46*, 980. (g) P. M. Kozlowski, T. Kamachi, T. Toraya, K. Yoshizawa, *J. Biol. Inorg. Chem.* **2011**, *17*, 293.

Conclusion

Methionine synthase, one of cobalamin-dependent methyltransferases, mediates an essential reaction of methyl group transfer using methylcobalamin as an organometallic cofactor in organisms. However, the detailed mechanism which suggests the transmethylation in the enzyme matrix has not been understood completely, because of the complicated molecular structures of the cofactor and the protein matrix. In the present study, the author has constructed and investigated the model system to reveal the reaction mechanism via the organometallic species possessing the unique reactivity in the enzyme matrix. Myoglobin reconstituted with a cobalt corrinoid as a newly-prepared model system provides the details of structure, reactivity and coordination behavior of the intermediates to understand the reaction mechanism.

As an enzyme model, a cobalt corrinoid complex with a simple protein matrix was designed and prepared to clarify the coordination behavior of the Co(I) species, one of the important intermediates. In the present work, the author chose cobalt tetradehydrocorrin (Co(TDHC)) as a model complex of cobalamin. Next, the author employed myoglobin as a simple protein matrix with an axial histidine residue, which is similar to the cobalamin binding domain. The model complex was inserted into the protein matrix by a conventional reconstitution method to obtain myoglobin reconstituted with Co^{II}(TDHC), rMb(Co^{II}(TDHC)). UV-vis and EPR spectroscopies clearly show that the Co(II) species is coordinated by the His93 residue as an axial ligand. Furthermore, the X-ray crystal structure of the rMb(Co^{II}(TDHC)) reveals the penta-coordinated Co(II) complex with the His93 ligation. Therefore, the reconstituted myoglobin can be regarded as a His-on model of methionine synthase. The Co(II) species was then reduced with dithionite to yield the Co(I) species, rMb(Co^{I}(TDHC)), which was characterized by UV-vis and EPR spectroscopies. The Co(I) species was also prepared in the protein crystals by soaking the protein crystals of rMb(Co^{II}(TDHC)) into the dithionite solution. In the X-ray crystal structure, de-ligation of the His93 residue coordinated to the Co(II) species occurs to form the tetra-coordinated Co(I) species in the heme-binding pocket.

To understand the reaction mechanism of the transmethylation occurring in methionine synthase, the model reactions by the reconstituted protein were investigated. The Co(I) species reacted with methyl iodide to generate the CH_3–Co(III) species in the myoglobin matrix, which is identified by UV-vis and EPR spectroscopies, and ESI mass spectrometry. Since the organometallic species are not obtained in organic solvents, this result suggests that the axial coordination of the His93 residue stabilizes the methylated complex. The theoretical calculations also support the stabilization of the methylated complex by the imidazole-ligation. Furthermore, the author observed the intraprotein transmethylation in the heme pocket over 24 h at 25 ˚C. The in source decay analysis by MALDI TOF MS indicates that the

methyl group on the cobalt center is transferred to the His64 residue in the heme pocket. The NMR spectra of the peptide fragment containing the His64 residue prepared by trypsin-digestion of the methylated protein indicate that the methyl group is transferred to the Nε atom of the His64 residue via a heterolytic cleavage of the Co–C bond. The HPLC analysis of the peptides shows the first-order reaction of the transmethylation. The theoretical study suggests that the stepwise pathway via a His-off intermediate is more plausible than the concerted pathway for the transmethylation, indicating that the de-ligation of the His93 residue activates the methyl group. The moderate coordination of His93 to the cobalt center in TDHC induces the transmethylation via the His-off species, because there is sufficient space to allow flipping of the imidazole ring in the proximal site. These findings proposed that dynamic structural changes of the enzyme would likely promote de-ligation in the cobalamin-binding domain.

Because of the difficulty for the characterization of the CH_3–Co(III) species, the author prepared and investigated the aqua- and cyano-Co(III) species to understand the coordination behavior of the Co–N(His93) bond. The X-ray crystal structures show that the hexa-coordinated aqua- and cyano-Co(III) species with the axial His93 ligation in the myoglobin matrix. The X-ray crystallography and IR spectroscopy show the elongation of the Co–CN bond of the cyano-Co(III) species compared to cyanocobalamin. This result is also supported the much lower affinity of cyanide for rMb($Co^{III}(OH_2)$(TDHC)) than that for aquacobalamin. The acid titration and theoretical results for cyano-Co(III) species indicate the relatively weak Co–N(Im) bond. The similar weak coordination of the histidine residue to the cobalt center is plausible in the CH_3–Co(III) species due to higher σ-donation of the methyl group. The theoretical calculations of the CH_3–Co(III) species also suggest the elongation of the Co–N(Im) bond, which would lead to the transient formation of the His-off intermediate promoting the transmethylation in the myoglobin matrix.

The author has developed myoglobin reconstituted with Co(TDHC) as an model of cobalamin-dependent methionine synthase. The author's model demonstrates the tetra-coordinated structure of the Co(I) species as an important intermediate and the model reactions of the transmethylation in the protein matrix. The theoretical study supports the mechanism that the axial histidine ligation and the de-ligation are significantly effective for the stabilization and activation of the CH_3–Co(III) species, respectively. Furthermore, the investigation of the coordination behavior of the Co(III) species suggests that the protein matrix would provide the flexible ligation. The present model system provides the understanding for the mechanism that the His-on/off switching controls the multi-step reactions in structurally complex cobalamin-dependent methionine synthase. These findings give an important insight into generating a new biocatalyst toward difficult alkylations of various substrates.

List of publications

1. Co(II)/Co(I) reduction-induced axial histidine flipping in myoglobin reconstituted with a cobalt tetradehydrocorrin as a methionine synthase model
   Takashi Hayashi, Yoshitsugu Morita, Eiichi Mizohata, Koji Oohora, Jun Ohbayashi, Tsuyoshi Inoue and Yoshio Hisaeda
   Chem. Commun., **2014**, *50*, 12560–12563.

2. Intraprotein transmethylation via a CH_3–Co(III) species in myoglobin reconstituted with a cobalt corrinoid complex
   Yoshitsugu Morita, Koji Oohora, Akiyoshi Sawada, Kazuki Doitomi, Jun Ohbayashi, Takashi Kamachi, Kazunari Yoshizawa, Yoshio Hisaeda and Takashi Hayashi
   Dalton Trans., **2016**, *45*, 3277.

3. Crystal Structures and Coordination Behaviors of Aqua- and Cyano-Co(III) Tetradehydrocorrins in the Heme Pocket of Myoglobin
   Yoshitsugu Morita, Koji Oohora, Eiichi Mizohata, Akiyoshi Sawada, Takashi
   Kamachi, Kazunari Yoshizawa, Tsuyoshi Inoue and Takashi Hayashi
   Inorg. Chem., **2016**, *55*, 1287

Supplementary publication

4. Correlation between Redox Potentials of Cobalt Corrinoids with Axial Ligands and the Co–C Bond Dissociation Energies
   Yoshitsugu Morita, Koji Oohora, Akiyoshi Sawada, Takashi Kamachi, Kazunari Yoshizawa and Takashi Hayashi
   in preparation.

Acknowledgments

The study presented in this thesis has been carried out at Department of Applied Chemistry, Graduate School of Engineering, Osaka University from April 2010 to March 2016. The author would like to express his deep gratitude to the supervisor, Professor Takashi Hayashi, for his continuous guidance, kind suggestions, constant discussions and warm encouragement throughout this research. The author would like to deeply thank Assistant Professor Koji Oohora for his valuable suggestion, helpful discussions and warm encouragement. The author would like to deeply thank Associate Professor Akira onoda for his valuable suggestion and discussions.

The author would like to express his gratitude to Professor Jean Weiss at Institut de Chimie, UMR 7177 CNRS-Université de Strasbourg for his kind suggestions, and warm encouragement. The author would like to express her gratitude to Dr. Jennifer Wytko at Institut de Chimie, UMR 7177 CNRS-Université de Strasbourg, for her meaningful suggestions and warm encouragement. The author would like to express his gratitude to Romain Ruppert at Institut de Chimie, UMR 7177 CNRS-Université de Strasbourg, for his fruitful discussion and warm encouragement.

The author also acknowledges Professor Hiroshi Uyama and Professor Hidehiro Sakurai for reviewing this thesis and valuable discussions.

The author expresses great gratitude to Dr. Kyoko Inoue at Department of Applied Chemistry, Graduate School of Engineering, Osaka University for technical assistance during the NMR measurements. The author gratefully acknowledges Professor Tsuyoshi Inoue and Associate Professor Eiichi Mizohata at Department of Applied Chemistry, Graduate School of Engineering, Osaka University for X-ray crystal structure analysis of the proteins and the staff for their excellent support during data collection on the BL44XU at SPring-8 and the BL-17A at Photon Factory. The author gratefully acknowledges Professor Kazunari Yoshizawa, Assistant Processor Takashi Kamachi, Dr. Kazuki Doitomi and Mr. Akiyoshi Sawada at Institute for Materials Chemistry and Engineering and International Research Center for Molecular Systems, Kyushu University for DFT calculations.

The author would like to highly thank to Dr. Yohei Sano for his meaningful suggestions and discussions. The author would like to express the author's gratitude to Dr. Yasuaki Kakikura for his significant suggestions and warm encouragement. The author would like to express his gratitude to Kazuki Hukumoto for his meaningful suggestions and warm encouragement. The author would like to deeply thank to Yasunori Okamoto for his meaningful suggestions and warm encouragement. Acknowledgement is also made to all members of Professor Takashi Hayashi's group and Professor Jean Weiss's group for their encouragements and friendship in the laboratory.

The author would like to express great gratitude to his family for their assistance.

Finally, the author is grateful for financial supports by Japan Society of the Promotion Science (JSPS) and a Japan-German Graduate Externship Program funded by JSPS.

Yoshitsugu Morita

January 2016